EIT InnoEnergy - MSc SELECT
Environomical Pathways for Sustainable Energy Systems

Energy Flexibility Strategies for Residential Buildings in Mediterranean Climates

Author: Riccardo Toffanin
Director: Joana Aina Ortiz Ferrà
Supervisor: Thibault Péan
Call: September 2018

Master's Thesis Submitted in Partial Fulfilment of the Requirements for the
Master's Degree in Energy Engineering

Universitat Politècnica de Catalunya – Barcelona Tech
Catalonia Institute for Energy Research - IREC

Abstract

European buildings, of which 75% are considered energy inefficient, account as much as 40% of the continent total energy consumption. To solve this issue, the European Union has set as goal the increase of building energy efficiency by 30% before 2030, and this objective has supported the electrification of heating and cooling systems, with the number of installed Heat Pumps (HPs) increasing four times from 2006 to 2015. However, this rise in electricity consumption and the higher presence of fluctuating energy sources, like solar and wind, in the energy mix may lead to electric grid congestion and instability since the grid was originally designed considering fossil-fuel boilers as the predominant heating technology, and centralized dispatchable generation as the standard for energy production. An increasing flexibility in building energy consumption might be an effective solution to mitigate these issues, especially since the thermal load can largely be shifted in time due to building inertia and the HP power draw can be moved to a certain extent without jeopardizing the occupants' comfort.

In this master's thesis, different energy flexibility strategies are applied in a residential building, which is located in the Mediterranean area of Spain and equipped with a HP. The control strategies make use of Model Predictive Control (MPC) in order to manage the HP operation, and their flexibility potential is assessed using a TRNSYS-MATLAB co-simulation platform. Moreover, this master's thesis presents the modelling of an air-to-water reversible Variable Speed HP (VSHP) in TRNSYS, because this software mostly models Fixed Capacity HPs (FCHP), thereby limiting the energy performance and flexibility analysis.

Simulations were conducted in both heating and cooling periods. The developed VSHP model proved to be more efficient than the FCHP model, achieving an electricity consumption reduction of 16.10% in winter and of 6.23% in summer, due to its ability to work at part load where the HP efficiency is higher. Four MPC energy flexibility strategies were implemented and their performance confronted with the operation of the building equipped with a VSHP controlled with a standard thermostat. The first strategy minimizes the electricity consumption of the HP, the second aims at minimizing the HP electricity cost using the two-period electricity tariff available in Spain, while the third and the fourth have as goal the CO_2 emission minimization. The signal used to trigger the shifting of the HP operation is the percentage of CO_2-free generation in the third case and the grid CO_2 emission factor in the fourth case. All the four strategies achieved their energy objective by reducing the electricity consumption on average by 39.70% in the first case, the electricity cost on average by 49.15% in the second case, the CO_2 emission on average by 28.02% in the third case and by 24.26% in the fourth case. In addition, the last three scenarios successfully achieved load shifting towards low-price or low-emission hours. However, the level of thermal comfort of the occupants was slightly reduced when flexibility was activated yet remains far from discomfort levels.

Acknowledgements

This thesis represents the conclusion of the EIT InnoEnergy master's degree SELECT - Environomical Pathways for Sustainable Energy Systems, which was undertaken at Royal Institute of Technology of Stockholm – KTH in Sweden and Universitat Politècnica de Catalunya – UPC in Spain. In these two years, I have met incredible people from all over the globe, and I would like to thank them for giving me beautiful insights of their cultures that helped me grow as a person, and for their support in my first experience living abroad, far from all the certainties that home can offer. Among these people, a special thanks goes to Jalomi, that was always there for everything I needed.

I would like to express my gratitude to my thesis supervisors, Thibault Péan and Joana Ortiz, that offered me the opportunity to perform this work at Catalonia Institute for Energy Research – IREC. They shared with me their experience, knowledge, and material that supported me in the understanding of the topic of energy flexibility in buildings, and to solve the doubts that I encountered during this work. I also would like to thank Attila Husar that accepted to be the rapporteur for this work, without previous knowledge of me or of my work.

I would especially like to thank all my friends back home in Italy, with a special regard to two of my journey companions at Politecnico di Milano, Federico and Giordano. Without all the laughs and good times we shared, I do not think I would have been able to complete the bachelor's degree and start the adventure that lead me to write this master's thesis. Grazie!

I personally dedicate this work to my family. To my parents, Gianpietro e Patrizia, for their unconditional love and support they always showed me. To my sister, Silvia, for her constant encouragement and inspiration. To my grandmother, Ines, that always nourished me with love, and to my grandfather, Erminio, that, even if is not here with us, is always here with me.

I would like to conclude the acknowledgments with a quote from my favourite artist, that always gives me hope and joy:

"C'est la vie, say the old folks, it goes to show you never can tell"

Chuck Berry

Table of Contents

List of Tables

List of Figures

Glossary

Term	*Abbreviation*
Active Demand Response	ADR
Balance Responsible Party	BRP
Carbon Dioxide	CO_2
Coefficient of Performance	COP
Demand-Side Management	DSM
Distribution System Operator	DSO
Domestic Hot Water	DHW
Economic Model Predictive Control	EMPC
Energy Flexibility	EF
Energy in Buildings and Communities	EBC
European Union	EU
Fixed Capacity Heat Pump	FCHP
Flexibility Factor	FF
Heat Pump	HP
International Energy Agency	IEA
Key Performance Indicator	KPI
Model Predictive Control	MPC
Net-Zero Energy Building	nZEB
Optimal Control Problem	OCP
Part Load Factor	PLF
Part Load Ratio	PLR
Photovoltaic	PV
Predicted Mean Vote	PMV
Proportional-Integral-Differential	PID
Pseudo-Random Binary Signal	PRBS
Renewable Energy Source	RES
Resistance-Capacity	RC
Rule-Based Control	RBC
Space Cooling	SC
Space Heating	SH
Strengths, Weaknesses, Opportunities, and Threats	SWOT
Strengths, Weaknesses, Opportunities, Threats	SWOT
Time-of-Use	ToU
Transmission System Operator	TSO
Variable Speed Heat Pump	VSHP
Voluntary Price for the Small Consumer	PVPC

1. Introduction

Buildings account as much as 40% of the total European energy consumption and approximately 75% of them are energy inefficient (1). To ameliorate the situation, the European Union (EU) has established an objective of a 30% improvement in energy efficiency by 2030 which has supported the electrification of heating and cooling systems, with the number of installed Heat Pumps (HPs) increasing by a factor of four from 2006 to 2015 (1, 2). This rise in electricity consumption may lead to electric grid congestion and instability since it was originally designed considering fossil-fuel boilers as the predominant heating technology. Furthermore, this higher electricity consumption trend will be amplified by the increasing share of electric vehicles in the automotive market (3).

Moreover, Renewable Energy Sources (RESs) are being more and more integrated into the global energy mix due to the expected reduction of fossil fuel availability, an increasing global warming effect, the rising global energy demand, and supporting policies (4–6). For example, the EU has decided to reach a renewable energy penetration in the national energy mix of every member state of 20% by 2020 and of 27% by 2030 (7). However, solar and wind energy suffer from a high fluctuation that can create serious stability problems in the energy system, in particular when a high percentage of the energy generation comes from these sources.

A possible solution to mitigate these issues is an increasing flexibility in the energy consumption, meaning a passage from generation on demand to consumption on demand, knows as Demand-Side Management (DSM). This concept can be applied to the different actors of the total energy demand system but concentrating on buildings will be crucial, knowing their high share in the total consumption and their potential for performance improvement.

Among the different buildings typologies, residential constructions are one of the most interesting for an energy flexibility analysis because they are the most common typology in Europe and, in addition, present the highest share in the final energy consumption (8, 9).

As a matter of fact, the energy consumption of a building, especially the thermal part, can largely be shifted in time (10–12). This means that, depending on the case, the consumption of electrical appliances used by the occupants can be varied and the demand for Domestic Hot Water (DHW), Space Heating (SH), Space Cooling (SC), and ventilation can be moved to a certain extent without jeopardizing the comfort of the occupants (3). This flexibility can be achieved, especially for the heating and cooling demand, thanks to the embedded thermal mass of the construction or other storage technologies that might be present in the buildings, e.g. DHW tanks, phase change materials storage systems, or batteries (3).

Different control strategies can be introduced in order to achieve flexibility in building energy consumption. They can be grouped into two different categories: Rule-Based Control (RBC) or

Model Predictive Control (MPC) (13). RBC are based on the introduction of certain rules (e.g. change in heating/cooling set-point, charging rate of an electric vehicle, etc.) when a trigger signal, for example the electricity price or the on-site photovoltaic (PV) production, reaches a pre-determined threshold (13). MPC are more complex but more effective (14) since they predict the future performance of the building with a simplified model and decide an operating strategy that minimizes the selected objective function, for instance the cost or the consumption of the system, over a receding horizon (15).

In conclusion, Energy Flexibility (EF) in buildings will become of utmost importance in the coming years, and for all the above-mentioned reasons, it is fundamental to examine and estimate the energy flexibility potential of residential buildings, especially if equipped with heat pumps.

1.1. Objective and Scope

In this master's thesis, a residential building – typical of the building stock of Catalonia, Spain, thus located in the Mediterranean climate – will be analysed through dynamic building simulations in a TRNSYS-MATLAB co-simulation platform. This project aims to implement different model predictive control flexibility strategies on the heating and cooling system in order to suggest answers to these major questions: how to better reproduce the behaviour of a variable speed heat pump in simulations? What are the advantages and drawbacks of MPC strategies compared to more standard control strategies like thermostatic control? What is the performance of these flexibility strategies in heating and cooling periods? What are the effects of different trigger signals on MPC strategies? Is the thermal comfort of the occupants maintained when flexibility is activated?

In this context, the project emphasizes the following points of the wide topic of energy flexibility in buildings:

- it focuses on residential buildings, being the most common typology in the EU building stock and the building category with the highest share in the final energy consumption;
- it concentrates on the Mediterranean climate, also exploring the possibility of controlling the cooling consumption, as seldom done in the available literature;
- the detailed model of the building is developed with a specific dynamic building simulation software, TRNSYS, while the MPC strategies, including the resolution of the algorithm and the simulation of the simplified model of the building, are implemented in MATLAB;
- dynamic simulations are the chosen mean of analysis, enabling the possibility of performing a wider range of scenarios compared to experiments;
- the effect of energy flexibility can be analysed from the building or from the energy grid point of view, and this study concentrates on the building side, focusing on the impact on the

performance of the building and on the wellness of its occupants.

1.2. General Methodology

The main tasks performed during the master's thesis were the:

- literature review of energy flexibility in residential buildings, with a focus on the key performance indicators used to quantify the EF and on the most common control strategies;
- assessment of the business opportunity potential of energy flexibility in residential buildings;
- study of the TRNSYS energy model of the chosen building for a detailed performance simulation;
- implementation of the part load performance of a variable speed heat pump based on manufacturer data in TRNSYS;
- study and modification of a simpler MATLAB energy model of the studied building, necessary for the implementation of MPC strategies;
- implementation of the TRNSYS/MATLAB co-simulation platform in order to use MPC strategies on the detailed building model;
- analysis of the energy flexibility potential of the chosen scenarios with the chosen key performance indicators;
- evaluation of the impact of EF on the thermal comfort of the occupants.

2. Literature Review

The concept of flexibility of demand is not recent; however, the research in this field applied to buildings is at its initial stage, and, at this time, an overview regarding the amount of flexibility that different types of buildings and their usage may offer is not available. For this reason, the International Energy Agency (IEA) Energy in Buildings and Communities (EBC) program Annex 67: "Energy Flexible Buildings" was created in 2015 (3). This project, which is an international collaboration between 16 countries, has as a scope the expansion of knowledge, the identification of the problematics and the relative solutions, the discovery of the means to quantify and control the energy flexibility that can be offered by buildings, and the creation of a common and uniform terminology, since various definitions concentrating on different aspects of the term are present in the literature.

In the extended review written by Reynders et al. (16), the available literature was classified into 5 categories depending on the focus that the authors gave to the definition of "Energy Flexibility in Buildings", although the majority of the papers does not explicitly define the term. The emphasis was, depending on the case, on the energy infrastructure context (e.g. grid support, time or fuel shifting), on the electricity grid, on the energy price, on the negative secondary effects of flexibility (e.g. reduction of building performance, such as thermal comfort of the occupants), or on the systems interacting with buildings, such as heat pumps or boilers. Notwithstanding, all definitions rely on the simple idea that (16):

> energy flexibility represents the ability of a building to adapt its energy consumption to provide specific services.

Among all the definitions, the one elaborated during the Energy Flexibility Workshop CITIES project (17) was based on a different flexibility potential:

> energy flexibility is an energy system service provided by a customer. For each energy carrier: the amount of power and energy within a given period that can be changed upon request – either permanently (fuel shifted) or temporary (time shifted).

This definition is interesting since it mentions the fuel shifting potential of flexibility, which may be important in countries where the energy infrastructure is heterogeneous with the presence of different energy carriers, such as gas network, electricity grid, or district heating.

However, IEA EBC Annex 67: "Energy Flexible Buildings" project proposed a more comprehensive and formal definition, which is still under discussion (3, 18):

> the energy flexibility of a building is the ability to manage its demand and generation according to local climate conditions, user needs, and energy network requirements. Energy flexibility of buildings will thus allow for demand side management/load control and thereby demand response based on the requirements of the surrounding energy networks.

Furthermore, there is also no agreement in the available literature on the sign convention of flexibility (19). De Coninck and Helsen (20) and Reynders et al. (16) consider as positive (or upward) flexibility an increase of load while as negative (or downward) flexibility a decrease of load; in contrast, other researchers (21), (22), (23) have defined the need for increased electricity generation (or reduced load) as positive flexibility whereas the need for decreased electricity generation (or increased load) as negative flexibility. Stinner et al. (19) adopt another approach deciding to change the sign convention depending on the type of load: if the heating system is a combined heat and power plant, an increase of load is positive while a reduction of load is negative, but if the heating system is a heat pump or a heating rod system, a load power increase is negative whereas a load power decrease is positive. In the rest of the document, an increase of load is considered as positive (or upward) flexibility while a decrease of load is considered as a negative (or downward) flexibility.

2.1. Quantification Methodologies of Energy Flexibility

The lack of international uniformity that characterises the definition of "energy flexibility in buildings" is even more pronounced for the quantification methodologies. However, under the scope of IEA EBC Annex 67: "Energy Flexible Buildings", first Lopes et al. (24) wrote a literature review and then Reynders et al. (16) expanded this work identifying two main approaches for the quantification of EF.

In the first one, energy flexibility is quantified indirectly in a specific energy system and/or energy market context in order to evaluate the performance of a specific control strategy (e.g. reduction of operation costs, or of CO_2 emission, or of peak power), which is also the case of this master's thesis project. In the second one, the quantification of the energy flexibility is direct and performed with a bottom-up method on the level of the individual technologies, enabling the decoupling of the analysis of the market operation and demand side technologies (16).

These two approaches can also be differentiated by the moment when flexibility is evaluated. The former quantifies the flexibility "after", evaluating the effect of a specific flexibility control strategy, while the latter analyses it "before", by predicting the potential without implementing any control strategy.

The authors of the review (16) focused on the second approach trying to identify the differences and the similarities of the six main methodologies based on it, and to compare them in a common case study. The methodologies and their characteristics can be summarized in Table 1 taken from (16).

Table 1: Direct quantification methodologies for energy flexibility (16)

Methodology	Authors	Flexibility quantified by the	Case study
A	Six et al. (25) Nuytten et al. (26)	Numbers of hours the respective energy consumption can be delayed or anticipated	EF of residential heat pumps combined with thermal energy storage (25) EF of a combined heat and power system with thermal energy storage (26)
B	D'hulst et al. (27)	Power increases or reductions combined with how long these changes can be sustained	Based on measured data, the authors quantified the EF offered by 5 different types of domestic electrical systems
C	Stinner et al. (19)	Temporal flexibility, power flexibility, and energy flexibility	Heating system with thermal energy storage tank used for space heating and DHW
D	De Coninck and Helsen (20, 28)	Cost functions, which comprise the amount of energy that can be shifted at a specific time and the associated cost compared to a reference plan	Heating system using structural thermal mass storage
E	Oldewurtel et al. (29)	Efficiency curves, depicting the maximum power increase or decrease against the power shifting efficiency	Heating system using structural thermal mass storage
F	Reynders, G. (30, 31)	Available storage capacity, the storage efficiency, and the power shifting potential	Heating system using structural thermal mass storage

These methodologies can, in turn, be divided into two categories (16). In methodologies A and B, EF is calculated from two extreme cases, which are the minimum and maximum state of charge if thermal storage is analysed. The thermal losses are neglected, since these methods calculate the energy in the buffer at time t as the difference between the maximum and minimum cumulated energy profile at time t, assuming that it can be recovered completely. This approach may have problems of interpretability when the system has high thermal losses, e.g. the structural thermal mass; furthermore, the EF is estimated when the system passes from an initial state to a finale state, that must be reached at a specific time. However, for continuous processes, such as space heating, the final state is not

defined, since there are not specific charging and discharging periods, but the system tries to satisfy the thermal comfort constraints.

In methodologies C, D, E, and F, energy flexibility is quantified from specific simulated flexibility events based on rule-based control (C and F) or on optimal control (D and E). These approaches may also present lack of interpretability in systems with high thermal losses and multiple time constants.

Nevertheless, three characteristics (time, power/energy, and cost) are found to be common to the different methods (3), (16), (19) since the building flexibility is described by:

1. the time during which the power or the energy can be moved;
2. the amount of power or energy that can be moved;
3. the associated monetary or energy cost (e.g. increase of the energy use due to the flexibility operation) from the activation of the flexibility.

Moreover, another point raised by the authors is that the available energy flexibility is estimated as a function of time: the estimation will change depending on the variation of the boundary conditions, especially weather (e.g. solar radiation and outdoor temperature) and occupancy time.

The methodologies were assessed on a common case study, a detached single-zone building with a heat pump and a simplified low temperature radiator heating system to fulfil the space heating demand. The system has high thermal losses and multiple time constants, since the building thermal mass is exploited. The authors concluded that the methodologies based on specific flexibility events (from C to F) have a better interpretability whereas the methodologies based on cumulated energy profiles (A and B) lose interpretability because they simplify multiple time constants system into single state systems. The results obtained from D, E, and F are similar, easy to compare and show the dependence of the estimated energy flexibility on the dynamic boundary conditions, such as weather and occupancy. Methodologies D and E present the same result in a different way, whereas methodologies D and F have limited differences, even if the former makes use of optimal control while the latter is based on rule-based control, as can be seen in Figure 1 and Figure 2 for the almost overlapping power shift and cost profiles, respectively. In addition, methodology C obtained physically meaningful results, but a comparison was not possible due to different starting hypothesis as it is shown in Figure 1.

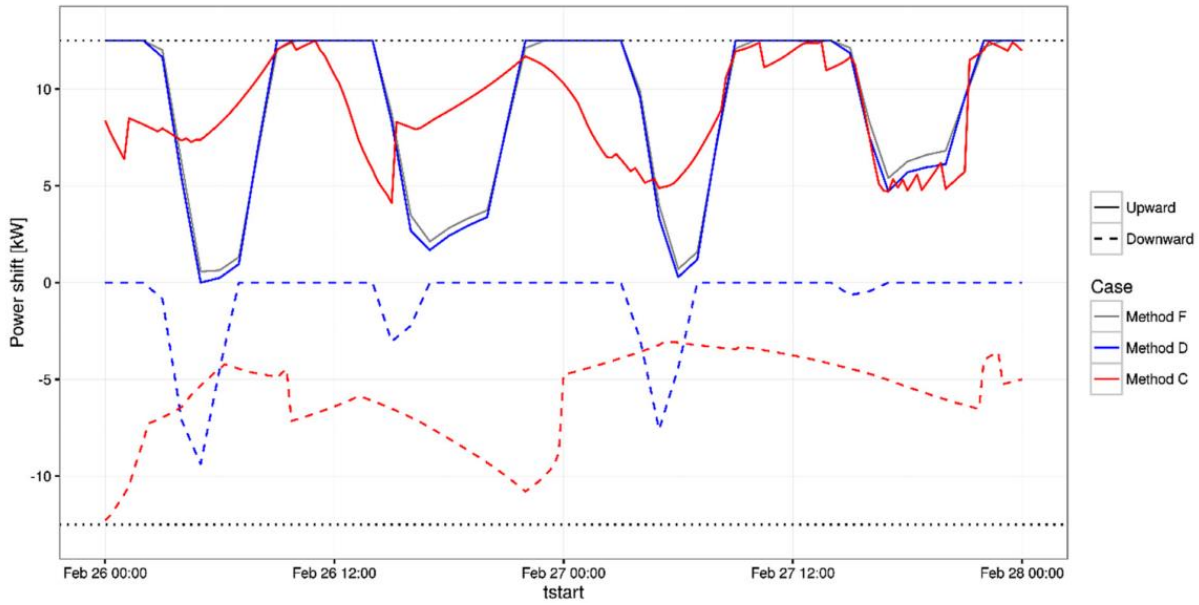

Figure 1: Comparison of results of methodologies C, D and F (F only considers upwards flexibility) (16)

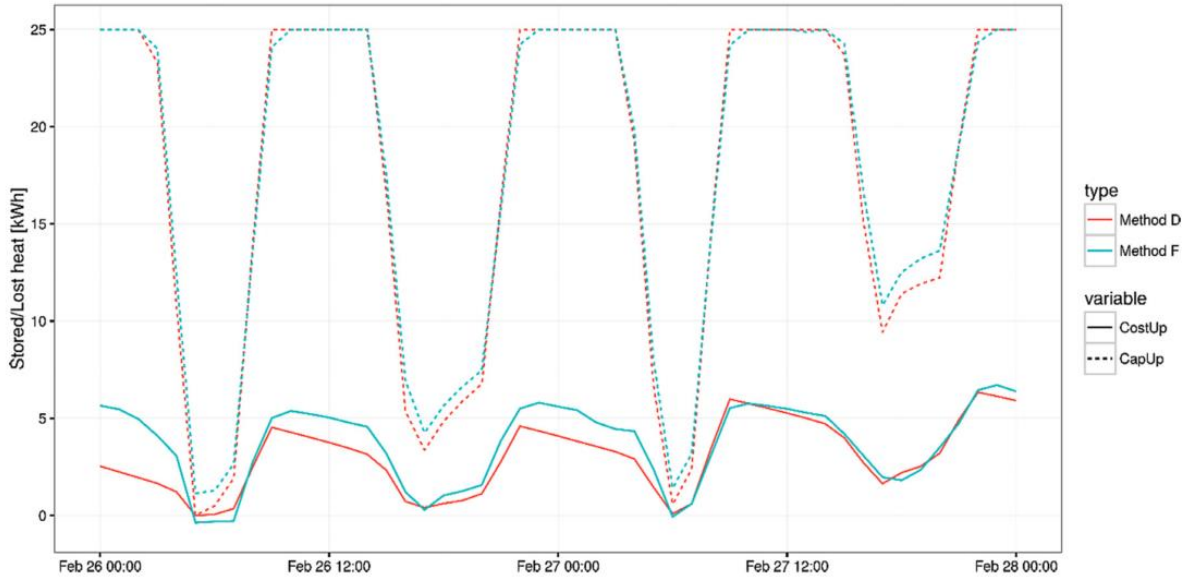

Figure 2: Comparison of results of methodologies D and F for upwards flexibility (16)

2.2. Key Performance Indicators

A Key Performance Indicator (KPI) is defined by Deru and Torricellini (32) as:

> a high-level performance metric that is used to simplify complex information and point to the general state or trends of a phenomenon.

The use of correct KPIs is fundamental since they are tools to provide a precise measurement of the status of the system in order to simplify and help the process of decision making (14). Moreover, they follow and measure the performance, and, when a control system is implemented, they are used to reach the required performance goals. For this reason, a building KPI must be applicable throughout the system's operational lifespan, during the different season and occupational levels. EF was evaluated using conventional KPIs, such as primary energy consumption, energy cost, CO_2 emissions, etc., or more specific indicators.

The major KPIs related to EF found in the literature are listed in this section. The majority of these indicators are summarized in the literature review written by Clauß et al. (14). Other more general KPIs included in Clauß et al. (14) are presented in Appendix 1: General Key Performance Indicators.

The name of the indicators, that presented the same designation in several references but different mathematical definition, are changed adding words that better express the focus point of view of the flexibility analysis.

2.2.1. KPIs for Post-Evaluation of Flexibility Potential

The KPIs presented in this section are used to quantify the energy flexibility "afterwards", subsequently to the introduction of a specific control strategy.

2.2.1.1. Flexibility Factor

The Flexibility Factor (FF) was presented in the literature with different formulations focusing on different aspects of the flexibility, but representing in every case a relative indicator of the tariff period in which the majority of the energy demand was done or, in other terms, a quantification of the ability to move the energy demand from high to low tariff periods (10, 33–35).

The **price flexibility factor** is defined as (10):

$$FF_E = \frac{\int_{LPT} l(t)dt - \int_{HPT} l(t)dt}{\int_{LPT} l(t)dt + \int_{HPT} l(t)dt} \quad (2.1)$$

where the two integrals represent the energy demand during low price and high price time, respectively. It is a simple indicator to quickly identify the time when the energy is consumed. $FF = 1$ means that there is no demand during the high-price period, while $FF = -1$ means the opposite case; $FF = 0$ represents the case when the energy consumption is equal in both periods.

The **power flexibility factor** (33) shows the capacity to increase or reduce power demand at a given

time step in relation to the reference daily peak power and it is defined as:

$$FF_P = \frac{P(t) - P_{ref}(t)}{\max[P_{ref}(d)]} \quad (2.2)$$

where $P(t)$ is the power demand of the energy flexible building at a given time step, $P_{ref}(t)$ is the power demand of the reference building at a given time step, and $\max[P_{ref}(d)]$ is the maximum power demand of the reference building during the day. The factor is above 0 (possible increase of daily peak power) when the power demand increases while the factor is below 0 (possible reduction of daily peak power) when the power demand decreases, in comparison with the reference. The factor is equal to 0 means that there is no variation of power demand, and, in turn, no possible variation of daily peak power.

Another definition, the **cost flexibility factor** (34, 35), is based on the monetary expense during the different price periods. The annual procurement cost of the energy depends on the electricity Time-of-Use (ToU) tariffs, therefore, the higher part of the demand satisfied during low price periods, the higher the cost flexibility factor. The following equation defines the indicator:

$$FF_{PC} = \frac{PC_{max} - PC}{PC_{max} - PC_{min}} \quad (2.3)$$

where PC_{max} and PC_{min} are the procurement cost of the high tariff period and low tariff period, respectively, while PC is the procurement cost of the studied case and are defined as:

$$PC_{max} = \frac{\int_0^T p_{EL,max} l(t) dt}{\int_0^T l(t) dt} \qquad PC_{min} = \frac{\int_0^T p_{EL,min} l(t) dt}{\int_0^T l(t) dt} \qquad PC = \frac{\int_0^T p_{EL}(t) l(t) dt}{\int_0^T l(t) dt} \quad (2.4)$$

where $p_{EL}(t)$ is the electricity price during the analysed period, and $p_{EL,max}$ and $p_{EL,min}$ represent the maximum and minimum electricity price over the same period, respectively.

FF_{PC} is maximum (equal to 1) when PC is equal to PC_{min} and minimum (equal to 0) when PC is equal to PC_{max}. This indicator was then utilised to quantify the energy shifted from a reference case:

$$FF_{PC,shift} = \frac{FF_{PC} - FF_{PC,ref}}{FF_{PC,ref}} \quad (2.5)$$

where FF_{PC} is the procurement cost flexibility factor of the studied case, and $FF_{PC,ref}$ is the procurement cost flexibility factor of the reference case with flat tariff.

2.2.1.2. Regulation Potential

It is the hourly absolute integral of the power flexibility factor. It gives a measure of how much the maximum daily power demand can be varied for one hour. This information is useful for grid balancing responsible parties because the regulation market works on a 24 hours horizon divided into intervals of 60 minutes. It is usually represented graphically with a daily curve. The mathematical definition is (33):

$$RP = \int_{\Delta t} FF_P(t)dt \quad (2.6)$$

where $FF_P(t)$ is the power flexibility factor at a given time step, and Δt is the time step relevant for the regulation market (1 hour).

2.2.2. KPIs for Pre-Evaluation of Flexibility Potential

The KPIs introduced in this section are used for an evaluation of the energy flexibility potential before implementing any control strategies.

2.2.2.1. Power Shifting Capability

The power flexibility of a building is the difference between the heating power during an Active Demand Response (ADR) event, e.g. charging of the embedded thermal mass of the building, and the reference heating power during normal operation. In mathematical terms the energy variation is (30, 31, 36, 37):

$$l_{shift} = l_{ADR} - l_{ref} \quad (2.7)$$

The power shifting capability is defined as the combination of l_{shift} and its time duration t_{shift}. If the temperature set-point of the reference case is chosen in the middle of the thermal comfort, both positive and negative flexibility are possible.

2.2.2.2. Storage Capacity

The storage capacity can be considered as a time-varying characteristic property of the building, related to the specific boundary conditions, heating system, and occupant behaviour of the studied case. It is expressed mathematically by the following equation (30, 31, 36, 37):

$$C_{ADR} = \int_0^{t_{shift}} l_{shift}dt \quad (2.8)$$

In case of positive flexibility (upwards modulation of the HP power), C_{ADR} represents the amount of energy that can be added to the embedded thermal mass of the building during a charging ADR event. In case of negative flexibility (downwards modulation of the HP power), C_{ADR} represents the amount of energy that can be saved during a discharging ADR event. Both cases are constrained by the thermal comfort need of the occupants.

2.2.2.3. Storage Efficiency

The previous indicator is important from a grid perspective since it considers the gross amount of energy shifted on the energy network. The net energy, useful for a building point of view, can be evaluated considering the storage efficiency; however, there is an on-going debate on the mathematical definition of this term, since it may lead to a value of efficiency higher than 1, creating confusion since efficiency is commonly recognised as a parameter lower than 1 (30, 31, 36, 37).

It may have the same definition for both positive and negative flexibility (30, 31, 36, 38):

$$\eta_{ADR} = 1 - \frac{\int_0^{\infty} l_{shift} dt}{|C_{ADR}|} \quad \text{in case of positive/negative flexibility} \tag{2.9}$$

In this case, $\eta_{ADR} > 1$ means that the overall energy consumption is lower than the reference scenario (typical for negative flexibility), while $\eta_{ADR} < 1$ means the opposite (typical for positive flexibility).

In another reference (37), two different formulations of the terms were presented:

$$\eta_{ADR} = 1 - \frac{\int_0^{\infty} l_{shift} dt}{|C_{ADR}|} = 1 - \frac{\text{energy losses}}{\text{stored energy}} \quad \text{in case of positive flexibility} \tag{2.10}$$

$$\eta_{ADR} = \frac{\int_0^{\infty} l_{shift} dt}{|C_{ADR}|} = \frac{\text{rebound effect}}{\text{ADR event}} \quad \text{in case of negative flexibility} \tag{2.11}$$

With these two definitions, the efficiency should be always lower than 1, respecting the convention.

The rebound effect can be defined as (39):

> The time before or after a flexibility activation (where a customer's consumption/generation has been shifted up or down) where the customer compensates for the activation by increasing/reducing consumption relative to its consumption profile.

In this situation, it is the surplus amount of energy consumed after the discharging ADR event as it can be seen in the grey part of Figure 3.

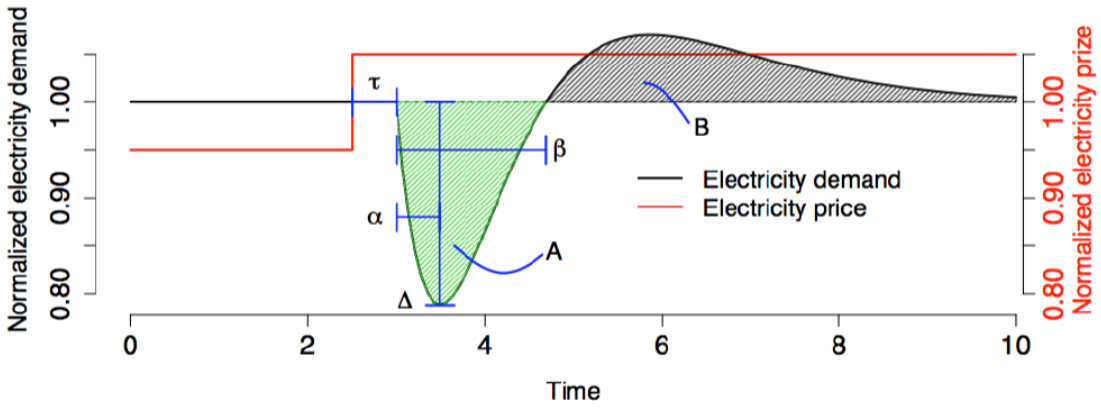

Figure 3: Example of "rebound effect" (40)

2.2.2.4. Shifting Efficiency

It can be used for both the embedded thermal mass and hot water tanks and it is defined as (10):

$$\eta_{shifting} = \frac{-\Delta l_{discharged\ heat}}{\Delta l_{charged\ heat}} \tag{2.12}$$

where $\Delta l_{discharged\ heat}$ is the decrease of load demand compared to the reference case, while $\Delta l_{charged\ heat}$ is the increase of load demand compared to the reference case, during the simulation period. In case of a charging ADR event, the term $\Delta l_{charged\ heat}$ represents the increase of load demand when the storage is purposely charged while $\Delta l_{discharged\ heat}$ is the decrease of load following the event. In case of a discharging ADR event, $\Delta l_{discharged\ heat}$ is the decrease of load due

to storage discharge done on purpose during the event, whereas $\Delta l_{charged\ heat}$ is the increase of load following the event. The shifting efficiency corresponds to the storage efficiency when the storage is being charged and it is lower than one, whereas it is higher one during a discharging event.

2.2.2.5. Demand Recovery Ratio

It quantifies the ratio between the energy consumption during an ADR event and the heating energy consumption of the reference case (no ADR participation) as (41):

$$DRR = \frac{\int_0^{t_{shift}} l(t)dt}{\int_0^{t_{shift}} l_{ref}(t)dt} \tag{2.13}$$

It can be used to describe the flexibility performance of one building or a cluster of buildings.

2.2.2.6. Temporal, Power, and Energy Flexibility

Forced temporal flexibility τ_{forced} is defined as the time required by an electrical-grid coupled heat generator working at maximum power to charge or heat the thermal energy storage until maximum storage capacity from an empty state (19).

Delayed temporal flexibility $\tau_{delayed}$ is defined as the time necessary to completely discharge the thermal energy storage from maximum capacity when the electrical-grid coupled heat generator is at minimum power, or, if possible, shut off (19).

Power flexibility can be measured by three different methods (19):

- Power curve: the forced power flexibility is calculated as the difference between the maximum possible power of the electrical-grid coupled heat generator and the reference case power demand curve, while the delayed power flexibility is calculated as the difference of the reference case curve and the minimum possible power of the electrical-grid coupled heat generator, which is often zero. Both power curves start at each time t and end after the calculated temporal flexibility time. In formula:

$$\pi_{flex,forced}(t, \xi - t) = \pi_{max}(\xi) - \pi_{ref}(\xi) \quad t \le \xi \le t + \tau_{forced}(t) \tag{2.14}$$

$$\pi_{flex,delayed}(t, \xi - t) = \pi_{ref}(\xi) - \pi_{min}(\xi) \quad t \le \xi \le t + \tau_{delayed}(t) \tag{2.15}$$

- Average power flexibility: it consists of the power for every time step calculated by averaging the power curves using the calculated temporal flexibility time; the mathematical expression:

$$\pi_{avg,forced}(t) = \begin{cases} \frac{\int_0^{\tau_{forced}(t)} \pi_{flex,forced}(t,\xi)d\xi}{\tau_{forced}(t)} \ if\ \tau_{forced}(t) > 0 \\ 0\ if\ \tau_{forced}(t) = 0 \end{cases} \tag{2.16}$$

$$\pi_{avg,delayed}(t) = \begin{cases} \frac{\int_0^{\tau_{delayed}(t)} \pi_{flex,delayed}(t,\xi)d\xi}{\tau_{delayed}(t)} \; if \; \tau_{delayed}(t) > 0 \\ 0 \; if \; \tau_{delayed}(t) = 0 \end{cases} \quad (2.17)$$

- Cycle power flexibility: it consists of the power for every time step calculated by averaging the power curves using the storage cycle time (sum of charging time and discharging time); it is defined as:

$$\pi_{cycle,forced}(t) = \begin{cases} \frac{\int_0^{\tau_{forced}(t)} \pi_{flex,forced}(t,\xi)d\xi}{\tau_{forced}(t)+\tau_{delayed}\left(t+\tau_{forced}(t)\right)} \; if \; \tau_{forced}(t) > 0 \\ 0 \; if \; \tau_{forced}(t) = 0 \end{cases} \quad (2.18)$$

$$\pi_{cycle,delayed}(t) = \begin{cases} \frac{\int_0^{\tau_{delayed}(t)} \pi_{flex,delayed}(t,\xi)d\xi}{\tau_{delayed}(t)+\tau_{forced}\left(t+\tau_{delayed}(t)\right)} \; if \; \tau_{delayed}(t) > 0 \\ 0 \; if \; \tau_{delayed}(t) = 0 \end{cases} \quad (2.19)$$

Energy flexibility is calculated as the integral of the power curve (19):

$$\epsilon_{forced}(t) = \int_0^{\tau_{forced}(t)} \pi_{flex,forced}(t,\xi)d\xi \quad (2.20)$$

$$\epsilon_{delayed}(t) = \int_0^{\tau_{delayed}(t)} \pi_{flex,delayed}(t,\xi)d\xi \quad (2.21)$$

The availability of EF depends on the use of a portion of the flexibility in the previous periods, thus, it is useful to calculate the annual building energy flexibility (19):

$$\epsilon_{forced,year} = \int_0^{t_{year}} \pi_{cycle,forced}(\xi)d\xi \quad (2.22)$$

$$\epsilon_{delayed,year} = \int_0^{t_{year}} \pi_{cycle,delayed}(\xi)d\xi \quad (2.23)$$

The energy flexibility for an entire year shows the maximum possible energy that can be delivered in either forced or delayed operation for one year considering the pauses due to the use of EF in the opposite operation.

2.2.2.7. Energy and Cost Flexibility (cost curve)

This indicator was developed using a bottom-up approach through the solution of optimal control problems with low-order models in order to create cost curves of the flexibility. The advantage of this method is its genericity and the possibility to aggregate different buildings. The mathematical formulation of the energy flexibility is (20):

$$\phi_{pos} = l_{max}(t) - l_{ref}(t) \geq 0 \quad (2.24)$$

$$\phi_{neg} = l_{min}(t) - l_{ref}(t) \leq 0 \quad (2.25)$$

where $l_{ref}(t)$ is the load demand of the reference case, which minimizes the cost, and $l_{max}(t)$ and $l_{min}(t)$ are the maximum and minimum possible load demand, respectively.

The relative cost variation is defined as:

$$\Gamma_{max} = J_{c,max} - J_{c,ref} \geq 0 \quad (2.26)$$

$$\Gamma_{min} = J_{c,min} - J_{c,ref} \geq 0 \quad (2.27)$$

where $J_{c,ref}$ is the total cost of the reference case, while $J_{c,max}$ and $J_{c,min}$ are the total cost of the scenario with the maximum and minimum possible consumption, respectively. It must be noted that, since the reference case minimizes the cost, the cost variation is always positive (introducing flexibility always increases the cost) both in the case of positive and negative flexibility scenarios.

2.3. Control Strategies

Buildings equipped with heat pump show promising prospective for EF, as was pointed out in the introduction of the study; therefore, the analysis presented in this section focuses on this category.

The general control system in this type of building can be summarized in Figure 4. There are two levels of control: the supervisory system, where the applied control strategy acts, and the local controller of the heat pump. The supervisory control system communicates not only with the different sensors present in the building, receiving information about e.g. room temperature, CO_2 level, PV generation, net power exchange with the grid, etc., but also with external services giving the price of energy and weather data. This system analyses this information and, based on its algorithm, decides an operating strategy, which is sent to the local controller of the heat pump (13).

There are two main types of control strategies implemented to achieve energy flexibility in buildings: rule-based control and model predictive control.

RBCs strategies are based on an "if-then" statement: if a certain condition applies, then a response action is triggered. The monitored parameters are, for example, the room or water temperature, the CO_2 level, or the PV generation, and when the predefined value is reached, the operation of the heat pump is varied, based on the corresponding strategy (13). These methods are simple and easy to implement into dynamic building simulation programs, such as TRNSYS, EnergyPlus, or IDA ICE (14).

MPCs strategies use a simplified model of the building in order to predict its future performance, and, relying on this prediction, the operating strategy is optimized over a sliding horizon depending on the selected objective function (14). These strategies are more complicated and require a higher computational time, and, moreover, the implementation into dynamic building simulation software is more difficult, requiring the use of other tools, like MATLAB or Modelica, for the application of the control strategy, and, in addition, an interface between the programs is necessary to coordinate between the software (14).

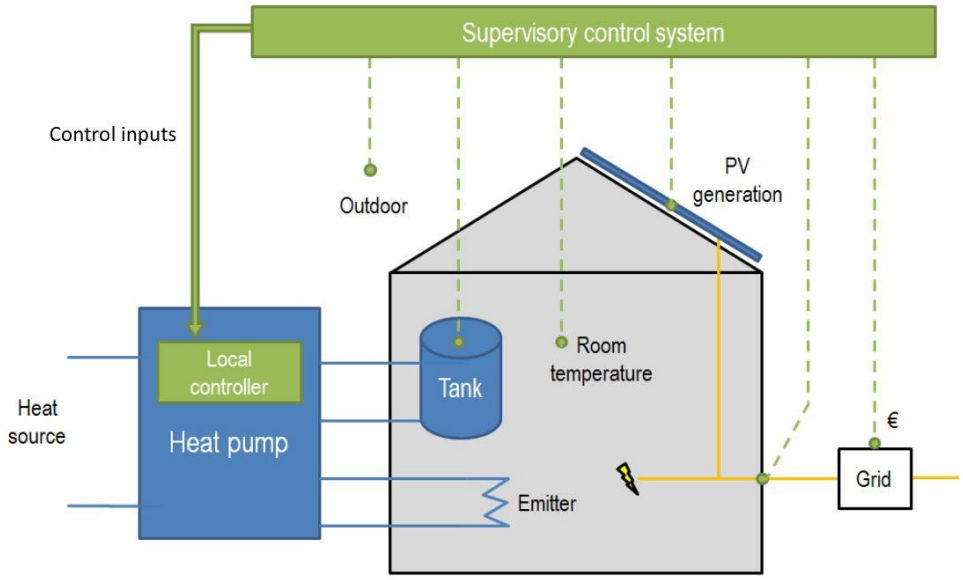

Figure 4: General control scheme for buildings equipped with heat pumps (13)

These strategies present multiple differences, however, some mutual characteristics can be noted: both methodologies are found to have in common the control inputs and sensor parameters (13).

The major control inputs are the temperature set-points and the power of the heat pump. The former can be the temperature of room thermostats (42, 43), of the hot water tank (43, 44), or of the supply system (45). The latter variable can be binary (heat pump on or off) (46), modulated between the minimum and maximum power by changing the speed of the compressor, if the heat pump is controlled by an inverter (47), or, indirectly, by modifying the temperature set points (34).

Data information is retrieved from different sensors, which most often measure temperatures, power, and outside conditions. The most important temperatures are the indoor temperature or the operative temperature (average of air temperature and mean radiant temperature of the room), controlled in order to satisfy the thermal comfort, and the hot water tank temperature; in case of radiant floor heating system, the dew point temperature, which is calculated by measuring the relative humidity, is also relevant to avoid surface condensation (13). With respect to power measurements, the building energy consumption, as well as, the on-site generation (e.g. from a PV installation) are monitored, or other more specific parameters, such as the voltage at the distribution feeder or the power exchange with the grid (48), that might be useful for certain control strategies.

2.3.1. Rule-Based Control

Several rule-based control strategies with different flexibility objectives, even if these were not explicitly clarified in the works, have been implemented in the literature. They can be grouped into four categories: load shifting with fixed scheduling, peak shaving, reduction of energy cost, and increase of RES consumption.

Load shifting with fixed scheduling is the major application of RBC for energy flexibility in buildings. Daily power peaks are easily identifiable, and operation can be avoided or reduced during these hours by fixing a proper schedule.

De Coninck et al. (49) forced the daytime charging of the DHW storage tank between 12:00 and 19:00, exploiting the higher seasonal performance factor during daytime, while De Coninck et al. (48) applied this strategy to the DHW production of a net-Zero Energy Building (nZEB) neighbourhood in Belgium by increasing the set-point temperature of 4 K between 12:00 and 16:00, achieving better results than more complicated RBC strategies. Lee at al. (43) reduced the power of the heat pump with set-point modulation during the assumed grid seasonal peak power periods (from 14:00 to 17:00 in summer and from 17:00 to 20:00 in winter), achieving a 80% and 64% reduction of cooling and heating energy consumption during peaks, respectively, whereas Carvalho et al. (50) used this strategy to stop the heat pump during morning peak hours (9:00 to 10:30) and evening peak hours (18:00 to 20:30), reducing the energy cost by 17 to 34%.

Peak shaving, which is useful for grid support operation by controlling the power exchange between the building and the grid, is another target of RBCs. Limits are typically set for either the import and export power, or for at least one of the two variables.

De Coninck et al. (49) defined a threshold of 3500 W for both import and export: if the PV production is higher/lower than 3500 W, the heat pump is started/stopped. Results showed a reduction of the number of peaks up to 50% and a decrease of 1% highest quarter hourly peaks up to 20%, but, the highest peaks were not created by controllable loads, and, therefore, impossible to be avoided. In (48), the authors used a similar strategy in a nZEB neighbourhood of 33 buildings, where the temperature set-point of the DHW tanks is increased when PV production overcomes the export threshold in order to have a higher self-consumption. Benefits are obtained, such as the reduction of curtailing losses, but in a lower magnitude than the simpler fixed scheduling strategy for load shifting, because this second method is active every day and, not only, during sunny days.

Other researchers (34) decided to control the operation of the heat pump of a nZEB with PV on-site generation system by setting an import limit of 2500 W and an export limit of 5000 W. As in (49), the heat pump is switched on/off when the limit is passed by the on-site production/building consumption. This strategy achieved a reduction of import hours above the threshold between 11% and 31% compared to the reference case.

Other strategies have the objective of reducing the energy cost of the final consumers exploiting ToU energy tariffs. Time-changing energy prices showed advantages for both the electricity grid, helping shifting loads or reducing peaks, and the consumers, reducing their expense for energy (51) (52). The trigger of the controller is the energy price, and a different control strategy is implemented depending on the decided high-price and low-price threshold values.

Two main strategies are used in the literature to identify the high and low-price limits: analysis of past price data or projection of future price data. The first approach was implemented studying the data over two years (53), over two weeks (10), over the previous 24 hours (54) (55), while the second for the next 12 hours (53) or 24 hours (54). This second hypothesis is viable on a scenario with a high deployment of smart meters, that enable communication between consumers and distribution system operator, and this scenario is already true for some regions as the EU has planned to substitute 80% of the electricity meters when it is economically feasible by 2020 (56).

Péan et al. (54) used price-based control strategies to improve the flexibility of a residential building located in Catalonia, Spain, by modulating the set-point temperature for space heating and DHW production according to the energy tariff. Results showed that the scenario using future price data was, unexpectedly, outperformed by scenarios using past price data, both in winter and in spring. The most promising case used as low-price threshold the 40^{th} percentile of the previous day price data while as high-price threshold the 60^{th} percentile of the previous day price data, varying the set-point for space heating of ± 1°C and for DHW of ± 5 °C in case these limits are surpassed. This configuration shifted an important part of the energy consumption to low-price periods, achieving an increase of price flexibility factor from -0.08 to 0.67 in spring and from -0.21 to 0.69 in winter; the energy cost was reduced by 22% to 26%, even though the energy consumption increased by 2% to 4%, whereas the comfort level is not compromised. In another paper, Péan et al. (55) extended the previous work, evaluating more deeply the impact on thermal comfort and the robustness of the chosen control strategy. The scenarios achieved energy cost savings of around 20% by shifting the energy consumption of the heat pump to low-price periods (price flexibility factor up to 0.9), but the electricity consumption increased by up to 7% due to higher thermal losses since the additional energy is stored in the embedded thermal mass of the building or in the DHW tank.

The last objective of RBC identified in the literature is the increase of RES consumption. In the work of (34) where a building equipped with a PV system is analysed, the heat pump is started when the on-site generation is higher than the non-heating loads, increasing the load cover factor from 19.6% to 32%. A simpler control strategy was implemented in (53), where the heat pump was simply forced to operate when the PV panels are producing electricity. Self-consumption was improved since the export to the grid was increased by up to 12% while the import from the grid was reduced by up to 22%. The voltage at the distribution feeder was also used as a trigger to activate the operation of the heat pump. De Coninck et al. (48) increased the temperature of the DHW tank when the voltage passed the chosen limit (approximately 250 V) to avoid the shutdown of the PV system. This strategy decreased the curtailing losses by up to 74%. A more general method to achieve this objective is to consider the residual load at the national level, that is the power demand minus the production from solar and wind (57). In (44), the residual load profile was used to elaborate a control strategy to increase the heat pump energy consumption during high residual load periods: the study concluded that

electrical HPs with storage are suitable devices for DSM without compromising the comfort, but load shifting increased the consumption up to 19%.

In conclusion, load shifting with fixed scheduling is a simple approach easy to implement that can obtain promising results, but this method emphasises the major problem of RBC, the lack of adaptation since the fixed schedule does not adjust to real conditions, even though it can be varied seasonally. With respect to peak shaving strategies, they are useful for grid support because the export to the grid or the peak demand is highly reduced showing great potential to control the influence of on-site generation on the grid. Regarding price-based control, this control strategy achieves not only the reduction of energy cost but also load shifting; however, it is related to the implementation of smart meters that enable the communication of price data to consumers. With reference to the strategies to increase the consumption of RES, there are multiple approaches that achieve positive flexibility results, but these methods are difficult to compare as they rely on different parameters. A common finding is that the results are highly influenced by the chosen thresholds, therefore, it is of great importance to choose these values with precaution. In general, it can be said that RBC strategies are characterised by simplicity, but their lack of adaptation limits their applications since the trigger parameters and the thresholds are fixed beforehand and do not adapt to varying external conditions.

2.3.2. Model Predictive Control

The MPC problem is based on the Optimal Control Problem (OCP), which is formulated as:

$$\min_{u} J(k) \tag{2.28}$$

subject to:

$$F(k, x(k), \dot{x}(k), y(k), u_C(k), u_X(k)) = 0 \tag{2.29}$$

$$g(k, x(k), \dot{x}(k), y(k), u_C(k), u_X(k)) = 0 \tag{2.30}$$

$$h(k, x(k), \dot{x}(k), y(k), u_C(k), u_X(k)) \geq 0 \tag{2.31}$$

$$x(0) = x_0 \tag{2.32}$$

where $k \in [0, N]$ is the time step, with N the prediction horizon, J is the objective function, $F(\cdot)$ is the model of the system, $g(\cdot)$ and $h(\cdot)$ are the equality and inequality constraints respectively, x and y are the states of the system, $u_C \in \mathbb{R}^n$ are the control signals or controlled inputs, and u_X are the disturbances. MPC relies on the solution at every control time step of the OCP, which is started from an estimation of the system state from measurements (feedback) and considers the disturbances that will affect the behaviour of the system and its dynamics (feedforward) (15). Figure 5 shows a visual representation of the process: the controller solves the optimization problem over the receding horizon finding the future control signal that will minimize the objective function, considering the effect of the disturbances (or external inputs), the constraints, and the simplified model of the system.

The first control input is applied to the detailed system model or to the real building, and, when the new measurements are obtained, the process is repeated.

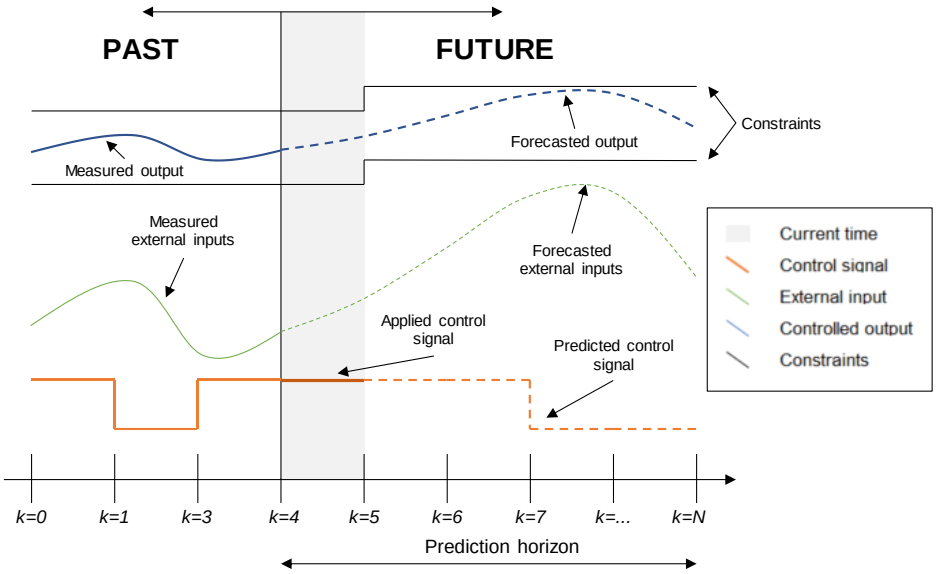

Figure 5: Example of an MPC algorithm

The most common disturbances are the outside weather conditions, namely the outdoor temperature and the solar radiation in the majority of the papers and more rarely the wind speed, and the internal gains (16). The former are usually assumed to be forecasted perfectly or, in case of a real building, retrieved from local measurement or external weather services, while the latter is obtained with a deterministic approach based on fixed schedule or, in case of a real building, an occupancy sensor or the measurement of plug and lighting consumption can be used. Moreover, the changing price of energy is considered in all the Economic MPC (EMPC) strategies (16). This can be an hourly tariff, based on day-ahead predictions, or a ToU electricity tariff (day/night or even three-period prices) (16). The prediction of the disturbances can be done assuming perfect, imperfect, or zero knowledge of the future (16). (58) analysed the effect of the three prediction techniques and concluded that the better the forecast, the better the performance, even if the improvement is small.

Being an optimization problem, the objectives are easy to identify since they are explicitly presented in the objective function (16). The most common type of MPC is the EMPC where the goal is the reduction of the monetary cost of energy. Other objective function terms found in the literature are directed to the minimization of the non-renewable primary energy consumption, peak shaving, the reduction of the emission of CO_2, energy flexibility (explicitly introduced), the thermal comfort of the occupants, and the increase of the robustness of the control strategy (13). The most common mathematical formulations of these terms are presented in Table 2. The objective function is often made by a combination (usually linear) of these terms, introducing different weights depending on their importance; however, their mathematical formulation might not be linear, and, thus, lead to an increase in the computational effort required.

Table 2: MPC objective function terms (13)

Term	Most common mathematical formulation	Variables	Reference
Economic	$J_c = \sum_k [P_{el}(k) W_{hp}(k) + \sum_i P_i(k) G_i(k)]$ (2.33)	P_{el}: price of electricity W_{hp}: heat pump power P_i: price of energy carrier i G_i: consumption of energy carrier i	(59), (35), (15, 60, 69–72, 61–68)
Energy	$J_e = \sum_k c_q(k) u_c(k)$ (2.34)	c_q: conversion factor of each control input	(29), (73)
Peak shaving	$J_p = P_p \max_k [W_{hp}(k)]$ (2.35)	P_p: peak demand cost	(74), (71)
CO_2 emission	$J_{CO_2} = \sum_k c_{CO_2}(k) u_c(k)$ (2.36)	c_{CO_2}: CO2 emission factor	(68)
Energy flexibility	$J_f = \left(\sum_{k_i}^{k_e} W_{hp}(k) \times k - E_{target}\right)^2$ (2.37)	E_{target}: energy consumption target $[k_i, k_e]$: flexibility time interval	(15), (67)
Thermal (dis)comfort (temperature)	$J_d = \sum_k \theta_{occ}(k) \times \left(T_{zon}(k) - T_{set}(k)\right)^2$ (2.38)	θ_{occ}: occupancy factor T_{zon}: actual zone temperature T_{set}: set-point temperature	(15, 35, 60–64, 72)
Thermal (dis)comfort (PMV)	$J_d = \sum_k (\theta_{occ}(k) \times PMV)^2$ (2.39)	θ_{occ}: occupancy factor PMV: predicted mean vote	
Robustness	$J_r = \sum_k \rho \times v(k)$ (2.40)	ρ: penalty factor v: slack variable	(64–66, 72)

EMPC can also shift the load towards low energy price periods, depending especially on the profile of the price data. This can be clearly seen in Figure 6 (left) which presents the results of Masy et al. (35), where the EMPC was used to compare the effect of three different price profile data: flat tariff, day/night tariff, and hourly tariff. The ToU and the day/night tariffs obtain an interesting shift of the heat pump load during low-price periods while the heat pump works whenever space heating is required with the flat rate tariff. The best configuration achieved an 80% shifting of the load, and a 15% reduction of producer cost, while the energy consumption increased by 20%.

De Coninck and Helsen (15) implemented an EMPC on day/night tariff in an office building, equipped with heat pumps and a gas boiler for heating, in Belgium comparing it to the reference RBC control strategy. Moreover, this study is experimental, and the impact of the control strategies were verified on the real building. Results showed that the MPC strategy provided similar thermal comfort while lowering the cost for energy. The main differences between MPC and RBC lie on the daily start-up time and on the switch between the different heating sources. MPC started pre-heating the buildings at midnight while RBC starts only at 5:00 in the morning and the operation was mostly done with heat pumps for MPC, using the gas boiler only for the peaks of demand, while heat pumps were shut off for most of the day for RBC. EMPC reduced the average cost up to 40% and the primary energy use by more than 20%, even if this term was not part of the objective function. The authors also stated that the days when MPC performed badly were due to inexact forecast, large model mismatch or bad estimation of the system state.

Halvgaard et al. (65) introduced EMPC in a residential building with ground-source heat pumps linked to a floor heating system. The day-ahead electricity price data were retrieved from the Nordic power exchange market, Nordpool. The demand of the heat pump was shifted to hours with low price, with monetary savings up to 35% compared to a scenario with flat electricity tariff, as can be seen Figure 6 (right).

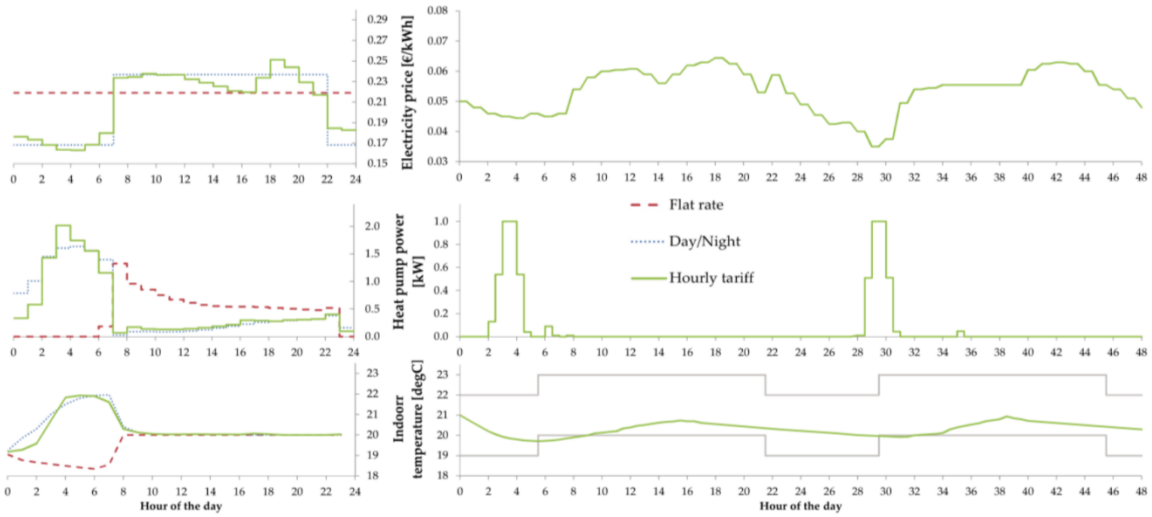

Figure 6: EMPC results of (35) (left) and of (65) (right)

The simplified model used in the controller is the major challenge of MPC. Building this model is challenging since it must be a trade-off between accuracy and computational effort. Most papers utilized a simplified resistance-capacity (RC) model, a network of thermal resistances and capacities, that can correspond to the real elements of the building or be lumped to create reduced order models. Another challenge resides on the amount of meta-information required (e.g. insulation levels, room sizes, occupancy time, etc.) that is difficult to obtain, and, especially for weather, it might be more complicated to obtain data from external services and this data might not be precise.

To sum up, the use of MPC strategies for energy flexibility in buildings will increase in the future, in spite of the problems connected to their complexity and the identification of a proper model, due to favouring conditions: increasing energy cost, availability of time-varying electricity prices, increase of computational power, and more standardised use of simulation tools.

2.3.3. Impact on Thermal Comfort

The impact of DSM strategies on the thermal comfort of the building occupants needs to be carefully controlled because there is the risk of comfort jeopardization if the implemented control strategies are not properly restrained. Several studies in the literature, regardless of being focused on RBC or MPC, implemented flexibility objectives considering thermal comfort boundaries and/or stressed the importance of respecting the temperature limit for thermal comfort (11, 15, 47, 48, 50, 53–55, 60–63, 16, 65, 67, 71–73, 75–77, 22, 30, 33, 35, 41–43). The major comfort constraints consist of variation ranges of the indoor temperature or of the DHW tank temperature, for example, to avoid the Legionella disease.

In papers dealing with rule-based control, the comfort constraints on the indoor temperature are satisfied in different ways: through a control loop that checks for every time step if the zone temperature is within the lower and upper limit and, if it lies between these boundaries, the flexibility strategy can be implemented, or through temperature set-point modulation of the heat pump by constraining the manipulated variable within the comfort limits (in this case the output temperature should, in turn, satisfy the boundaries unless the system is not dimensioned correctly).

MPC strategies can include comfort constraint as hard or soft constraints. The first approach consists in defining temperature ranges where the indoor temperature, a control output, should remain; the ranges can be removed during non-occupancy periods or changed based on time (e.g. night). However, this tactic can complicate the optimisation problem since an explicit solution may be impossible to find. Comfort constraints can also be included in the objective function as a weighted term; the advantage is that small comfort violations, that might be beneficial for the performance, are allowed, but penalised in the same time, a trade-off that is impossible for RBC. Some papers defined the term based on the absolute or squared value of the error between the zone temperature and the set-point temperature, or on the squared PMV (see Table 2) but, in this second case, the computational

effort is considerably increased because the calculation of PMV is complicated, depending on occupants characteristics (metabolic rate and clothing) as well as building parameters, such as the air speed and the indoor temperature.

3. Business Potential of Energy Flexibility

This section contains a brief overview on the business opportunities for energy flexibility in the electricity market, presenting the different stakeholders, the drivers and the barriers that can be encountered, the issues related to user's acceptance, and, in conclusion, the different business models for the implementation of energy flexibility in residential buildings.

For sake of clarification, it is here introduced the difference between explicit and implicit demand-side flexibility (39, 78), taking into account that a prosumer is an entity or an individual that is both a energy consumer and producer, and an aggregator is an entity that has the permission to manage the flexible consumption and/or generation of various customers in the electricity market.

In explicit, or incentive-based, flexibility (39, 78):

> monetary incentives are given to prosumers to change their consumption/generation behaviour upon request, using as trigger, for example, differences in electricity prices or a constraint on the grid or local production. Prosumers can decide to trade their flexibility individually or in group by entering into agreement with an aggregator, which can be either a third-party aggregator or an existing player of market with already established relations with the prosumers. The activation of flexibility is upon request of a third party and mandatory according to the agreement between the two parties.

while in implicit, or price-based, flexibility (39, 78):

> ToU electricity prices are used as a trigger to shift prosumers consumption/generation yet, in this case, customers decide autonomously to apply energy flexibility strategies in order to achieve monetary savings and not upon request of a third party. The introduction by the electricity supplier of time-varying prices for prosumers does not require the role of the aggregator. The activation of flexibility is a personal choice of the prosumer, based on his/her will to change its consumption/generation behaviour.

3.1. Stakeholders

Different actors are involved in the market of flexibility, ranging from the final end-users of the building to governments passing through energy utilities, all playing a different but important role in this framework. The list of the major stakeholders is presented below:

- **building owners** (79, 80) are the actual proprietors of the building but do not necessarily reside in the dwelling; however, their role coincides with the occupants if they reside in the building. They play an important role because they have the last word on the implementation of any measures in their premises;
- **building occupants** (also **consumers**, or **prosumers** if the building is equipped with energy generators) (79, 80) are the people living in the building and, thus, directly affected by the

implementation of flexibility measures; their approval and acceptance, along with the one of the owners, is fundamental and it will be analysed in detail in Section 3.3;

- **real estate developers/owners** (80) are individuals or corporations involved in land acquisition, property development or selling of the developed properties;
- **contractors** (80) are the construction companies and builders performing the construction work necessary to build or retrofit the building;
- **designers** (architects, energy consultants, engineers) (79, 80) are individual or companies involved in the design process of the building, especially regarding the energy supply or consumption;
- **utility partners**, such as Transmission System Operators (TSOs), Distribution System Operator (DSOs), Balance Responsible Parties (BRPs), or electricity supplier (79, 80), are the controller of the energy grid system generation, transportation, distribution and balance;
- **governments or regulators** (79, 80) are the entities developing policies (e.g. incentives campaigns) or standards (e.g. building codes);
- **financial institution** (80) are public or private companies that might finance the introduction of flexibility or the construction of energy flexible buildings;
- **aggregators** (39, 78, 81) are companies that aggregates multiple willing building owners/occupants to contract their flexibility potential with utilities; it is a key role since the EF of a single user is limited and difficultly interesting for the market; this role is discussed in more detail in Section 3.4 where the different implementation business models for flexibility are introduced.

3.2. Drivers and Barriers

The market of energy flexibility in residential buildings has multiple drivers and barriers. For example, owners/occupants may be attracted to the monetary savings on the energy bill that they can achieve, even if they will reduce their ability to personally control their energy consumption and/or comfort (e.g. due to heating/cooling temperature set-point variation) (79). On the other hand, from a grid perspective, demand-side management can reduce problems in the electricity grid by ensuring a better exploitation of variable RESs and helping the decongestion of the grid with peak shaving and load shifting (3).

However, the implementation of energy flexibility on a large scale is slowed down by a lack of homogeneity in the technical standard or in the methodologies to quantify its potential (82). On this side, the IEA EBC Annex 67: Energy Flexible Buildings is working on harmonizing the terminology and developing more uniform indicators and methodologies (3).

Moreover, another barrier consists in the fact that the energy and construction business sector are slow in adapting to changes (79): as a result, the modifications that are necessary to implement flexibility strategies, such as high diffusion of smart appliances, smart meters, and consumption information sharing, may face opposition, delaying the process. In addition to this, the different stakeholders might have contrasting interests: for instance, occupants might like to increase their heating power when there is a need for peak shaving from the grid, and this can result in a refusal from the prosumers to apply the required demand-side flexibility (83).

Furthermore, in some regions (Flanders in Belgium (84) and Netherlands (84)) favourable legislation on EF is starting to be introduced and this can clearly simplify the bureaucracy and foster the market potential, ensuring the law base for the entrance in the market of new actors, like aggregators (79); however, this should not only be an effort of single states but an endeavour of over-national entities, e.g. EU, in order to guarantee uniformity and homogeneity in the market, which is fundamental for the development of flexibility in buildings. The drivers and the barriers are summarized in the strengths, weaknesses, opportunities, and threats (SWOT) analysis of Table 3.

Table 3: SWOT analysis

Strength	Weaknesses
• Possible monetary savings • Decongestion of the energy grid • Better exploitation of variable renewable sources • Incomes for party working as aggregator	• Lack of uniform technical standard for the adoption of EF • Lack of common terminology and quantification methodologies • Possible rebound effect (85) • User's acceptance
Opportunities	**Threats**
• Favourable legislation (e.g. Flanders in Belgium, Netherlands) • Creation of the IEA EBC Annex 67: Energy Flexible Buildings	• Difficult adaptation to novel approaches for designers • Contrasting interests of the stakeholders • Unclear business cases and return on investment • Slow business sector

3.3. User's Acceptance

As previously mentioned in Section 3.1, user's acceptance is of key importance for the implementation of flexibility. An interesting insight on this aspect is given by the work of Rongling Li et al. (86) who conducted a large-scale survey in the Netherlands.

From the results of the survey, certain arbitrary criteria were decided in order to estimate the number

of potential flexible building users. These individuals are:

- willing to postpone the start time of half or more of their appliances;
- willing to use half or more of the smart technologies listed in the questionnaire;
- willing to turn off their heating or air-conditioning;
- willing to reduce the heating temperature setting.

Based on these assumptions, 11% of the respondents were identified as possible flexible building users, but, taking into account that more than 60% of the interviewees were unaware of the smart grid concept, this corresponds to 28% of the respondents who are aware of smart grid. The awareness of smart grid concept was the highest among people between 20 and 29 years old, and the smart appliances respondents were more willing to use were dishwasher and fridge/refrigerator.

Another interesting finding is that the majority of the answerers were eager to change their energy use behaviour, including switching off their heating or cooling system for a short time, diminishing the room temperature set-point for the heating system, or postponing the start time of electrical appliances, and that there is a correlation between the willingness of adopting smart appliances and the availability of changing the energy use behaviour in the respondents. The major motivating factors to adopt flexibility measures were found to be decreased energy bills, financial incentive from the energy supplier, and seeing the effects of energy use actions. Regarding the type of control strategy, most of the respondents accepted one of the four control options:

- grid remote control,
- home automatic control,
- manual control,
- try manual control first and later switch to grid remote control or home automatic control

This shows that users should be offered different types of control strategies, less or more intrusive, in order to match their desires and needs.

It can be said that it is necessary to increase awareness on smart grid in the population, especially in the older part, and that adoption of flexibility strategies can be increased using financial incentives, directed in particular to customers with medium level energy expenses that appeared as the most prone to reducing the energy bills.

3.4. Business Models

In the report of the Smart Energy Demand Coalition "Explicit Demand Response in Europe - Mapping the Market 2017" (87), the market aperture for active demand response is assessed in Europe and it is graphically presented in Figure 7, where it can be seen that Spain is considered as a closed

market. Indeed, this type of demand-side management is not legal in Spain; however, it is the first country in the world where the default price for residential buildings is based on the spot market hourly price, offering possibility of implicit demand-side flexibility, since all consumers are able to take advantage of ToU contracts. There is one programme for explicit demand-side flexibility, the Interruptible Load programme reserved for large consumers (>5 MW without possibility of aggregation), and it is controlled by the TSO, Red Eléctrica de España, even if it was not active in the last years. There are rumours, however, that the TSO and the relevant stakeholders have been talking about the introduction of explicit demand-side flexibility strategies for other typologies of customers as well (87).

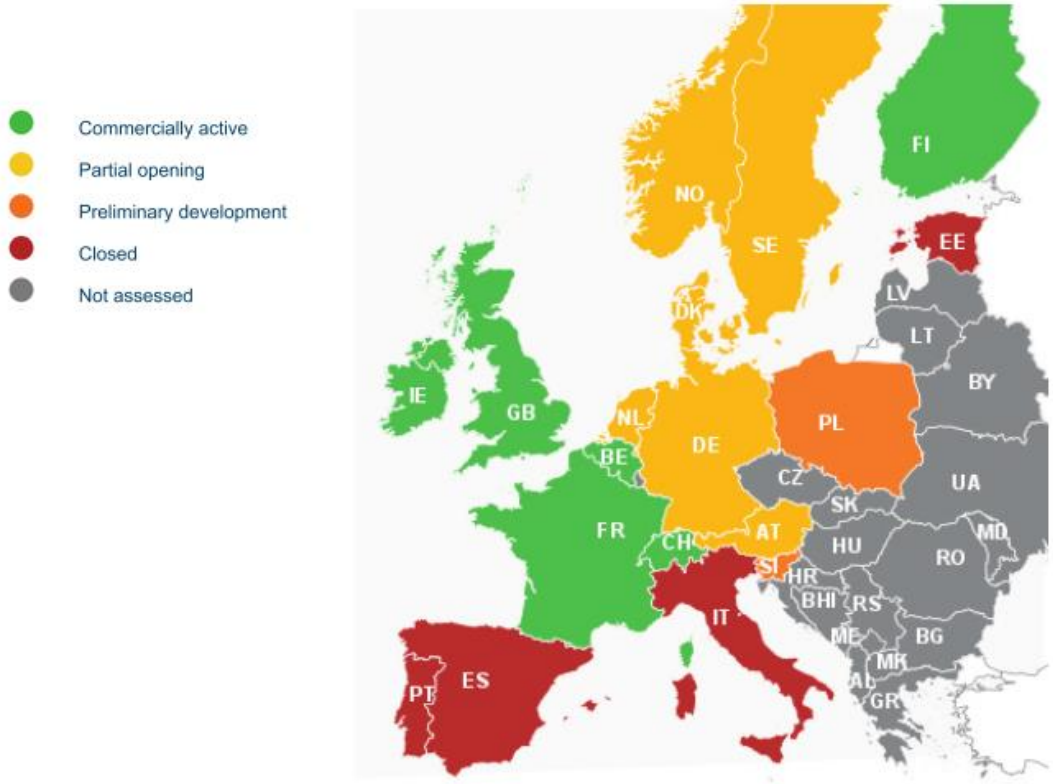

Figure 7: market aperture for active demand response (87)

Regardless of the current closed situation in Spain, it is useful to describe the possible business models in the market of residential buildings flexibility. Considering that the available flexibility of an individual users is small, a new role in the energy grid is needed to exploit the overall potential (78). The new actor is called **aggregator** and it is defined as (39):

> an entity that has entered into an agreement with an electricity customer on access to disposing of the electricity customer's flexible consumption and/or generation in the electricity market. The aggregator pools flexibility from customers and converts it into electricity market services, for example for use by the TSO, DSO and/or BRP. The aggregator can help to stabilise the electricity system and minimise the risk of power failures at times when the energy system is under pressure.

It operates between the suppliers, prosumers, and the utilizers, such as TSOs, DSOs or BRPs, of flexibility, as can be seen in Figure 8, merging many small flexibility resources into a useful flexibility volume. Many complexities are introduced, such as the difficulty in differentiating between implicit and explicit flexibility or in measuring and validating the activation of flexible resources, by the addition of the aggregator, which can be an existing actor or a new player.

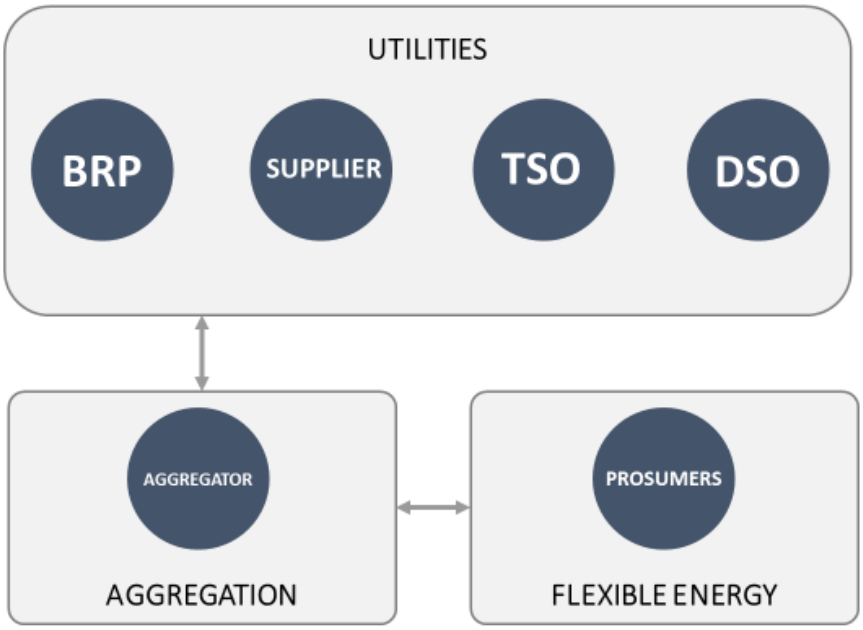

Figure 8: general scheme of the flexibility market (39)

There are multiple business models available for the integration of the aggregator in the existing market (refer to Table 4) that vary on the functions and roles that the aggregator does and occupies:

- in **model 0**, the aggregator role is occupied by an existing player of the electricity market, like a supplier or a balance responsible party;
- in **model 1**, the aggregator is an independent entity and performs frequency control on the grid using the flexible energy of the prosumers;
- in **model 2**, the aggregator works with its own BRP to deliver flexibility;
- in **model 3,** the aggregator along with its own BRP delivers flexibility and energy, being a supplier as well.

The aggregator needs an BRP to deliver flexibility or energy for the following reasons (78):

- If it fails to deliver the required amount of flexibility to his customer, his failure might cause imbalance in the grid, and, as a consequence, must compensate for this disequilibrium with the help of the BRP.
- If it wants to trade energy in the market.

Table 4: business model comparison

Name	Aggregator is independent?	Aggregator deals with:	Entry cost	Challenges
Model 0	No	Frequency control and/or flexibility and/or supply	Medium	Cost of bilateral agreement
Model 1	Yes	Frequency control	Low	Market rules
Model 2	Yes	Flexibility	Low	Market rules Verification of EF
Model 3	Yes	Flexibility and supply	High	Market rules Verification of EF Cost of meters

3.5. Conclusion

The different actors that are involved in energy flexibility in buildings are summarized in Figure 9. Among the different stakeholders, it is important to obtain the acceptance of the users, that are also known as building occupants or consumers/prosumers. The literature shows that 11% of the population can be considered a potential flexible building user, but this value rises to almost 1 out of 3 people when the part of the population that is aware of smart grids is considered. As a consequence, this willing group of people represents the most promising customer sector and it should be addressed for preliminary implementation of flexibility measures.

Moreover, an over-national effort should be made to introduce harmonized legislations that will help the market growth and provide a clear law base, useful for the entrance of new actors, such as aggregators, in the market. This entity is important since the flexibility of a single user is of modest quantity and, thus, not so interesting for the market. This creates the need of customer aggregation to achieve an amount of flexible energy that is relevant for grid stabilization purposes. Four major business models are identified, and they differ from each other as the aggregator can be an existing or a new entity, independent or dependent, and can deliver different grid services, such as frequency control and/or flexibility and/or energy supply.

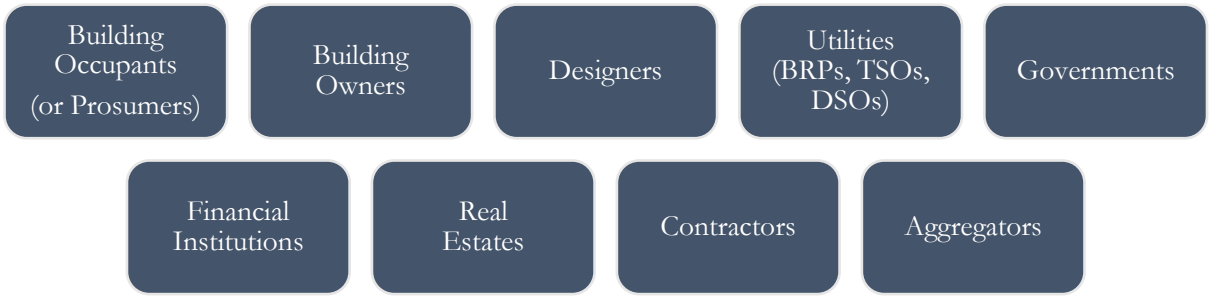

Figure 9: visual summary of the key stakeholders of energy flexibility

4. Methodology

In this section, the methodology of the work performed during the project is presented. The study case is detailed, focusing on the characteristics of the TRNSYS model of the building, then the chosen performance indicators are described, and, in conclusion, the different scenarios are presented.

4.1. Study Case

The dwelling is located in Terrassa (41.570° N, 2.013° E), close to Barcelona, in the region of Catalonia, Spain, and, therefore, it is located in the Mediterranean region as can be seen in Figure 10 (88). According to long-term climate data, the maximum daily average temperature is 31°C experienced in July whereas the minimum daily average temperature is 3°C during the months of December, January, and February (89), as shown in Figure 11.

Figure 10: aerial view of the Iberic peninsula with Terrassa circled in green (88)

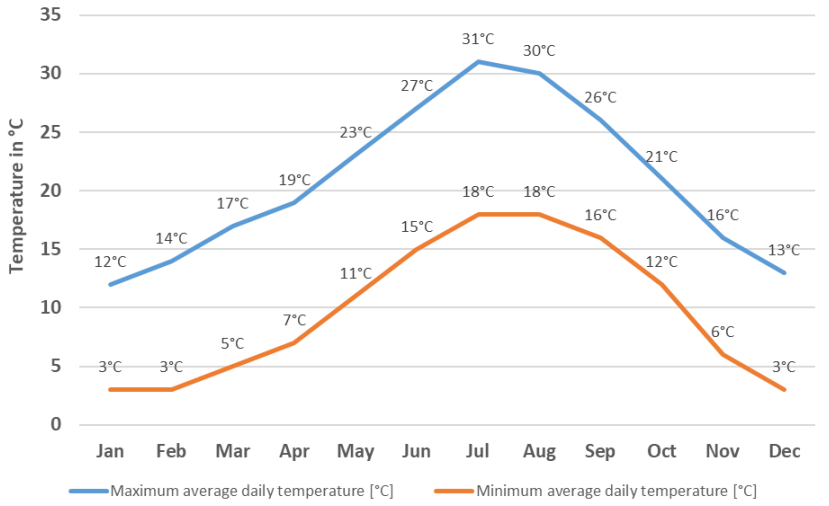

Figure 11: maximum and minimum average daily temperature per month for Terrassa (89)

The building is representative of a multi-storey building typology of the period from 1991 to 2007 (90), which is built under the Catalan building regulation NRE-AT-87 (91). The building typology was analysed previously (92) from the point of view of the energy efficiency renovation, considering the thermal comfort, the energy savings, and the economic evaluation. More details model hypothesis are described in (93, 94). As can be seen in Figure 12, the dwelling has two external façades, north-oriented and west-oriented, and it is located on the first floor of a multi-storey building. A family composed by two adults and two children lives in the apartment and its occupation profile has been adapted according to the habits of the family during a typical week, dividing the dwelling into day zone and night zone. The building is modelled in TRNSYS, and was previously presented in (94), and its main characteristics are summarized in Table 5.

Figure 12: 3D division of the building and picture of the outside

Table 5: main characteristics of the building

Parameter	Value	Unit
Location	Spain	-
Building date	1991 – 2007	-
Floor area	108.5	m^2
Window area	19.6	m^2
Protected volume	263.6	m^3
***U-value* of the walls**	0.6	W/m^2K
***U-value* of the windows**	2.5 to 5.7	W/m^2K
***g-value* of the windows**	0.5 to 0.76	W/m^2K
Infiltration n_{50}	3	1/h
Hot and cold water production	Reversible air-to-water heat pump Heating: 4.30 kW with a COP of 3.00 Cooling: 1.64 kW with a COP of 3.80	-
SC and SC emitter	Fan Coil	-
DHW storage	250 litres tank at 60°C	-

4.1.1. DHW System

The domestic hot water is stored in a 250 L tank. The water is withdrawn according to the standard tapping programme M (95) and the demand for DHW has priority over the need of SH or SC. The temperature in the tank is kept at 60°C and it is controlled by a thermostat with a downward asymmetric dead band of 5°C, that activates the HP when the tank temperature reaches the threshold, in order to keep the temperature stable, because it is advised not to have a temperature lower than 50°C due to the possibility of spread of the bacteria Legionella, which is really harmful for the health of the dwellers (96).

4.1.2. Space Heating and Cooling Emitter System

The emitter system is modelled with single fixed speed Fan Coil (FC) units capable of working in both heating and cooling mode. The units are placed in the major rooms of the dwelling (bathroom, toilet, bedrooms, living room, and kitchen), and their operation, therefore the SH and SC demand, is controlled by a central thermostat with an asymmetric dead band of 2°C placed in the living room. The heating and cooling set-point during occupation periods are shown in Table 6. A night set-back of the set-point is introduced to adapt to the habit of the dwellers and their different metabolic rate and activity level.

Table 6: space heating and cooling set-point

Parameter	Day (07:00 – 21:00)	Night (21:00 – 07:00) and non-occupancy periods
Space heating set-point	20.0°C	18.0°C
Space cooling set-point	25.5°C	27.0°C

4.1.3. Hot and Cold Water Production System: Reversible Air-to-Water HP

4.1.3.1. Case with Fixed Capacity Heat Pump

In this scenario, the heat pump, modelled in TRNSYS with Type 941, is a fixed capacity heat pump (FCHP) and, only has two operating modes, on at full load or off, and is controlled with a two-level control system. The first level is the DHW aquastat or zone temperature thermostat that activates the HP when there is need of DHW, SH, or SC, but a second control is necessary to control the HP supply water. Therefore, when the first level control is on, the HP is turning on and off in order to respect the limit on the temperature at its outlet. This on-off behaviour, necessary to respect the desired set-points (on the zone temperature and the water supply temperature), creates inefficiencies due to the parasitic losses related to cycling and it mines the overall performance by increasing the total electricity consumption (97–99). This on-off condition is taken into account with a coefficient that reduces the efficiency due to the frequent start-up and/or long stand-by periods (97, 98, 100–103).

The actual value of the COP is obtained using the equation given in Fuentes et al. (98), which is similar

to the correlation presented in the standard EN14825 for air-to-water heat pumps (103), but it is more conservative since it considers not only stand-by losses but also start-up losses:

$$PLF = \frac{1}{1+\frac{C_d(1-PLR)}{1-C_d(1-PLR)}+(1-C_c)\frac{1-PLR}{PLR}} \quad (4.41)$$

where:

- PLF is the part load factor, defined as the ratio between the COP at part load and the steady state COP at equivalent full load operating conditions;
- PLR is the part load ratio, defined as the ratio between the building thermal load and the capacity of the heat pump at full load;
- C_d is the degradation coefficient due to start-up losses;
- C_c is the degradation coefficient of the heat pump due to stand-by losses.

The supply water set-points are 60 °C for DHW and 40°C for SH, with an upward asymmetric dead band of 2.5 °C, and 15°C for SC with a downward asymmetric dead band of 2.5 °C.

4.1.3.2. Case with Variable Speed Heat Pump

In this scenario, the heat pump model is adapted from Type 941, because this type works with an on-off operation mode, and, therefore, it does not reflect the real operation of a variable speed heat pump (VSHP), which is capable of modulating the frequency of the compressor and, thus, changing the delivered capacity according to the needs of the building.

VSHP performance estimation

The reversible air-to-water heat pump, whose data is available, is HITACHI Yutaki S Combi RAS-4WHVNPE (outdoor unit) RWD-4.0NWE (indoor unit with tank). In heating standard conditions (outlet water temperature of 35°C and outdoor air temperature of 7°C) the COP is 5.00 and the heating capacity is 11.00 kW, whereas in cooling standard conditions (outlet water temperature of 7°C and outdoor air temperature of 35°C) the COP is 3.30 and the cooling capacity is 7.20 kW. Data regarding the performance of the heat pump are available in the manufacturer catalogue presented in Table A2.20, Table A2.21, Table A2.22 and Table A2.23 (104) of Appendix 2: Heat Pump Performance Data.

This heat pump is, however, oversized for the heating and cooling need of the dwelling, and in TRNSYS the model is scaled to a smaller size, since normalized full load and part load performance map are developed. The rated parameters are 4.30 kW of heating capacity with a COP of 3.00 and 1.64 kW of cooling capacity with a COP of 3.80, which are retrieved from a smaller HITACHI heat pump (104).

However, the part load performance data given by the manufacturer are not sufficient to create a

complete part load performance map, and, therefore, it is assumed a linear relationship between the available data at different operating conditions in order to build a complete performance map. The available (in orange) and estimated part load data for COP is presented in Table 7 for easier understanding of the estimation procedure. All the tables are available in Appendix 2: Heat Pump Performance Data.

The steps to obtain the missing part load operating points are:

1. available part load performance data is collected (heating capacity, COP);
2. missing values along rows (fixed water outlet temperature and variable outdoor air temperature) of the performance table are estimated;
3. missing values along the columns (fixed outdoor air temperature and variable water outlet temperature) of the performance table are estimated.

Table 7: coefficient of performance at part load (in brackets the PLR of the different points)

Manufacturer and estimated part load data						
COP at part load [-]		**Ambient temperature [°C]**				
		-7	**-2**	**2**	**7**	**12**
Water outlet temperature [°C]	**60**	1.57 (1.23)	2.47 (0.95)	3.20 (0.73)	4.55 (0.41)	5.65 (0.35)
	55	1.80 (0.89)	2.80 (0.68)	3.60 (0.50)	4.80 (0.26)	5.80 (0.25)
	50	2.04 (0.90)	3.13 (0.69)	4.00 (0.49)	5.05 (0.26)	5.95 (0.24)
	45	2.27 (0.91)	3.45 (0.67)	4.40 (0.48)	5.30 (0.26)	6.10 (0.24)
	40	2.51 (0.91)	3.78 (0.67)	4.80 (0.48)	5.55 (0.25)	6.25 (0.23)
	35	2.74 (0.90)	4.11 (0.63)	5.20 (0.46)	5.80 (0.25)	6.40 (0.23)
	30	2.98 (0.82)	4.43 (0.61)	5.60 (0.45)	6.05 (0.24)	6.55 (0.22)
	25	3.21 (0.78)	4.76 (0.58)	6.00 (0.45)	6.30 (0.24)	6.70 (0.22)
	20	3.45 (0.74)	5.09 (0.55)	6.40 (0.46)	6.55 (0.24)	6.85 (0.22)

The PLF-PLR curve is obtained by interpolating the available part load data until the minimum PLR of the heat pump, using a quadratic fit of data ($R^2 = 0.92$). For PLR values falling below the minimum percentage of continuous modulation, the on-off behaviour takes place, therefore Equation 4.41 is adapted and used. A graphical representation of the curve with a scatter of the part load points is presented in Figure 13 (left), where it can be seen that the data points confirm the typical increase of COP at part load for VSHP (100, 102) and that the decay of the COP shows that the HP shifts to on-off operation around 0.25 of the PLR, consistent with the information obtained from the manufacturer (104). The switch to on-off mode is represented by the decay of the part load factor as

can be seen in Figure 13 (left).

The PLF-PLR relation is calculated as follows:

$$\begin{cases} PLF = \dfrac{2.317}{1+\frac{C_d(1-PLR)}{1-C_d(1-PLR)}+(1-C_c)\frac{1-PLR}{PLR}} & PLR < 0.25 \\ PLF = 1.6458 \times PLF^2 - 3.5876 \times PLF + 2.9315 & PLR \geq 0.25 \end{cases} \quad (4.42)$$

Since part load data for cooling operation are not available, it is assumed that the PLF-PLR curve is valid also for cooling mode. Reference (53) presents the part load curve of a variable speed heat pump for both heating and cooling operation, and the average absolute difference of the PLF between the two curves at same PLR is less than 0.09, therefore the previous hypothesis is considered feasible.

A note of caution is due here since the part load curve highly influences the final results, and, being a hypothetical relation not based on experimental data, might differ from the real part load curve of the heat pump. Nevertheless, a similar approach of part load performance estimation was used in (105). Moreover, the estimated performance curve of the VSHP was compared to the performance curves of 8 air-to-water VSHP retrieved from the database of the Swedish Energy Agency (106). The analysed heat pumps have a similar quadratic trend for the COP at part load and, therefore, the estimated curve was considered to be reliable, as can be seen in Figure 13 (right). In addition, in (107) and (108) a part load curve of an air-conditioning system reached values of PLF around 2.0 before dropping, similarly to the current study.

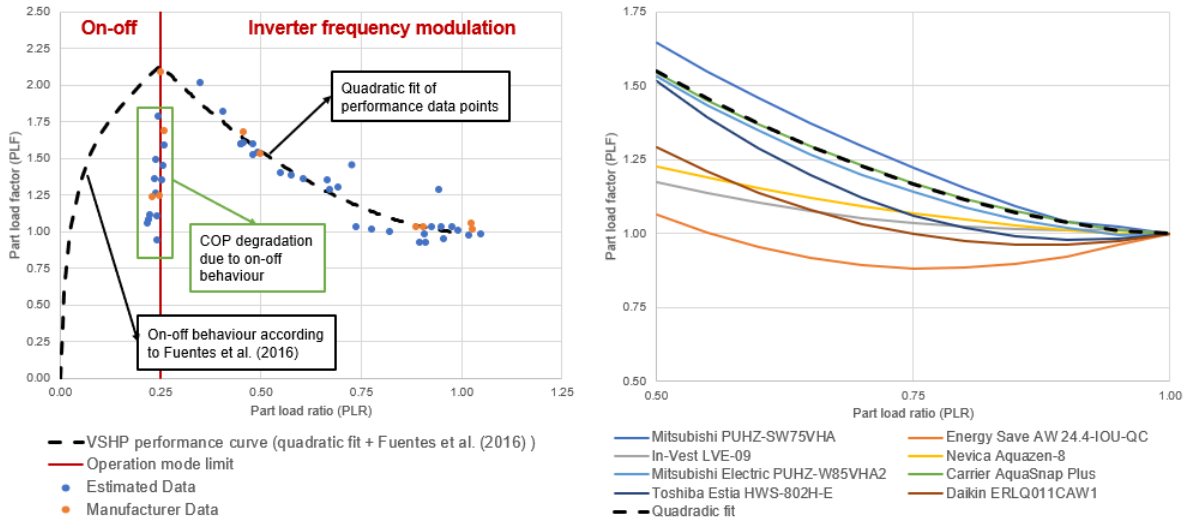

Figure 13: part load performance of the VSHP (left) and comparison of the estimated part load curve with literature (right) (106)

VSHP implementation in TRNSYS

A variable speed heat pump (VSHP) was modelled during this master's thesis project by combining Type 941 and Type 43 which uses the data presented in the previous section to calculate the coefficient of performance at part load COP_{PL}. Additional equations are added in order to recalculate the outputs

of the heat pump, along with Type 23, a PID[1] (proportional-integral-differential) controller on the supply water temperature of the heat pump (104, 109). Figure 14 shows the combination of the different TRNSYS types and equations.

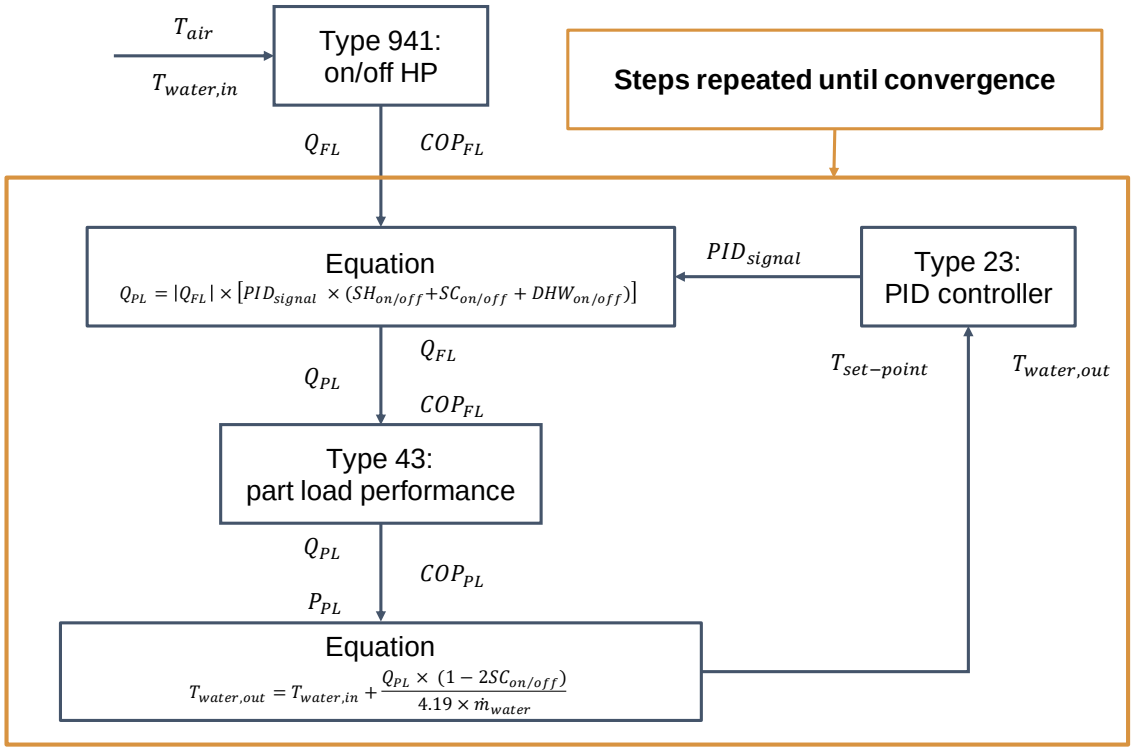

Figure 14: flowchart of the part load performance calculation methodology

This controller works when there is demand for space heating or cooling with a water set-point of 40°C and 15°C, respectively, and of 62.5°C for domestic hot water. The output control signal, representing the part load ratio of the heat pump, is limited between 0.25 and 1.00, with the lower limit being the minimum part load operation of the heat pump from manufacturer (104).

The control signal is calculated as (110):

$$PID_{signal}(t) = K\left[e(t) + \frac{1}{T_i}\int_0^t e(t)\,dt + T_d\frac{de(t)}{dt}\right] \tag{4.43}$$

where $Ke(t)$ represents the proportional term, $K\,(1/T_i)\int_0^t e(t)\,dt$ is the integral term, while $K\,T_d\frac{de(t)}{dt}$ is the derivative term. The value of the gain constant K, of the integral time T_i, and of derivative time T_d requires accurate tuning in order to achieve an accurate performance. The final values are presented in Table 8.

[1] A PID controller calculates the error value $e(t)$ at every time step as the difference between a desired set-point and a controlled variable and applies a correction based on proportional, integral, and derivative terms, from which derives the name of the controller, PID.

Table 8: PID controller parameters

Parameter	SH	SC	DHW
Gain constant K	0.0275	0.0275	0.0500
Integral time T_i	0.1250	0.1250	0.1250
Derivative time T_d	0.0000	0.0000	0.0000

The behaviour of control system is graphically presented in Figure 14 and it follows these steps repeated every iteration until the convergence of the TRNSYS calculations:

1. Type 941 receives as input the outdoor air temperature T_{air} in °C and the inlet temperature of the water $T_{water,return}$ in °C and calculates the full load capacity Q_{FL} in kJ/h and coefficient of performance COP_{FL} at the current operating conditions.
2. Type 23 calculates the PID control signal, equivalent to the PLR, according to Equation 2.2 where the error is $e(t) = T_{set-point} - T_{water,supply}$.
3. The first output of Type 941 along with the control signal PID_{signal} generated by the PID are used to calculate the part load capacity $Q_{PL} = |Q_{FL}| \times [PID_{signal} \times (SH_{on/off} + SC_{on/off} + DHW_{on/off})]$ in kJ/h where $SH_{on/off}$, $SC_{on/off}$, and $DHW_{on/off}$ are binary variables that are equal to 1 when there is demand of space heating, space cooling, and DHW, respectively (only one binary variable can be equal to 1 at the same time).
4. Q_{PL}, $|Q_{FL}|$, and COP_{FL} are the inputs of the part load performance Type 43 that calculates the power input at part load P_{PL} in kJ/h and the coefficient of performance COP_{PL}.
5. The outlet water temperature is then calculated with $T_{water,out} = T_{water,in} + \frac{Q_{PL} \times (1 - 2SC_{on/off})}{4.19 \times \dot{m}_{water}}$ where $\dot{m}_{water}$ is the mass flow rate of water in kg/h. The term $(1 - 2SC_{on/off})$ makes the fraction negative in case of cooling.

It is necessary to use the absolute value of Q_{FL} as input of Type 43, because it does not work with negative values (the minimum allowed value of the inputs is 0). The value of Q_{PL} is always positive (refer to the equation).

A VSHP modulates the frequency of the compressor, therefore, the PID control signal should be the required frequency (or in other terms the ratio between the desired frequency and the maximum frequency). However, in the control system explained above the control signal represents the ratio of the desired capacity and the maximum capacity of the heat pump. This simplification is justified because the equality of the frequency ratio and the capacity ratio was proved with an extensive part load testing of air-to-water heat pumps by the Swedish Energy Agency (106). The average difference between the two values was lower than 1%, and, therefore, considered negligible. Furthermore, in the control of a real heat pump, the frequency cannot be directly controlled, and, other signals need to be

sent, e.g. capacity ratio, temperature set-point, etc.

4.2. Key Performance Indicators

In this section the selected performance indicators are presented. In the following equations, T is the total simulation time, while $l_{HP}(t)$ indicates the electrical consumption of the heat pump.

4.2.1. Thermal Demand

The thermal demand of the building in kWh is defined as:

$$Q_{HP} = \int_0^T q_{HP}(t)dt \tag{4.44}$$

where $q_{HP}(t)$ represents the thermal power delivered by the heat pump in kW.

4.2.2. Electricity Consumption

The electricity consumption of the heat pump in kWh is defined as:

$$E_{HP} = \int_0^T l_{HP}(t)dt \tag{4.45}$$

where $l_{HP}(t)$ represents the electrical power consumption of the heat pump in kW.

4.2.3. Electricity Cost

It is interesting to study the electricity cost, because Spain offers an hourly varying price for residential customers (87); otherwise it would have been proportional to the electricity consumption if the price had been fixed.

The electricity cost is calculated using the Voluntary Price for the Small Consumer (PVPC, in its Spanish acronym) available on the website of the Red Electrica de Espana (111). The two-period hourly price with a high daily variation was used due to its better applicability for flexibility purposes. The cost in EUR is calculated with the following equation:

$$C_{EL} = \int_0^T p_{EL}(t) l_{HP}(t)dt \tag{4.46}$$

where $p_{EL}(t)$ is the hourly price of electricity in EUR/kWh.

4.2.4. CO_2 Emission

The CO_2 emission in g is calculated with the following equation:

$$P_{CO_2} = \int_0^T e_{CO_2}(t) l_{HP}(t)dt \tag{4.47}$$

where $p_{CO_2}(t)$ is the average hourly CO_2 emission factor in g/kWh of the electrical grid, considering the electricity mix and the CO_2 emissions of every kind of technology.

4.2.5. Average Part Load Ratio and Average Part Load Factor

The average part load ratio and the average part load factor are defined as for the VSHP:

$$\overline{PLR}_{VSHP} = \frac{\int_0^{T_{ON}} PLR(t)dt}{T_{ON}} \tag{4.48}$$

$$\overline{PLF}_{VSHP} = \frac{\int_0^{T_{ON}} PLF(t)dt}{T_{ON}} \tag{4.49}$$

while for the FCHP as:

$$\overline{PLR}_{FCHP} = \frac{Q_{HP}}{q_{RATED-FCHP} \times T_{ON}} \tag{4.50}$$

$$\overline{PLF}_{FCHP} = \frac{1}{1+\frac{C_d(1-\overline{PLR}_{FCHP})}{1-C_d(1-\overline{PLR}_{FCHP})}+(1-C_c)\frac{1-\overline{PLR}_{FCHP}}{\overline{PLR}_{FCHP}}} \tag{4.51}$$

where T_{ON} is the period of time in h when the HP is on and $q_{RATED-FCHP}$ is the rated thermal capacity of the FCHP in kW. The denominator represents the energy that the heat pump would have used if it was working at full load during the same amount of time (when the zone thermostat is on).

The difference in the definition is due to the fact that the FCHP is not actually able to operate at part load and, as a consequence, the losses related to repeated on-off cycling are added after the simulation using Equation 4.51. As a result, the PLR of a FCHP is an indicator of the losses related to repeated on-off cycling and stand-by.

4.2.6. Price Flexibility Factor

The price flexibility factor is defined in Section 2.2.1.1 as (10) [26]:

$$FF_E = \frac{\int_{LPT} l_{HP}(t)dt - \int_{HPT} l_{HP}(t)dt}{\int_{LPT} l_{HP}(t)dt + \int_{HPT} l_{HP}(t)dt} \tag{4.52}$$

where the two integrals represent the electricity demand in kWh during low price and high price time, respectively, defined using the 30th and 70th percentiles as thresholds.

4.2.7. CO_2 Flexibility Factor

The CO_2 flexibility factor is defined as:

$$FF_{CO_2} = \frac{\int_{LET} l_{HP}(t)dt - \int_{HET} l_{HP}(t)dt}{\int_{LET} l_{HP}(t)dt + \int_{HET} l_{HP}(t)dt} \tag{4.53}$$

where the two integrals represent the electricity consumption in kWh during low emission and high emission time, respectively, defined using the 30th and 70th percentiles as thresholds.

4.2.8. Percentage Outside the Range

This indicator is defined as the percentage of time when the operative temperature or the PMV are outside the specified comfort range during occupancy hours. The comfort ranges of the operative

temperature considered are developed by Péan et al. (55) and differ from the normative (e.g. EN 15251 for Residential) since two different temperature bands are defined for day and night zone in accordance with the different occupants activity level and clothing insulation between day and night. These ranges are used because (55) showed that offer a better estimation of the discomfort level, in case of night set-back of the set-point. For the heating season ranges, the following values are assumed: 1.2 met, 1 clo, 0.1 m/s for the day range and 0.8 met, 2.5 clo, 0.1 m/s for the night range; while for the cooling season ranges, 1.2 met, 0.5 clo, 0.1 m/s for the day range and 0.8 met, 1.0 clo, 0.1 m/s for the night range. The ranges are presented in Table 9 for the heating season and in Table 10 for the cooling season.

Table 9: Operative temperature ranges for different comfort categories for heating season

Category	Day zone range [°C]	Night zone range [°C]
I	20.60 – 22.50	19.30 – 21.30
II	19.20 – 23.80	17.80 – 22.70
III	18.30 – 24.70	16.80 – 23.70
IV	< 18.30 and > 24.70	< 16.80 and > 23.70

Table 10: Operative temperature ranges for different comfort categories for cooling season

Category	Day zone range [°C]	Night zone range [°C]
I	24.00 – 25.40	25.60 – 26.70
II	23.00 – 26.40	24.80 – 27.60
III	22.30 – 27.10	24.20 – 28.10
IV	< 22.30 and > 27.10	< 24.20 and > 28.10

4.2.9. Long-term Percentage of Dissatisfied

This long-term index summarizes the overheating and the overcooling of the building, and depending on the calculation period (annual, warm or cold season), stresses the strong and the weak points of the dwelling. It is a general indicator because it is normalised over the calculation period, the analysed zones of the building and the number of occupants (113). It is a function of a short-term index; in this case the PPD (predicted percentage of dissatisfied) defined by Fanger is used. It is defined as:

$$LPD = \frac{\sum_{t=1}^{T} \sum_{z=1}^{Z} (p_{z,t} PPD_{z,t} h_t)}{\sum_{t=1}^{T} \sum_{z=1}^{Z} (p_{z,t} h_t)} \tag{4.54}$$

where t is the counter of simulation time step, z is the counter of the building zone, Z is the total number of zones analysed in the building, $p_{z,t}$ is the number of occupants of zone z at time t, h_t is the duration of the time step. Thermal comfort is achieved when the long-term percentage of dissatisfied is lower than 20% (114).

4.3. Model Predictive Control Strategies

MPC is based on a simplified model of the building that is used to predict the future performance of the system, and, for this purpose, the building envelope is modelled using a second-order RC (resistance-capacity) grey-box model (refer to Figure 15). Two-state models were already proved to be sufficient for the purpose of this analysis in the literature (115).

The parameters of this simplified model are estimated with datasets created using the more detailed TRNSYS model, previously presented (94), in combination with a Pseudo-Random Binary Signal (PRBS) that controls the space heating and cooling operation of the HP (116). The PRBS is a binary sequence that is used to excite the building with different frequencies in order to simplify the identification of the model.

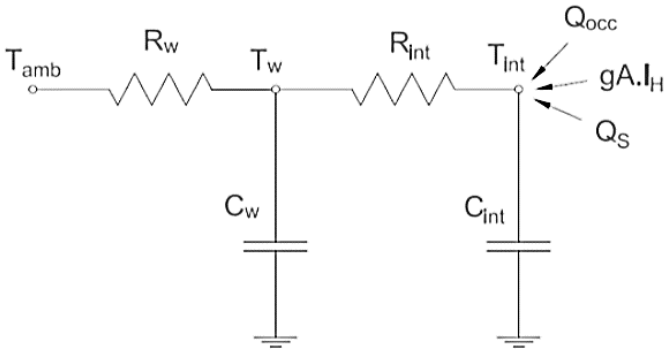

Figure 15: scheme of the second order RC grey-box model

The node temperatures of the simplified model are governed by the following set of ordinary differential equations:

$$C_{INT} \times \dot{T}_{INT} = \frac{1}{R_{INT}}(T_W - T_{INT}) + gA \times I_H + Q_S + Q_{OCC} \tag{4.55}$$

$$C_W \times \dot{T}_W = \frac{1}{R_{INT}}(T_{INT} - T_W) + \frac{1}{R_W}(T_A - T_W) \tag{4.56}$$

whose variables are explained below.

The outputs of the model are:

- $T_{INT} \in \mathbb{R}$ [°C], the indoor operative temperature, that corresponds to the average operative temperature of the different zones of the building; this variable is constrained by the thermal comfort range $[\underline{T_{INT}}; \overline{T_{INT}}]$ varying depending on the time of the day and on the season of the year;
- $T_W \in \mathbb{R}$ [°C], an intermediate temperature, that represents the average internal surface temperature of the external walls of the dwelling.

The external inputs (or disturbances) of the model are:

- $Q_S \in \mathbb{R}$ [kW] the delivered thermal power by the heat pump (positive in case of heating and negative in case of cooling). This input is the variable controlled by the algorithm of the MPC in order to optimise the objective function, and it is constrained by operational limit of the heat pump $[\underline{Q_{HP}}; \overline{Q_{HP}}]$ which varies from space heating or cooling operation mode;
- $T_A \in \mathbb{R}$ [°C] the outdoor ambient temperature obtained from weather data of the chosen location;
- $I_H \in \mathbb{R}^+$ [kW/m^2] the ground horizontal solar irradiation obtained from weather data of the chosen location;
- $Q_{OCC} \in \mathbb{R}^+$ [kW] the heat gain within the envelope, mostly due by equipment and occupants.

The parameters to be estimated in the model are:

- C_{INT} and $C_W \in (\mathbb{R}^+)^2$ [kWh/K] the thermal capacities of the two states, that represents the thermal capacities of the building;
- R_{INT} and $R_W \in (\mathbb{R}^+)^2$ [kWh/K] the thermal resistance between the internal node and the wall node, and between the wall state and the outside state;
- $gA \in \mathbb{R}^+$ [m^2] the aperture area of the windows, which is proportion of solar irradiation passing through the glazing.

Moreover, it is necessary to model the Thermal Energy Storage (TES) system, composed of a tank of 250 L. The following state variable is introduced:

- $T_{TES} \in \mathbb{R}$ [°C], the temperature of the water inside the tank; as previously mentioned in Section 4.1.1, the minimum temperature for the TES temperature is 50°C for health reason, therefore the constraints on this variable are $[\underline{T_{TES}}; +\infty]$.

The governing equation of the tank temperature T_{TES} is:

$$C_{TES} \times \dot{T}_{TES} = Q_{TES} + \frac{1}{R_{TES}}(T_{INT} - T_{TES}) - Q_{DHW} \tag{4.57}$$

where:

- $Q_{TES} \in \mathbb{R}^+$ [kW], the thermal heating power delivered by the HP to the TES system. This variable is controlled by the algorithm of the MPC in order to optimise the objective function, and it is constrained by operational limit of the heat pump $[\underline{Q_{HP}}; \overline{Q_{HP}}]$;
- $Q_{DHW} \in \mathbb{R}^+$ [kW], the thermal power required by the occupants of the building for DHW and withdrawn according to the normative (refer to Section 4.1.1);
- $R_{TES} \in \mathbb{R}^+$ [K/kW] the thermal resistance of the tank insulation, which the resistance between the water in the TES and its surroundings;
- $C_{TES} \in \mathbb{R}^+$ [kWh/K] the thermal capacity of the water in the tank given by the product

between its mass and the specific heat of water.

The controlled variables are Q_S and Q_{TES}, the thermal power delivered by the heat pump for space heating or cooling, and domestic hot water, respectively, for sake of simplification; however, it is necessary to transform into temperatures since these variables need to be constrained, and it can be done by assuming linear relationships. The first equation is:

$$Q_S = \gamma \times (T_{SUP,S} - T_{INT}) \tag{4.58}$$

which represents the final emitter to the space. In the present case, FCU are used so that both heating and cooling operation are possible. A linear regression from data generated with a detailed FCU model in TRNSYS estimated γ to be equal to 0.23757851 kW/K as it can be seen in Figure 16. γ depends on the water and air flow rates on both sides of the FCU, and the efficiency of the heat exchange between the two heat carriers.

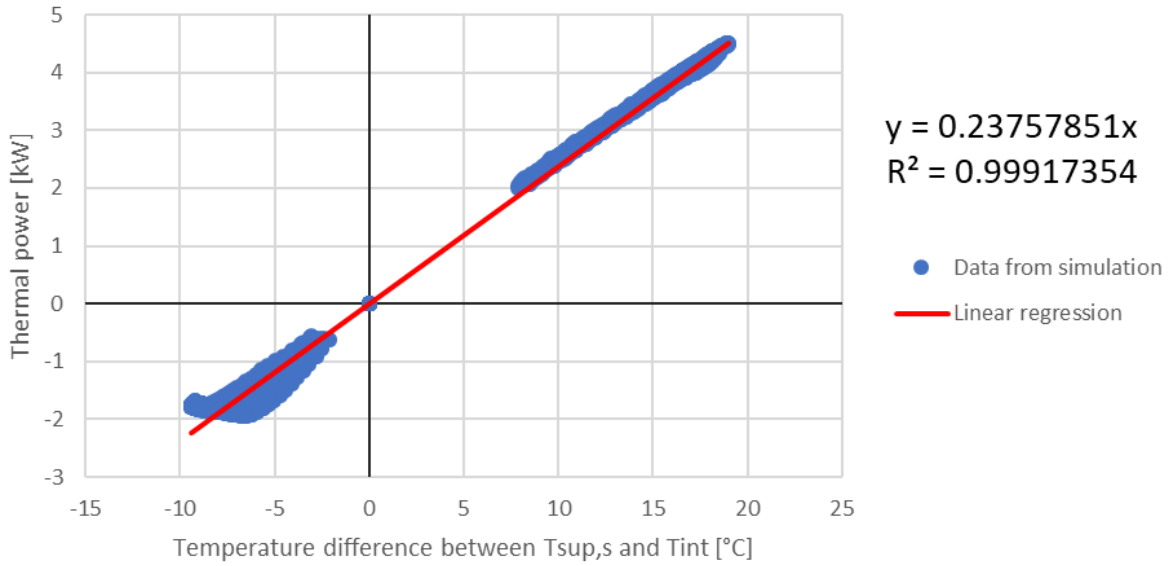

Figure 16: linear regression to estimate γ

The second equation is:

$$Q_{TES} = \beta \times (T_{SUP,TES} - T_{TES}) \tag{4.59}$$

representing the heat exchange from the heat pump circuit to the TES tank with $\beta = \dot{m}_W \times c_{P,W}$ where $\dot{m}_W$ is the water mass flow rate on the heat pump side in kg/s. β is equal to 0.896194444 kW/K considering that the water flow rate is 770 kg/h and the heat capacity of water is 4.19 kJ/kgK.

4.3.1. Reduced Model Identification

The process to find the parameters of the reduced model is composed of the following steps:

- the TRNSYS model of the building is adapted, removing the normal control system, in order to be able to excite the model with the PRBS;

- annual, winter, and summer simulations are performed in TRNSYS in order to create datasets with the useful inputs and outputs for different seasons;
- a MATLAB code based on the System Identification Toolbox (117) is used to estimate the parameters using the previously generated datasets choosing which parameters are fixed and which are free. The process is repeated until an optimum level of accuracy is achieved;
- the performance of the estimated models is then assessed using the datasets from which the parameters were not retrieved; in this case, it may be useful to re-estimate some parameters using the different dataset and check if the accuracy has improved.

In this master's thesis, the most accurate model (fit of 91.12%) is obtained from the dataset of the annual simulation, because models estimated from seasonal datasets did not reach an adequate level of accuracy over the entire year, even if they were slightly more accurate in the respective seasons in some cases. The estimated parameters of the reduced model are summarized in Table 11, while Figure 17 shows the performance of the reduced model (in blue) compared to the data originated in TRNSYS (in grey) and used to estimate the parameters.

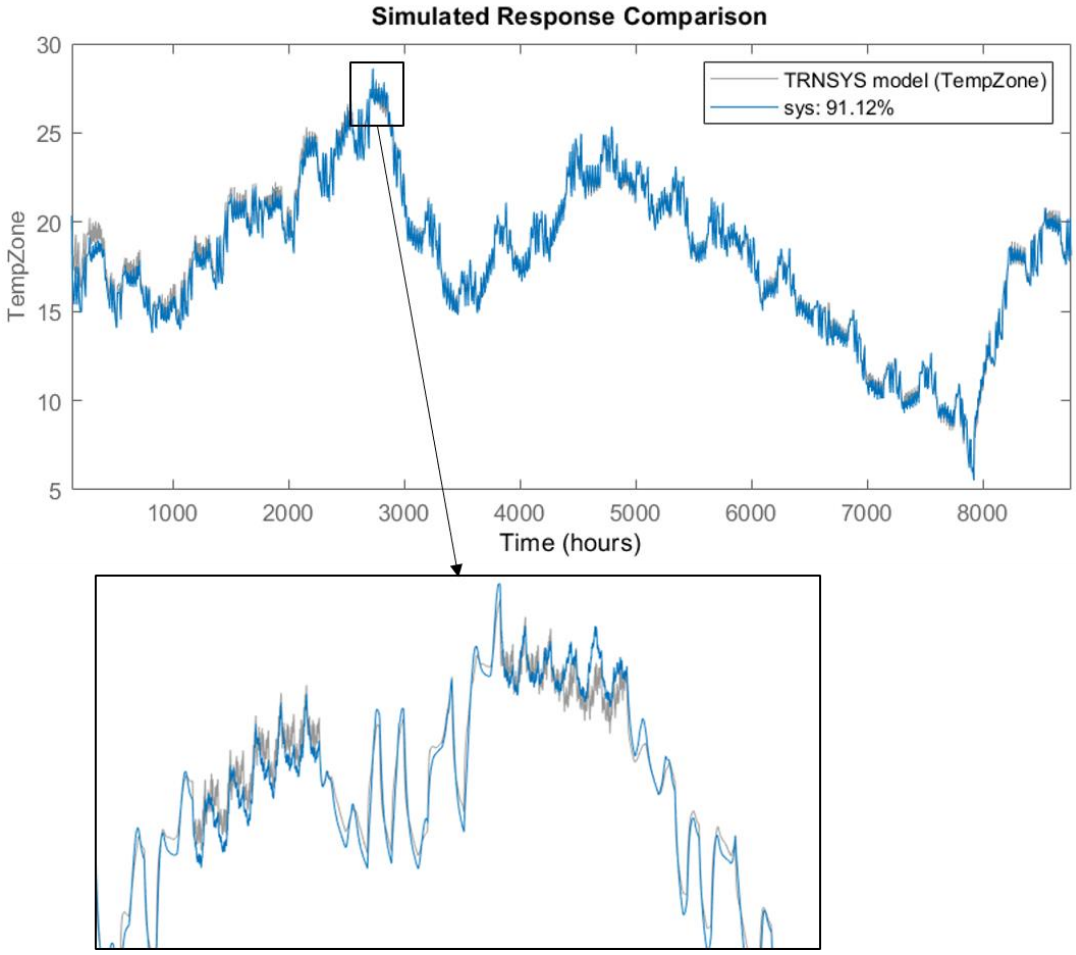

Figure 17: performance of the reduced model compared to the TRNSYS data along with a zoom snippet

Table 11: summary of the RC model parameters

Variable	Value	Unit
$\boldsymbol{C_{INT}}$	3.1329	kWh/K
$\boldsymbol{C_W}$	25.5372	kWh/K
$\boldsymbol{R_{INT}}$	1.0681	K/kW
$\boldsymbol{R_W}$	7.6499	K/kW
$\boldsymbol{gA}$	1.6646	m²
$\boldsymbol{\gamma}$	0.2376	kW/K
$\boldsymbol{\beta}$	0.8962	kW/K

4.3.2. State-Space Model Formulation

Equations (4.46) to (4.50) can be summarized into a generic state-space model:

$$\begin{cases} \dot{\boldsymbol{x}} = \boldsymbol{A}\boldsymbol{x} + \boldsymbol{B_C}\boldsymbol{u_C} + \boldsymbol{B_x}\boldsymbol{u_x} \\ \boldsymbol{y} = \boldsymbol{C}\boldsymbol{x} \end{cases} \tag{4.60}$$

In this formulation, the classic $\dot{\boldsymbol{x}} = \boldsymbol{A}\boldsymbol{x} + \boldsymbol{B}\boldsymbol{u}$ is modified by separating the input vector into the controlled variable vector $\boldsymbol{u_C}$ and the exogenous variables $\boldsymbol{u_X}$. The vectors are:

$$x = \begin{bmatrix} T_{INT} \\ T_W \\ T_{TES} \end{bmatrix} \qquad u_c = \begin{bmatrix} Q_S \\ Q_{TES} \end{bmatrix} \qquad u_x = \begin{bmatrix} T_A \\ I_H \\ Q_{OCC} \\ Q_{DHW} \end{bmatrix} \qquad \text{and} \qquad y = \begin{bmatrix} T_{INT} \\ T_{TES} \end{bmatrix};$$

while the matrices are:

$$A = \begin{bmatrix} -\frac{1}{R_{INT}C_{INT}} & \frac{1}{R_{INT}C_{INT}} & 0 \\ \frac{1}{R_{INT}C_W} & -\frac{1}{R_WC_W} - \frac{1}{R_{INT}C_W} & 0 \\ \frac{1}{R_{TES}C_{TES}} & 0 & -\frac{1}{R_{TES}C_{TES}} \end{bmatrix}, \qquad B_C = \begin{bmatrix} \frac{1}{C_{INT}} & 0 \\ 0 & 0 \\ 0 & \frac{1}{C_{TES}} \end{bmatrix},$$

$$B_X = \begin{bmatrix} 0 & \frac{gA}{C_{INT}} & \frac{1}{C_{INT}} & 0 \\ \frac{1}{R_WC_W} & 0 & 0 & 0 \\ 0 & 0 & 0 & -\frac{1}{C_{TES}} \end{bmatrix}, \qquad \text{and} \qquad C = \begin{bmatrix} 1 & 0 & 0 \\ 0 & 0 & 1 \end{bmatrix}.$$

The constraints of the model are relative to the thermal power delivered by the heat pump (Q_S or Q_{TES}), which is the controlled input of the model, constrained by the operation limit of the HP in heating and cooling mode. Moreover, there are limits on the outputs: the average temperature of the zones is limited due to the need of respecting the thermal comfort of the occupants and the temperature of the TES tank is constrained for health reason. The constraints are presented in Table 12.

Table 12: constraints of the state-space model parameters

Variable	Boundaries	Note
$\boldsymbol{Q_S}$	$\left[\underline{Q_{HP}}; \overline{Q_{HP}}\right] = [1.075\ \text{kW};\ 4.300\ \text{kW}]$	in space heating operation mode
	$\left[\underline{Q_{HP}}; \overline{Q_{HP}}\right] = [-1.640\ \text{kW};\ -0.410\ \text{kW}]$	in space cooling operation mode
$\boldsymbol{Q_{TES}}$	$\left[\underline{Q_{HP}}; \overline{Q_{HP}}\right] = [1.075\ \text{kW};\ 4.300\ \text{kW}]$	in DHW operation mode
$\boldsymbol{T_{INT}}$	$\left[\underline{T_{INT}}; \overline{T_{INT}}\right] = [20.0\ °\text{C};\ 24.0\ °\text{C}]$	in winter during the day
	$\left[\underline{T_{INT}}; \overline{T_{INT}}\right] = [18.0\ °\text{C};\ 24.0\ °\text{C}]$	in winter during the night and unoccupied periods
	$[\underline{T_{INT}}; \overline{T_{INT}}] = [23.0\ °\text{C};\ 26.4\ °\text{C}]$	in summer during the day
	$[\underline{T_{INT}}; \overline{T_{INT}}] = [24.8\ °\text{C};\ 27.0\ °\text{C}]$	in summer during the night and unoccupied periods
$\boldsymbol{T_{TES}}$	$[\underline{T_{TES}}; \overline{T_{TES}}] = [50\ °\text{C};\ +\infty]$	-

4.3.3. Optimal Control Problem Formulation

In order to consider that the space heating/cooling operation and DHW operation of the HP cannot be contemporaneous, two binary variables δ_S and δ_{TES} are introduced. In the TRNSYS model of the system, this aspect is modelled with a control system on the divergent valve that directs the output flow of the HP accordingly to the operation mode.

The OCP is described as follows:

$$\min_{u_C,\delta} J = \alpha_{OBJ} \times J_{\Delta u} + (1 - \alpha_{OBJ}) \times J_{OBJ} \tag{4.61}$$

so that $\forall k \in [\![1, N]\!]$:

the model is:

$$\begin{cases} \boldsymbol{x}(k+1) = \boldsymbol{A}\boldsymbol{x}(k) + \boldsymbol{B_C}\boldsymbol{u_C}(k) + \boldsymbol{B_x}\boldsymbol{u_x}(k) \\ \boldsymbol{y}(k+1) = \boldsymbol{C}\boldsymbol{x}(k) \end{cases} \tag{4.62}$$

the input constraints are:

$$\delta_S(k) \times \underline{Q_{HP}} \leq Q_S(k) \leq \delta_S(k) \times \overline{Q_{HP}} \tag{4.63}$$

$$\delta_{TES}(k) \times \underline{Q_{HP}} \leq Q_{TES}(k) \leq \delta_{TES}(k) \times \overline{Q_{HP}} \tag{4.64}$$

$$\delta_S(k) + \delta_{TES}(k) \leq 1 \tag{4.65}$$

the output constraints are:

$$\underline{T_{INT}} \leq T_{INT}(k) \leq \overline{T_{INT}} \tag{4.66}$$

$$\underline{T_{TES}} \leq T_{TES}(k) \tag{4.67}$$

The tool used to formulate the mixed integer linear programming OCP is MATLAB, with the help of Yalmip (118). The problem is solved with the Gurobi solver (119) using a discretization time step of $t_s = 12$ min and a time horizon is $N = 120$ time steps, corresponding to 24 hours, enabling to cover the daily patterns observed in both occupancy and weather.

4.3.4. Objective Function

Three main objectives are analysed in this master's thesis project: the minimization of the electricity consumption of the heat pump, the minimization of the HP electricity cost, and the minimization of the CO_2 emissions of the heat pump.

The HP performance, modelled by the COP, can be assumed to be quadratic function (62). However, in (120) it was shown that a linear approximation achieves a good accuracy as well for most of the HP operating range and this approach is adopted in this study. From the heat pump performance map, it can be estimated a linear model of the COP reciprocal $\frac{1}{COP} = \frac{P_{HP}}{Q_S+Q_{TES}}$, which is the quantity used in the objective function:

$$\frac{1}{COP} = \frac{P_{HP}}{Q_S+Q_{TES}} = \alpha_0 + \alpha_1 T_A + \alpha_2 T_{SUP} \tag{4.68}$$

where α_0, α_1, and α_2 are estimated from manufacturer full performance data and presented in Table 13.

Table 13: *1/COP* equation coefficients

Variable	Value	Unit
$\boldsymbol{\alpha_0}$	0.0259	-
$\boldsymbol{\alpha_1}$	0.0084	°C^{-1}
$\boldsymbol{\alpha_2}$	-0.0070	°C^{-1}

In this model, the COP only depends on the outdoor condition T_A and the level of supply temperature T_{SUP}. Moreover, the smoothing term of the HP operation $J_{\Delta u} = \sum_{k=2}^{N} \|\boldsymbol{u_C}(k) - \boldsymbol{u_C}(k-1)\|$ is introduced in the objective function in order to penalize power peaks and switch of operating mode, since it was proved to be an effective method in (47).

The mathematical formulation of the first objective is:

$$J_{EL} = \sum_{k=1}^{N} \frac{\|\boldsymbol{u_C}(k)\|}{COP(k)} = \sum_{k=1}^{N} \frac{Q_S+Q_{TES}}{COP(k)} = \sum_{k=1}^{N} P_{HP}(k) \tag{4.69}$$

Moreover, in order to take advantage of the variable electricity price present in Spain for flexibility purposes, the minimization of the cost is considered:

$$J_{EL} = \sum_{k=1}^{N} p_{EL}(k) \frac{\|\boldsymbol{u_C}(k)\|}{COP(k)} = \sum_{k=1}^{N} p_{EL}(k) \frac{Q_S+Q_{TES}}{COP(k)} = \sum_{k=1}^{N} p_{EL}(k) P_{HP}(k) \tag{4.70}$$

The third objective is the minimization of the CO_2 emission, and in this case two different triggers are

utilized: the percentage of grid electricity generation CO_2-free f_{CO_2} and the average grid emission factor of CO_2 per kWh of electricity consumed e_{CO_2}. The first variable is easily retrievable from the website of the Spanish TSO, Red Eléctrica de España, while the second needs to be calculated considering the generation of every energy source, available on the same website, and its respective CO_2 emission factor, which can be found in literature (121).

In the first case, the objective to be minimized is not strictly the CO_2 emission but the CO_2-emitting electricity consumption of the HP and it is defined as:

$$J_{CO_2-free} = \sum_{k=1}^{N}[1 - f_{CO_2}(k)]\frac{\|\boldsymbol{u_C}(k)\|}{COP(k)} = \sum_{k=1}^{N}[1 - f_{CO_2}(k)]P_{HP}(k) \quad (4.71)$$

while in the second case is:

$$J_{CO_2} = \sum_{k=1}^{N} e_{CO_2}(k)\frac{\|\boldsymbol{u_C}(k)\|}{COP(k)} = \sum_{k=1}^{N} e_{CO_2}(k)P_{HP}(k) \quad (4.72)$$

As a result, the complete objective function is defined by the following equation:

$$J = \alpha_{OBJ} \times J_{\Delta u} + (1 - \alpha_{OBJ}) \times J_{OBJ} \quad (4.73)$$

where the term J_{OBJ} is the main objective that the MPC algorithm has to minimise while $J_{\Delta u}$ is a smoothing/modulation term introduced to avoid power peaks by penalizing changes in the control action, which is present in any of the four cases.

The weighing coefficient α_{OBJ} has different values depending on the objective since these variable affects the computational time and the predominance of one term on the other. In order to find the accurate value for the coefficient, Pareto fronts were developed for the different objectives, they show the trade-off between the 2 objectives for different values of alpha. The curves are presented in Figure 18 and Figure 19, while the chosen values of α_{OBJ} are shown in Table 14 and are highlighted in red in the figures. The values were selected considering a trade-off between the required computational time to solve the MPC algorithm and the weight between the major objective and the modulation term.

Table 14: values of the coefficient α_{OBJ} for the different objectives

Minimization objective	α_{OBJ} during heating period	α_{OBJ} during cooling period
Electricity consumption	0.20	0.20
Electricity cost	0.20	0.10
CO_2 emission (trigger CO_2-free generation)	0.60	0.30
CO_2 emission (trigger CO_2 emission factor)	0.70	0.30

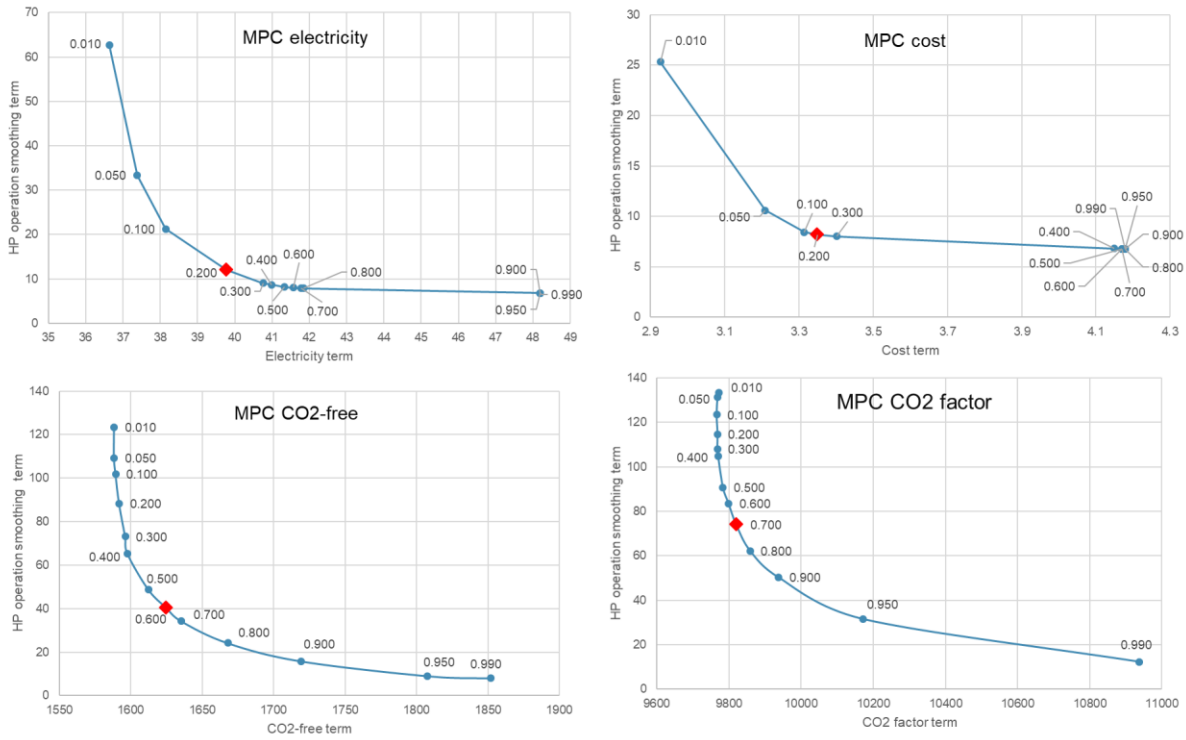

Figure 18: Pareto front for heating scenarios

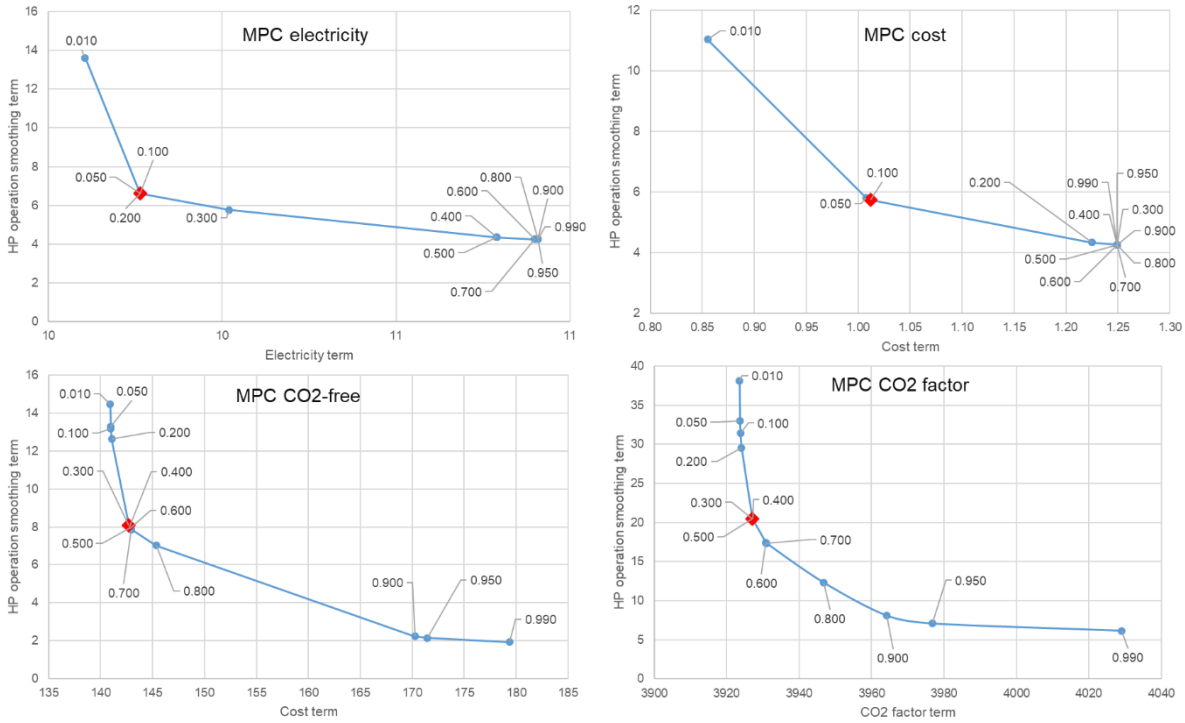

Figure 19: Pareto front for cooling scenarios

4.3.5. Co-simulation Platform

In order to implement the MPC strategy explained in the previous sections, a TRNSYS-MATLAB co-simulation platform is used, as previously done in (77). The detailed building model in TRNSYS enables to test the control strategy without having to implement it in a real building.

For the co-simulation, MATLAB is called every hour through Type 155 from TRNSYS and it runs the MPC controller, determining the optimal operation for the next day (N = 120 time steps of 12 minutes). Only the first 5 control actions (supply temperature set-points and on-off signals) are then sent back to TRNSYS, which simulates the dynamic behaviour with a more accurate model and a higher time resolution (3 minutes time steps).

Unfortunately, it can happen that the algorithm is not able to solve the problem (for example because the temperature coming from TRNSYS is out of bounds). In these cases, an if-else statement is implemented containing control signals for the heat pump so as to manually solve the problem and avoid a continuous chain of errors in the simulation.

5. Scenarios

Six different scenarios were analysed in this master's thesis. A first scenario, named **FCHP**, were the building model is equipped with the FCHP and a second scenario, called **VSHP**, were the building model has a VSHP controlled by a PID controller. In the other four scenarios, the building is equipped with the VSHP whose operation is managed by the MPC strategy. The four objectives are the minimization of: the HP electricity consumption (scenario **MPC electricity**), the electricity cost (scenario **MPC cost**), the reduction of the CO_2 emission using as trigger the percentage of CO_2-free grid generation (scenario **MPC CO_2-free**) and the minimization of the CO_2 emission using as trigger the grid CO_2 emission factor (scenario **MPC CO_2 factor**). The scenarios with their most relevant characteristics are summarised in Table 15. In the following sections of the document, the name of the scenarios is written in **bold** for sake of clarity.

The simulations are conducted for winter and summer season using weather data of 2015. The chosen simulation periods are the week of January from 18-01-2015 00:00 to 25-01-2015 00:00 and the week of July from 08-07-2015 00:00 to 15-07-2015 00:00.

Table 15: summary of the scenarios

Scenario	FCHP	VSHP	MPC
HP mode	On-off	Variable speed	Variable speed
Starting of HP with	1st level priority: zone temperature or DHW thermostat 2nd level priority: supply temperature proportional controller	Zone temperature or DHW thermostat	MPC (switching on-off the HP)
Control of HP with		PID controller on supply temperature	MPC (deciding the supply temperature)
Starting of FCU with	Zone temperature thermostat	Zone temperature thermostat (synchronized with the on-off of the HP for SH/SC)	MPC (synchronized with the on-off of the HP for SH/SC)
Minimization objective	-	-	Electricity consumption Cost CO_2 emission (trigger CO_2-free generation) CO_2 emission (trigger CO_2 emission factor)

6. Results

In this section the main results of the different analysed scenarios are presented. It is divided into section 6.1 and 6.2, where the results for the winter and summer period are shown respectively. Every section is, in turn, divided into a chapter where the **VSHP** scenario is compared to the **FCHP** scenario (section 6.1.1 and 6.2.1), in order to present similarities and differences of the developed VSHP model, and another chapter where the **MPC** cases are compared to the **VSHP** scenarios (section 6.1.2 and 6.2.2) to assess the potential of the energy flexibility strategies.

It must be noted that in the following sections, whenever a percentage change of a variable is given, it represents a relative change of the value in case of non-percent data, while it indicates an absolute change of the value for data that can be interpreted as percent, e.g. the flexibility factor, PLR, PLF, POR, and LPD.

6.1. Winter

In this section, the results of the simulation conducted between the 18th of January 2015 at 00:00 and the 25th of January 2015 at 00:00 are presented.

6.1.1. FCHP vs VSHP

Table 16 provides an overview of the results obtained from the winter simulation of the scenarios **FCHP** and **VSHP**. What stands out in the table is the reduction of electricity consumption by 16.19%, and the consequent decrease of electricity cost (-18.01%) and CO_2 emission (-16.10%), in the **VSHP** scenario compared to the case with fixed capacity heat pump. This interesting result is explained by the exploitation of the part load of the VSHP – the heat pump works at an average PLR of 0.84 – where the efficiency is higher, in fact the average PLF is 1.12. This trend is also noticeable in Figure 20 where the HP electricity consumption is presented: the VSHP is able to reduce the on-off behaviour, represented by the full light grey areas of the FCHP where the heat pump is on one timestep and off the next one in repetition, and to decrease the electricity consumption peaks during the period.

Comfort results are illustrated in Figure 21 and Figure 22, showing the POR for every comfort category and the long-term percentage of dissatisfied, respectively. The comfort of the occupants is similar since the average operating temperature of the apartment is outside category II for the 18.21% and the 23.93% of the simulation time for **FCHP** and **VSHP**, respectively, and, moreover, the LPD increases of only 0.16% in the **VSHP** scenario compared to the **FCHP** case. The living room temperature follows a remarkably similar trend in the two scenarios as the control system is based on the temperature of the room in both cases, as can be seen in Figure 23.

Table 16: energy results of FCHP and VSHP scenarios in winter

Variable	FCHP	VSHP
SH demand [kWh]	216.95	214.08 (-1.32%)
DHW demand [kWh]	57.12	57.15 (+0.05%)
Electricity consumption [kWh]	103.57	86.80 (-16.19%)
Electricity cost [EUR]	11.75	9.64 (-18.01%)
CO_2 emission [kg]	30.35	25.47 (-16.10%)
Average PLR [-]	0.776	0.842 (+6.64%)
Average PLF [-]	0.930	1.116 (+18.70%)

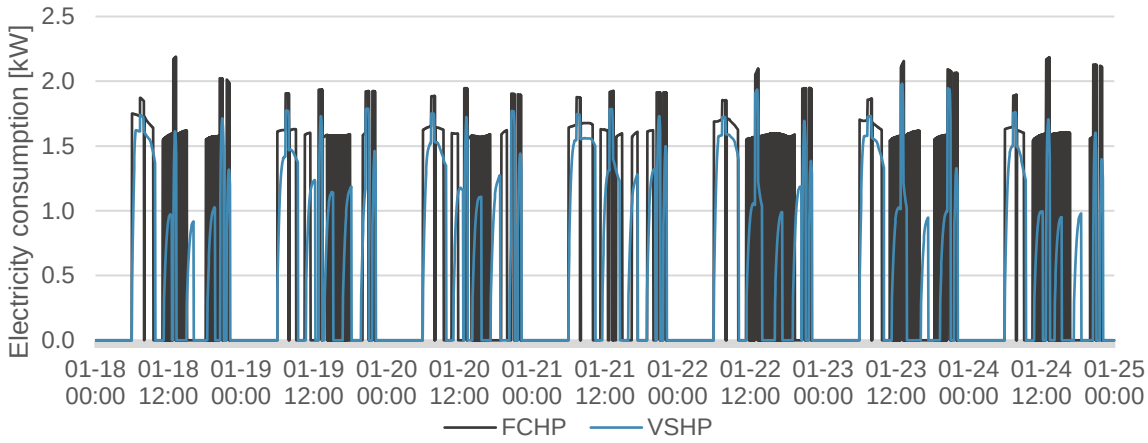

Figure 20: HP electricity consumption for FCHP and VSHP scenarios in winter

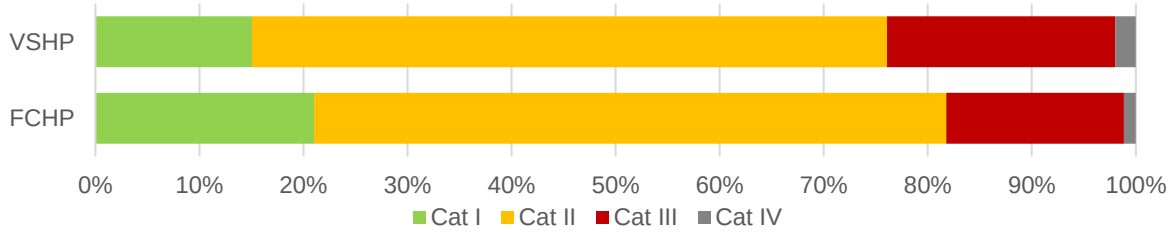

Figure 21: POR for FCHP and VSHP scenarios in winter

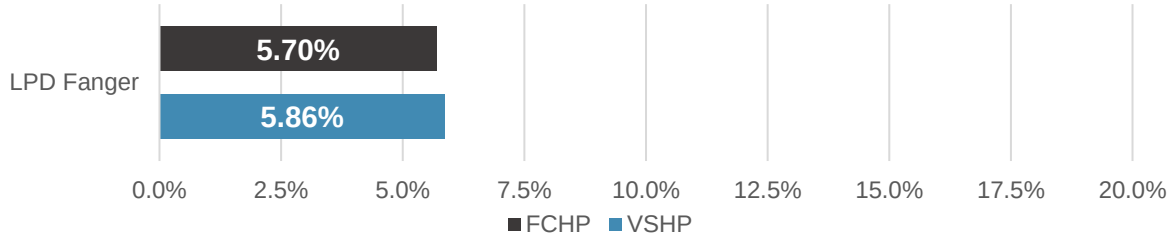

Figure 22: LPD for FCHP and VSHP scenarios in winter

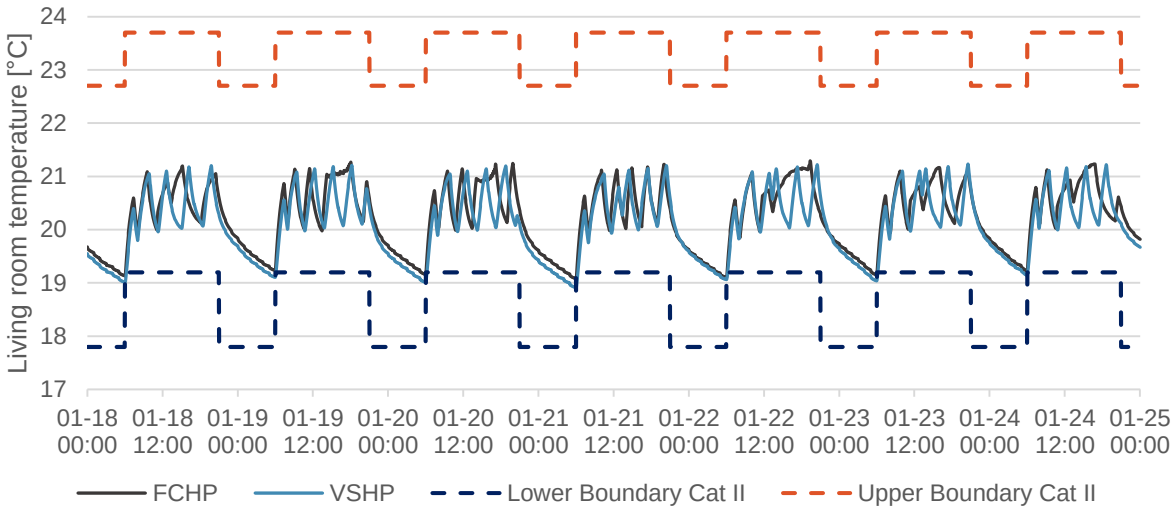

Figure 23: Living room temperature for FCHP and VSHP scenarios in winter

6.1.2. VSHP vs MPC

Table 17 shows the main results for the **VSHP** case and the **MPC** scenarios for the simulations conducted in January while Figure 24 to Figure 27 represents the HP electricity consumption during the simulation period compared to the one of the **VSHP** scenario for the **MPC electricity**, the **MPC cost**, the **MPC CO_2-free**, and the **MPC CO_2 factor** cases.

What is interesting about the data in the table is that every MPC strategy achieves its objective. The **MPC electricity** scenario reduces the electricity consumption by 38.06%, having the highest decrease among the energy flexibility strategies, and it also achieves unexpectedly the highest reduction in electricity cost (-47.47%) and CO_2 emission (-38.64%) compared to the **VSHP** case, even if these were not its primary objectives. A possible explanation for this might be that **MPC cost** uses energy during the first half of the low-price periods (night), where the efficiency of the heat pump is not that high due to the low outdoor temperature. On the other hand, **MPC electricity** uses energy during the second half of the low-price periods (mornings), where the price is still low, but the outdoor temperature is higher, and the COP as well. The difference can be seen in Figure 24 and Figure 25. Moreover, **MPC electricity** has the highest CO_2 reduction most probably because it reduces the electricity consumption of **VSHP** up to 18.46% compared to the CO_2 minimization cases. The **MPC cost** scenario effectively shifts the electricity consumption of the heat pump to low-price periods (see Figure 25) achieving an price flexibility factor of +0.642 with a rise of 1.160 compared to the **VSHP** scenario along with an electricity cost decrease of 41.04%. The **MPC CO_2-free** and the **MPC CO_2 factor** scenarios achieve a CO_2 flexibility factor of -0.004 and +0.098 with an increase of 0.250 and 0.351 compared to the **VSHP** scenario shifting the HP consumption to low-emission periods (see Figure 26 and Figure 27, respectively); moreover, the CO_2 emission drop by 24.88% for **MPC CO_2-free** and by 20.91% for **MPC CO_2 emission**.

Table 17: energy results of VSHP and MPC scenarios in winter

Variable	VSHP	MPC electricity	MPC cost	MPC CO_2-free	MPC CO_2 factor
SH demand [kWh]	214.08	209.51 (-2.14%)	249.95 (+16.76%)	207.62 (-3.02%)	207.41 (-3.12%)
DHW demand [kWh]	57.15	60.07 (+5.11%)	59.17 (+3.54%)	55.99 (-2.04%)	57.83 (+1.18%)
Electricity consumption [kWh]	86.80	53.77 (-38.06%)	72.55 (-16.42%)	65.77 (-24.23%)	69.79 (-19.60%)
Electricity cost [EUR]	9.64	5.06 (-47.47%)	5.68 (-41.04%)	6.64 (-31.10%)	6.88 (-28.59%)
CO_2 emission [kg]	25.47	15.63 (-38.64%)	21.18 (-16.84%)	19.13 (-24.88%)	20.14 (-20.91%)
Average PLR [-]	0.842	0.390 (-45.26%)	0.435 (-40.75%)	0.534 (-30.79%)	0.581 (-26.07%)
Average PLF [-]	1.116	1.813 (+69.64%)	1.770 (+65.36%)	1.570 (+45.38%)	1.493 (+37.61%)
Price FF [-]	-0.519	+0.226 (+0.745)	+0.642 (+1.160)	+0.043 (+0.562)	+0.102 (+0.621)
CO_2 FF [-]	-0.253	-0.118 (+0.135)	-0.046 (+0.207)	-0.004 (+0.250)	+0.098 (+0.351)

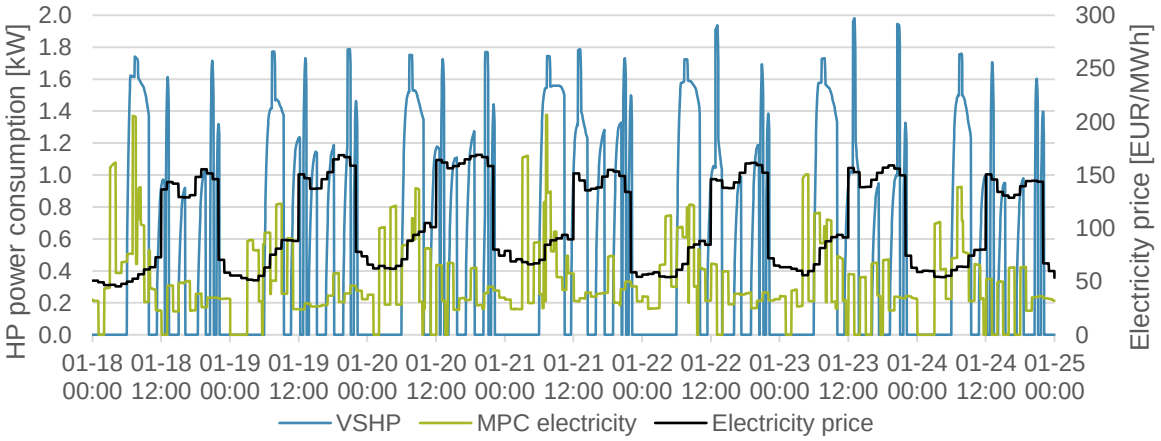

Figure 24: HP electricity consumption for VSHP and MPC electricity scenarios in winter

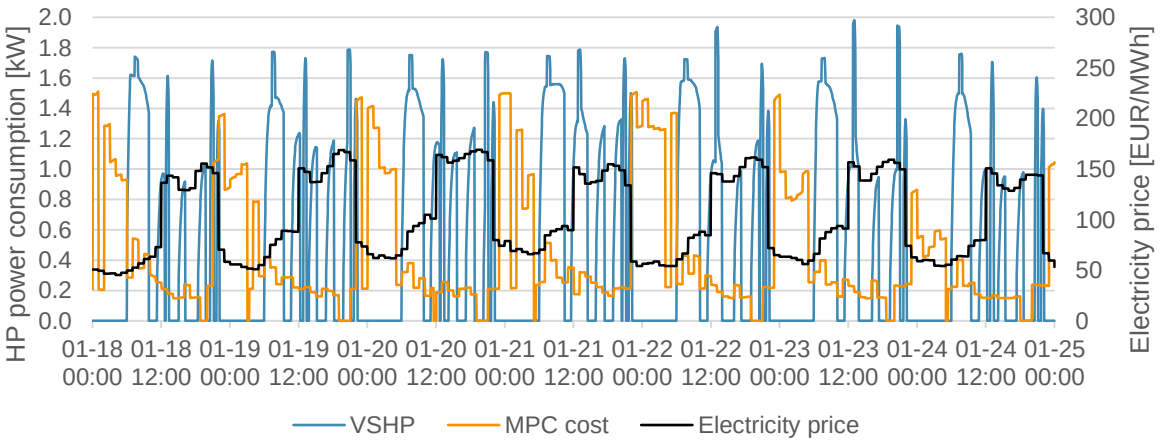

Figure 25: HP electricity consumption for VSHP and MPC cost scenarios in winter

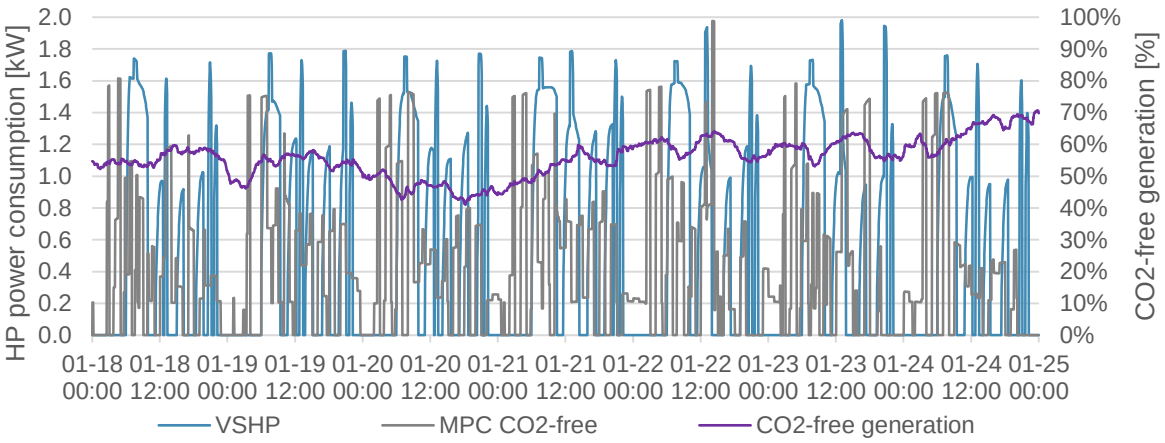

Figure 26: HP electricity consumption for VSHP and MPC CO_2-free scenarios in winter

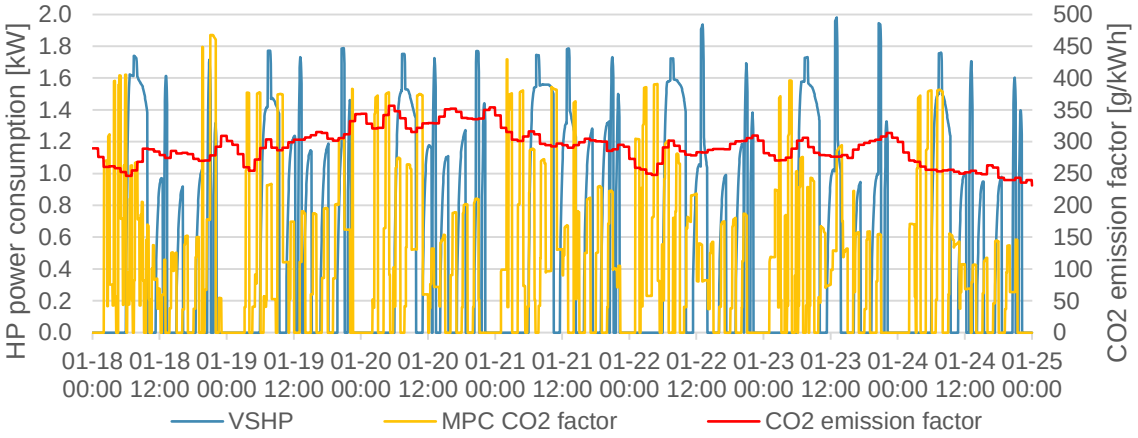

Figure 27: HP electricity consumption for VSHP and MPC CO_2 factor scenarios in winter

With respect to the thermal comfort, the **MPC** strategies achieve worse results, except for the **MPC cost** scenario, since the POR of category III and IV combined increases from 23.93% in the **VSHP** scenario to 27.79% for **MPC electricity**, to 37.96% for **MPC CO_2-free**, and to 35.85% for **MPC CO_2 factor**, as it is shown in Figure 28. However, the **MPC cost** scenario achieves a striking result reaching a percentage outside category II of only 2.42% and, furthermore, the average operative temperature of the apartment lies in category I for the 68.99% of the time, meaning an increase of 53.93% compared to the **VSHP** scenario. Figure 29 illustrates the values of the LPD for the different scenarios and this indicator shows that all the **MPC** scenarios perform worse than the **VSHP**, nevertheless all the scenarios provide comfortable conditions (LPD < 20%). This discrepancy between the indicators can be explained by the living room temperature profile presented in Figure 30 where it can be seen that the **MPC cost** scenario extremely changes the temperature profile since the apartment is heated during the nights – the profile is almost symmetrical to the other cases – in order to take advantage of the lower electricity price, while the other **MPC** scenarios maintain a close but less fluctuating profile to the one of the **VSHP** case. This can highly influence the LPD value since it is an indicator that considers the nearness to the midpoint of category II temperature range,

which is 21.50 °C during the day and 20.25 °C. Indeed, the temperature of **MPC cost** is within category II (upper limit 22.70 °C) but almost 2 °C far from the midpoint of category II during the night. Nevertheless, the indicator is well below the maximum limit of 20%, therefore the same comfort level of **VSHP** is maintained in the **MPC** scenarios.

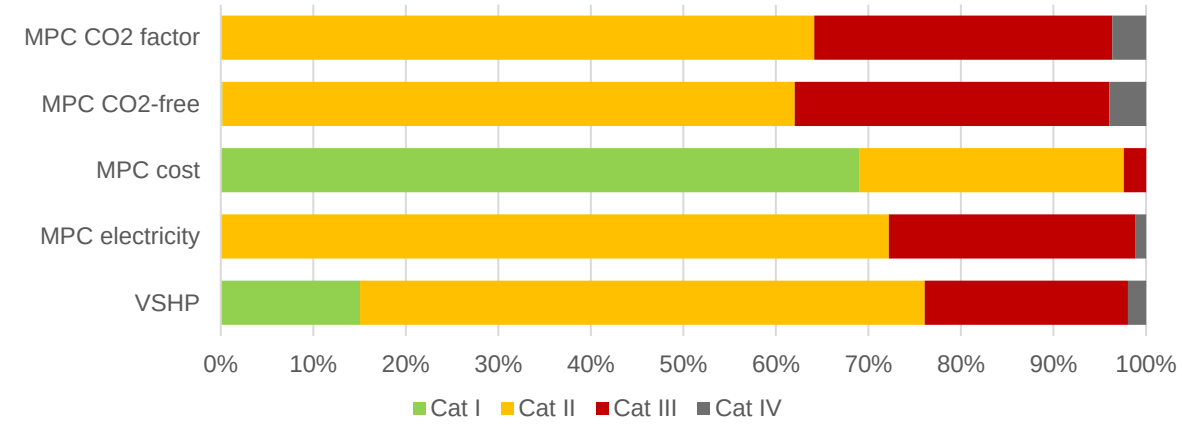

Figure 28: POR for FCHP and VSHP scenarios in winter

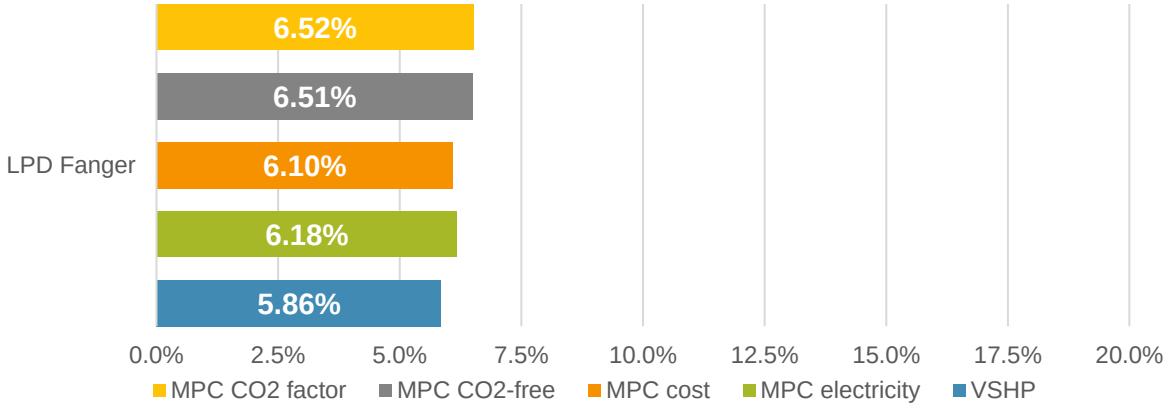

Figure 29: LPD for VSHP and MPC scenarios in winter

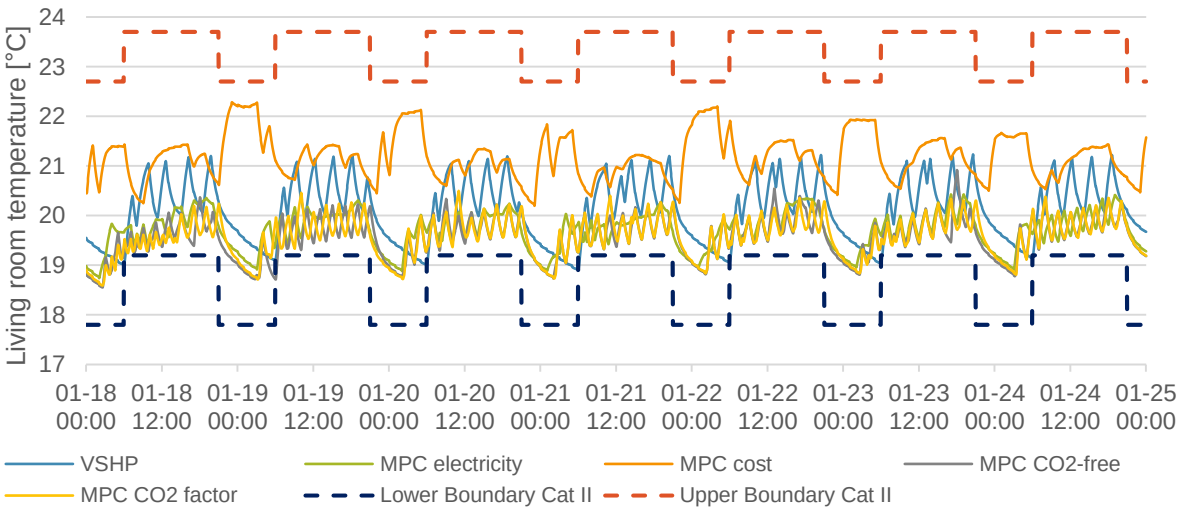

Figure 30: Living room temperature for VSHP and MPC scenarios in winter

6.2. Summer

In this section, the results of the simulation conducted between the 7th of July 2015 at 00:00 and the 15th of July 2015 at 00:00 are presented.

6.2.1. FCHP vs VSHP

The KPIs of the **FCHP** and **VSHP** scenarios for the summer simulation period are shown in Table 18. The VSHP works at an average PLR of 0.949 with an average PLF of 1.047 and it allows the reduction of the electricity consumption of the heat pump by 6.23%, which causes the electricity cost and the CO_2 emission to diminish by 3.11% and 6.28%, respectively. Moreover, the VSHP has a similar consumption trend with a slightly lower consumption during the peaks created by DHW demand while the operation during SC demand (consumption around 0.4 kW) is almost the same as the **FCHP** scenario, as can be noted in Figure 31.

Regarding the thermal comfort of the occupants, the LPD increases of only 0.09% (see Figure 33) and the POR of category III differs of 0.43% between the two scenarios (see Figure 29). Figure 30 confirms these results by showing that the living room temperature trend is almost coincident for the entire simulation period. Therefore, the same level of comfort is maintained in the two cases.

Table 18: energy results of FCHP and VSHP scenarios in summer

Variable	FCHP	VSHP
SC demand [kWh]	118.94	118.65 (-0.24%)
DHW demand [kWh]	49.78	49.71 (-0.13%)
Electricity consumption [kWh]	39.31	36.86 (-6.23%)
Electricity cost [EUR]	5.07	4.91 (-3.11%)
CO_2 emission [kg]	13.20	12.37 (-6.28%)
Average PLR [-]	0.957	0.949 (-0.81%)
Average PLF [-]	0.987	1.047 (+6.01%)

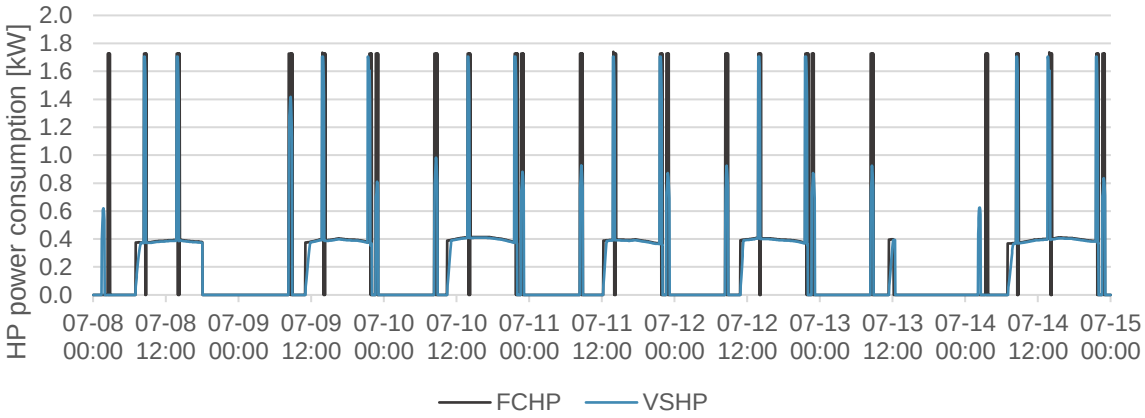

Figure 31: HP electricity consumption for FCHP and VSHP scenarios in summer

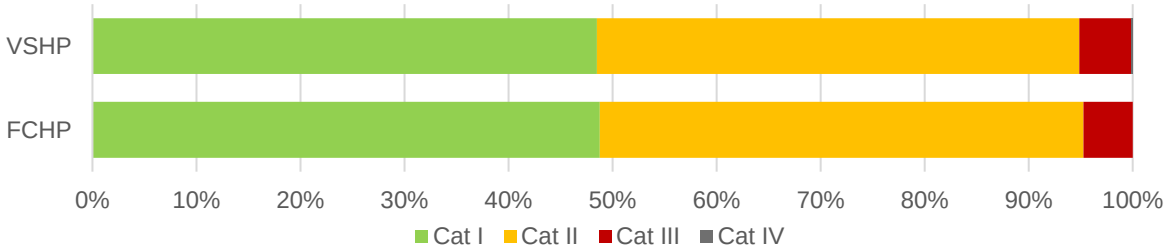

Figure 32: POR for FCHP and VSHP scenarios in summer

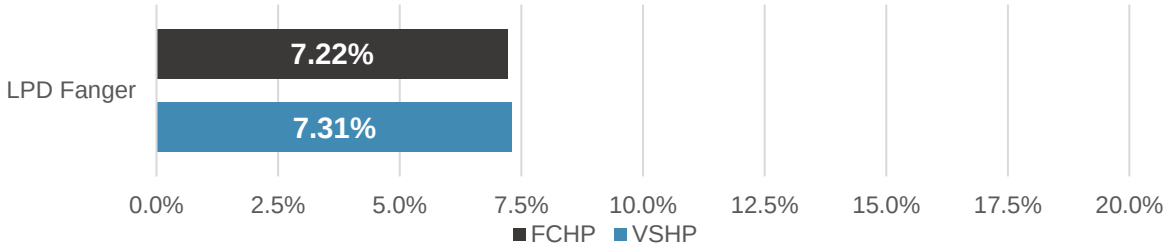

Figure 33: LPD for FCHP and VSHP scenarios in summer

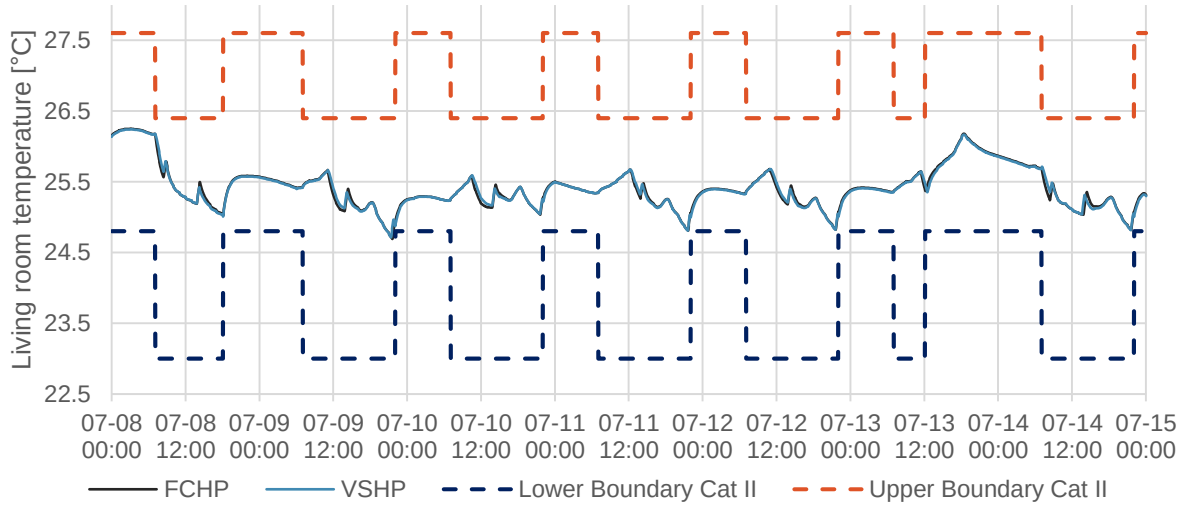

Figure 34: living room temperature for FCHP and VSHP scenarios in summer

6.2.2. VSHP vs MPC

An overview of the summer energy results of the scenarios equipped with a variable speed heat pump is presented in Table 19 whereas Figure 35 to Figure 38 compare the electricity consumption of the **VSHP** scenario, with the one of the **MPC electricity** scenario, of the **MPC cost** scenario, of the **MPC CO_2-free** scenario, and of the **MPC CO_2 factor** scenario for the same simulation period, respectively.

It is apparent from the table and the graphs that the **MPC** strategies manage to achieve their goal. The **MPC electricity** scenario reduces the electricity consumption by more than 40% compared to the **VSHP** scenario, even if the highest decrease was achieved by the **MPC cost** scenario (-46.90%). The **MPC cost** scenario is able to diminish the monetary expenses for electricity by 59.64% and vastly shifts the electrical load because the price flexibility factor varies from -0.838 of the **VSHP** case to +0.126, achieving an increase of 0.964. The CO_2 flexibility factor increases from +0.278 to +0.392 for the **MPC CO_2-free** scenario and to +0.436 for the **MPC CO_2 factor** scenario, therefore, the two cases move a part of the HP electricity consumption to low CO_2 emission hours and, in turn, reduce the CO_2 emission of the system from 12.37 kg to 8.52 kg (-31.15%) and to 8.96 kg (-27.61%), respectively. However, a higher drop of the emission is reached in the **MPC** strategies focusing on the minimization of the electricity consumption (-40.40%) and cost (-46.08%). This result may be explained by the fact that, in the MPC strategies aiming at the minimization of the CO_2 emissions, there are higher power peaks compared to **MPC electricity** and **MPC cost**, and, as a consequence, the average PLF is lower, and, in turn, the total electricity consumption, which directly influences the total CO_2 emission.

Table 19: energy results of VSHP and MPC scenarios in summer

Variable	VSHP	MPC electricity	MPC cost	MPC CO_2-free	MPC CO_2 factor
SC demand [kWh]	118.65	109.26 (-7.92%)	94.84 (-20.07%)	105.97 (-10.69%)	105.00 (-11.51%)
DHW demand [kWh]	49.71	46.32 (-6.43%)	46.22 (-7.03%)	48.20 (-3.03%)	48.38 (-2.68%)
Electricity consumption [kWh]	36.86	21.63 (-41.33%)	19.57 (-46.90%)	25.28 (-31.42%)	26.60 (-27.84%)
Electricity cost [EUR]	4.91	2.42 (-50.83%)	1.98 (-59.64%)	2.84 (-42.28%)	3.09 (-37.20%)
CO_2 emission [kg]	12.37	7.38 (-40.40%)	6.67 (-46.08%)	8.52 (-31.15%)	8.96 (-27.61%)
Average PLR [-]	0.949	0.437 (-51.17%)	0.435 (-51.39%)	0.553 (-39.65%)	0.611 (-33.82%)
Average PLF [-]	1.047	1.738 (+69.07%)	1.764 (+71.72%)	1.558 (+51.04%)	1.479 (+43.22%)
Price FF [-]	-0.838	-0.105 (+0.733)	0.126 (+0.964)	-0.095 (+0.743)	-0.221 (+0.616)
CO_2 FF [-]	0.278	0.045 (-0.233)	0.139 (-0.139)	0.392 (+0.114)	0.436 (+0.159)

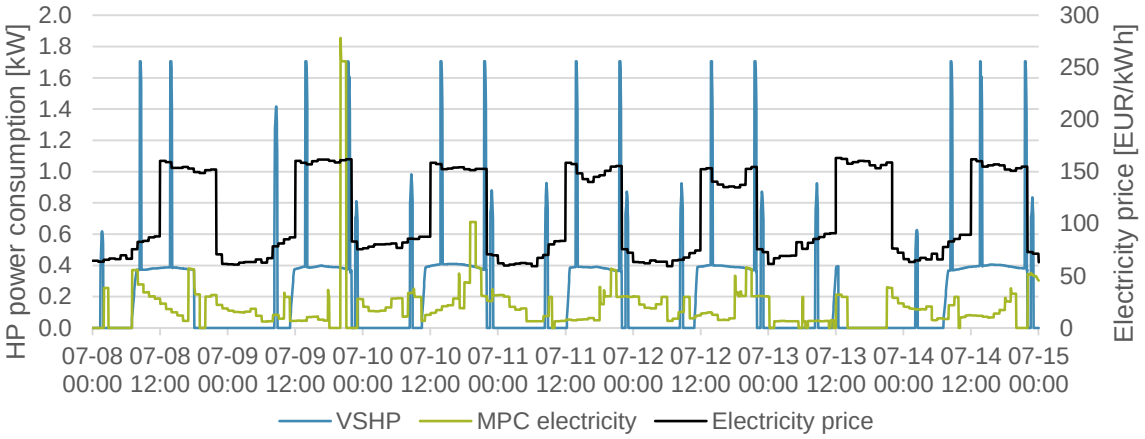

Figure 35: HP electricity consumption for VSHP and MPC electricity scenarios in summer

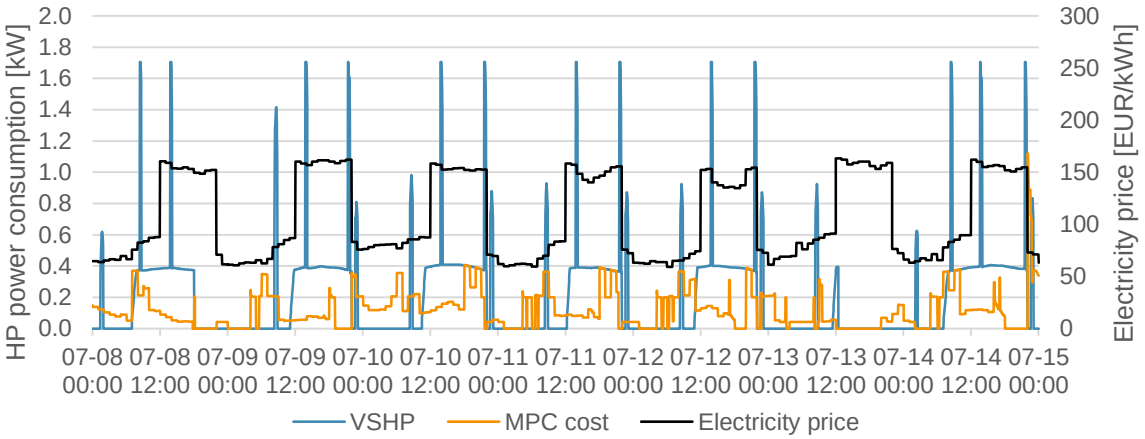

Figure 36: HP electricity consumption for VSHP and MPC cost scenarios in summer

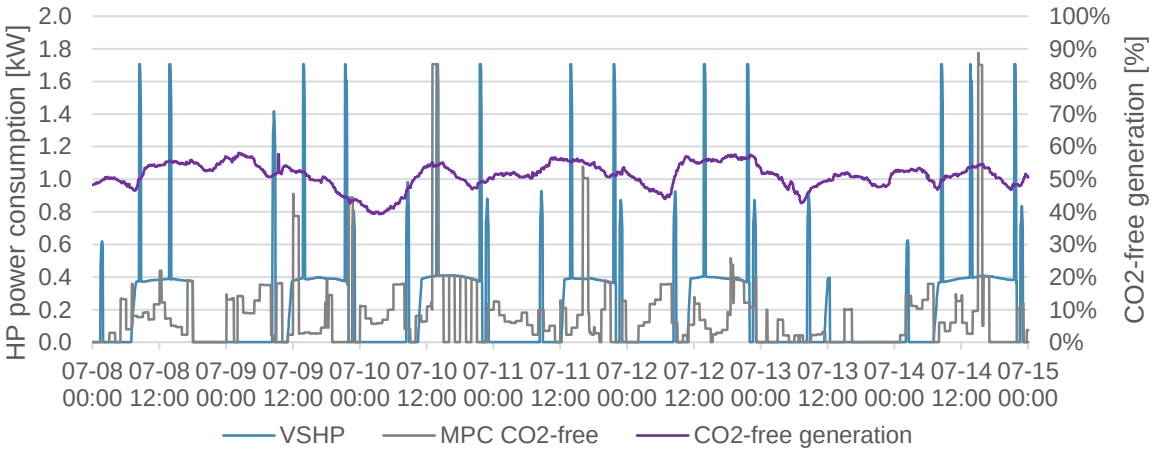

Figure 37: HP electricity consumption for VSHP and MPC CO_2-free scenarios in summer

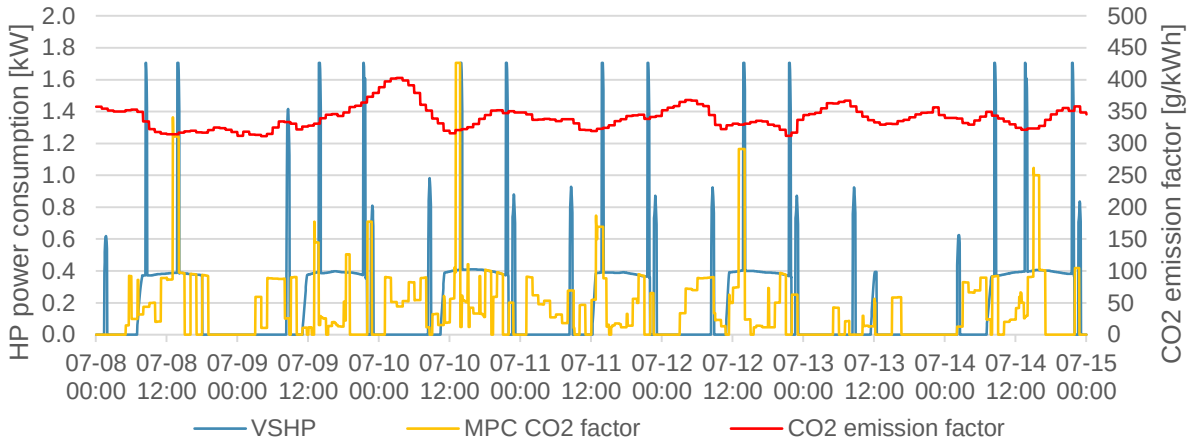

Figure 38: HP electricity consumption for VSHP and MPC CO_2 factor scenarios in summer

In summer simulations, in the **MPC** flexibility strategies the average operative temperature of the apartment is within category I or II for more than 85% of the occupied time, except for **MPC electricity**, as can be seen in Figure 39. However, if the LPD analysed, the increase for this scenario is only of 0.60%, while the indicator rises of 0.55% for **MPC cost**, of 0.38% for **MPC CO_2-free**, and of 0.37% for **MPC CO_2 factor**, as shown in Figure 40. Thus, the **MPC** scenarios reach a similar level of comfort.

Figure 41 represents the living room temperature profile of the scenarios. The flexibility strategies tend to have a similar temperature profile, where the building is cooled in the last part of the night, but this trend differs from scenario **VSHP**, because the latter usually cools the building around 12:00 when the temperature starts to go above the set-point.

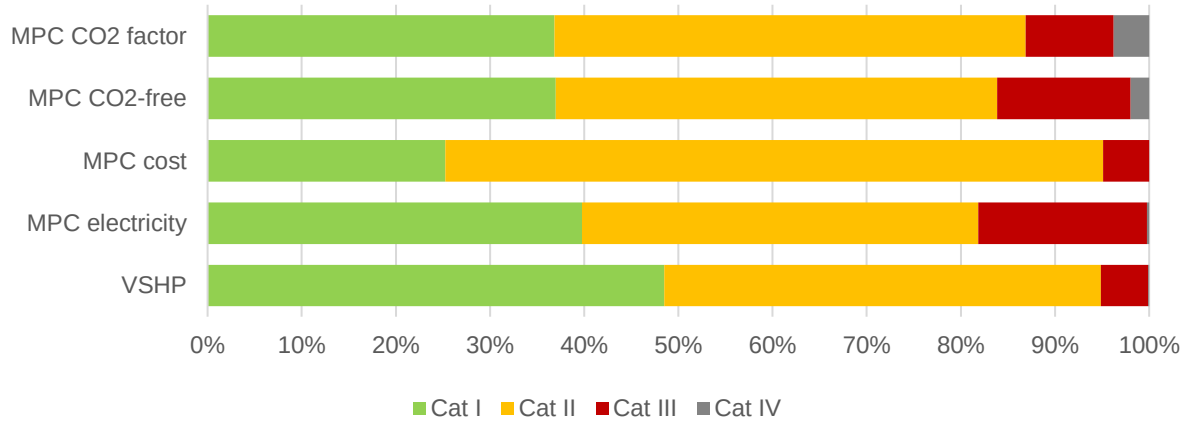

Figure 39: POR for FCHP and VSHP scenarios in summer

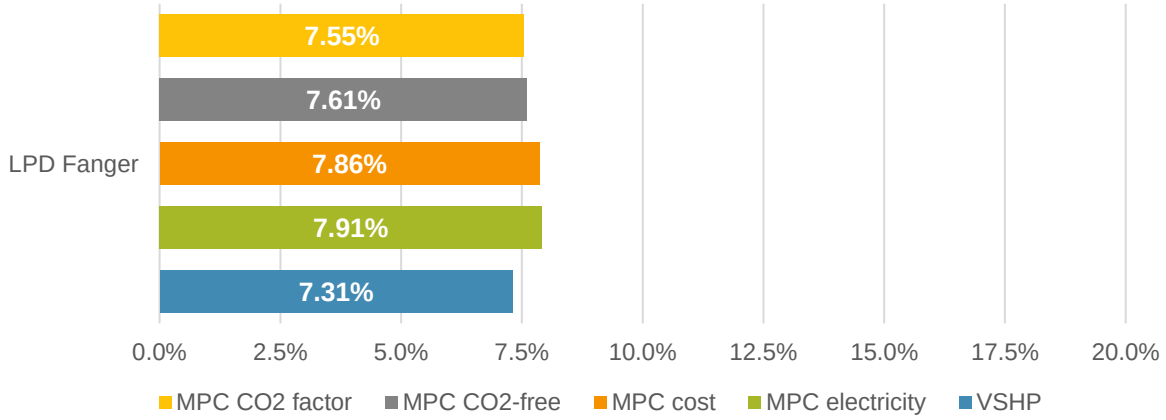

Figure 40: LPD for VSHP and MPC scenarios in summer

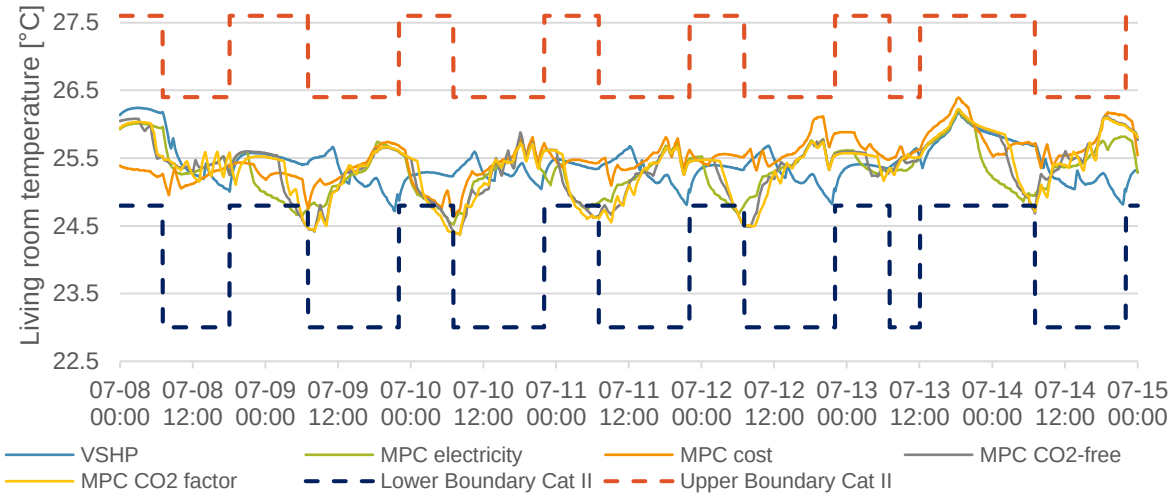

Figure 41: Living room temperature for VSHP and MPC scenarios in summer

7. Discussion

In the previous section, it was stated that every **MPC** strategy achieved its objective, however the cost minimization scenarios performed better than the CO_2 emission minimization cases. One of the reasons for this difference lies in the profile of the trigger signal. The electricity price has a more constant and recurring daily trend since it has a steady low-price period around 50 EUR/MWh during the night that increases at approximately 150 EUR/MWh at 12:00 during the day. On the other hand, the CO_2-free generation and the CO_2 emission factor do not have a clear daily trend and moreover their maximum and minimum values greatly change depending on the date. This reflects the fact that the two-period price signal is already created with the intention to achieve implicit energy flexibility, whereas the CO_2 signals are solely related to the type of energy-producing sources, of which fluctuating renewables, like wind and solar, really depend on weather conditions. Therefore, the profile is highly influenced by these variations, and the MPC algorithm is less capable of exploiting the low-emission periods because the amplitude of these valleys is less important. Figure 42 illustrates as an example of the profile difference, the electricity price, and the CO_2 emission factor for the analysed week of January 2015.

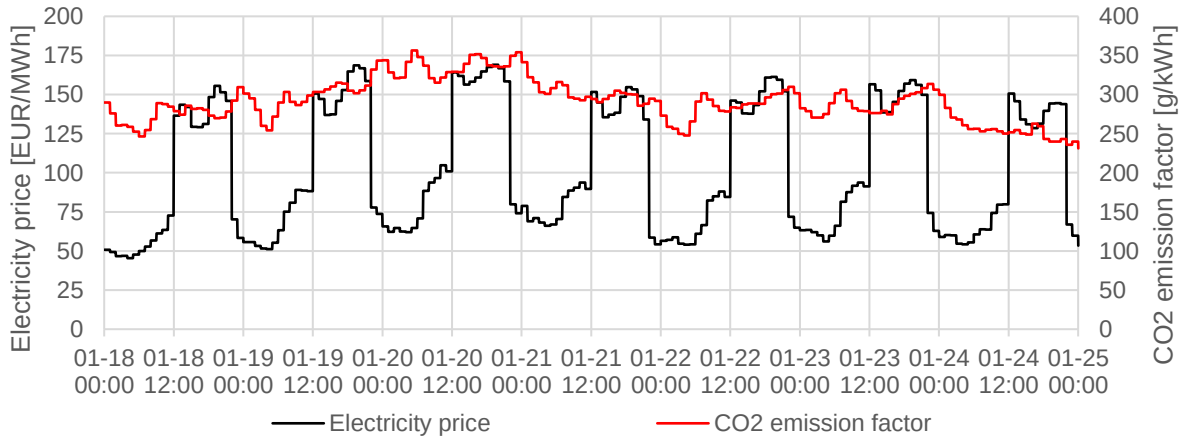

Figure 42: Electricity price and CO_2 emission factor for the analysed week of January

Moreover, the results demonstrated that using the percentage of CO_2-free grid generation is a less efficient method for obtaining load shifting towards low CO_2 emission hours, but this signal achieves a higher reduction in CO_2 emission than when using the CO_2 emission factor signal. Another advantage of this signal is that it is readily available in real time with a 10-minutes resolution on the website of Red Eléctrica de España (121) whereas the CO_2 emission factor is not accessible by the public on the TSO website and, therefore, needs to be calculated considering the generation of the different type of energy and assuming the emission factors for the different types of the generation sources.

Regarding thermal comfort, the **MPC** scenarios achieve a similar comfort level than the base case, when the LPD is analysed. However, the POR indicates that scenario **MPC cost** has a better level of

comfort in winter, even if this is not reflected in the LPD; this may be explained by the fact that **MPC cost** completely changes the temperature profile increasing the temperature at night compared to scenario **VSHP**, while the other **MPC** scenarios tend to have a similar trend to the **VSHP** case, but closer to the lower comfort boundary. As a result, the LPD that considers the nearness to the mid-point of category II is lower because the temperature stays within category II but it is close to the upper boundary.

In addition, it is interesting to note that in all the **MPC** scenarios, both in summer and winter, the VSHP works at very low part load ratio for a significant amount of time in comparison with the normal operation of the heat pump in scenario **VSHP**, as it is shown in Figure 43 and Figure 44 that represent the part load usage of the HP for winter and summer simulations, respectively. Because of this preference for low PLR of the MPC algorithm, the average PLR of all the **MPC** scenarios is on average 39.86% lower than the **VSHP** case, reaching the highest reductions in the winter **MPC electricity** scenario (-45.26%) and in the summer **MPC cost** scenario (-51.39%). This effect allows to use the higher COP at low PLR for most of the time, thereby achieving an important reduction of electricity consumption and cost, and CO_2 emissions. It is important to bear in mind that, if the variable speed heat pump had a different part load curve, the PLF/PLR relation might not have been as good at low PLR, and in such case the savings could be less significant.

Moreover, Figure 43 and Figure 44 highlight that the electricity minimization scenario almost never uses the heat pump at part load ratio higher than 0.85, suggesting that maybe a smaller HP could have been equally able to satisfy the thermal requirement of the building. However, only one week per season is analysed in this study, and this might not be true for other periods.

Furthermore, the current study found that the time when the HP is off was significantly reduced in the **MPC** scenarios, yet savings were still achieved. When considering the average of the flexibility strategies, the HP off time passed from 54.72% of **VSHP** to 32.14% in winter, and from 57.78% of **VSHP** to 24.09% in summer.

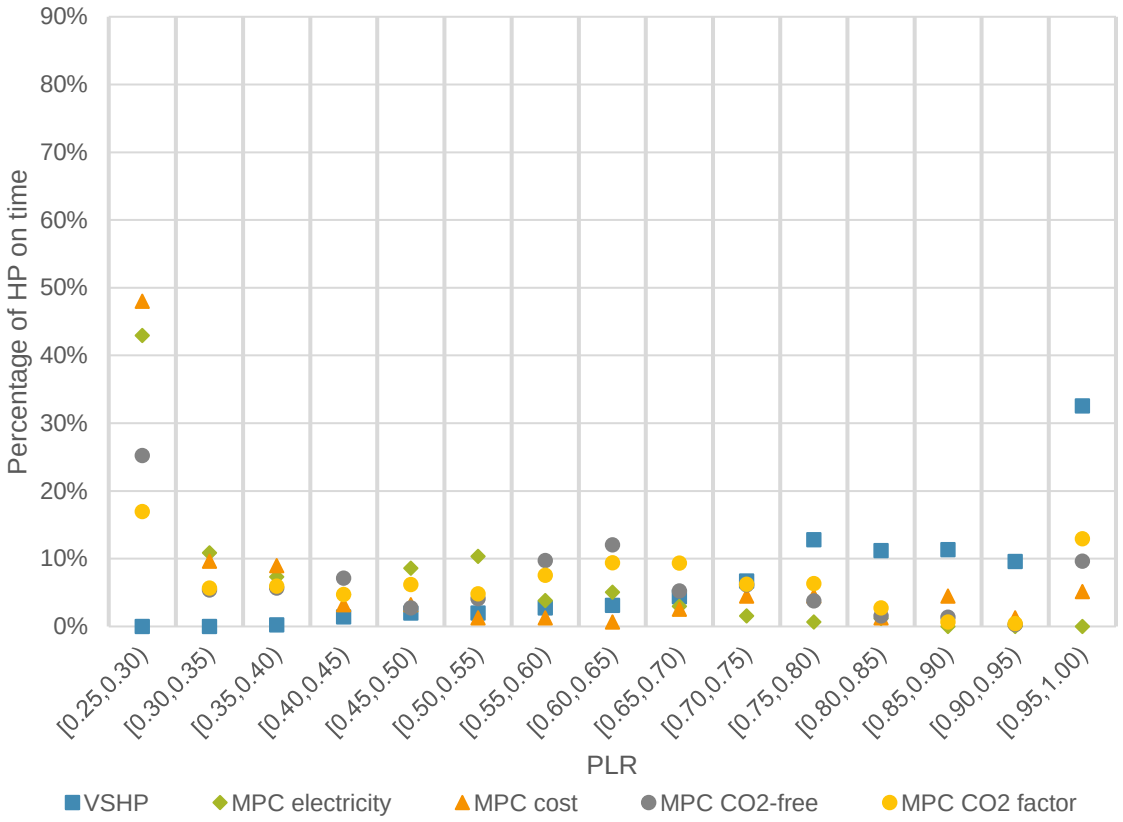

Figure 43: Part load usage of the HP for VSHP and MPC scenarios in winter

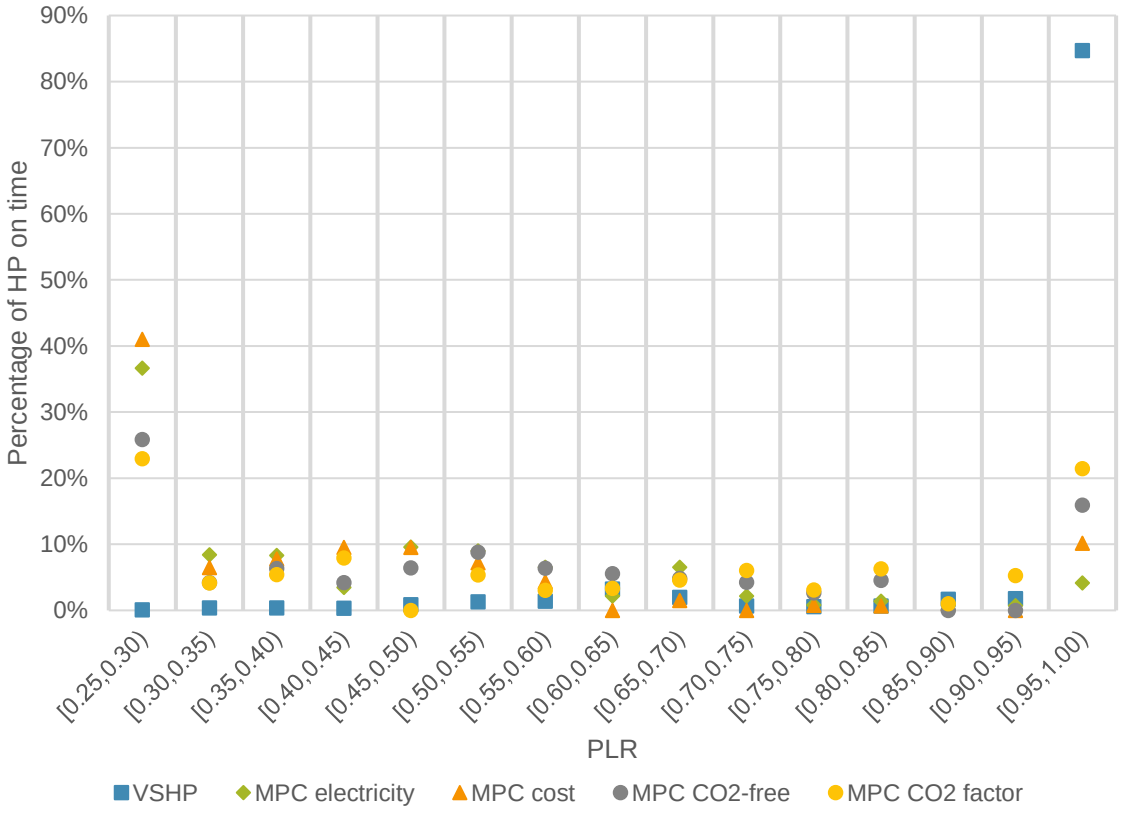

Figure 44: Part load usage of the HP for VSHP and MPC scenarios in summer

Moreover, for the analysed VSHP model, the part load factor increases when the part load ratio decreases, and this produces a positive side effect. In fact, even if it is not explicitly the objective of any of the strategies, peak shaving is achieved in every **MPC** scenario, due to the use of the heat pump at lower PLR, even more than the **VSHP** scenario that already uses the HP at part load. In fact, the percentage of time when the HP has an electrical consumption higher than 1.114 kW (80% of the HP rated input power) decreases on average by 70.24% in winter and by 57.80% in summer in the energy flexibility strategies compared to **VSHP**. This is most significantly observed in **MPC electricity** with an average reduction in both season of 94.07%, passing from 34.01% of the HP working time in the base case to the 0.75%.

Moreover, it is of great interest to analyse the seasonal differences among the results. The **VSHP** scenario achieves better results in January than in July. This result may be explained by the fact that the PID controller uses the heat pump usually at a higher part load ratio for space cooling than space heating, as it is shown in Figure 45. This characteristic may be explained by the fact that the VSHP might be sized for the specific summer week that was analysed, while, in other dates it might have been able to work at a lower part load ratio. Moreover, another possible explanation is that, in the analysed week, the space cooling demand is almost half of the space heating, thus there is less margin of improvement.

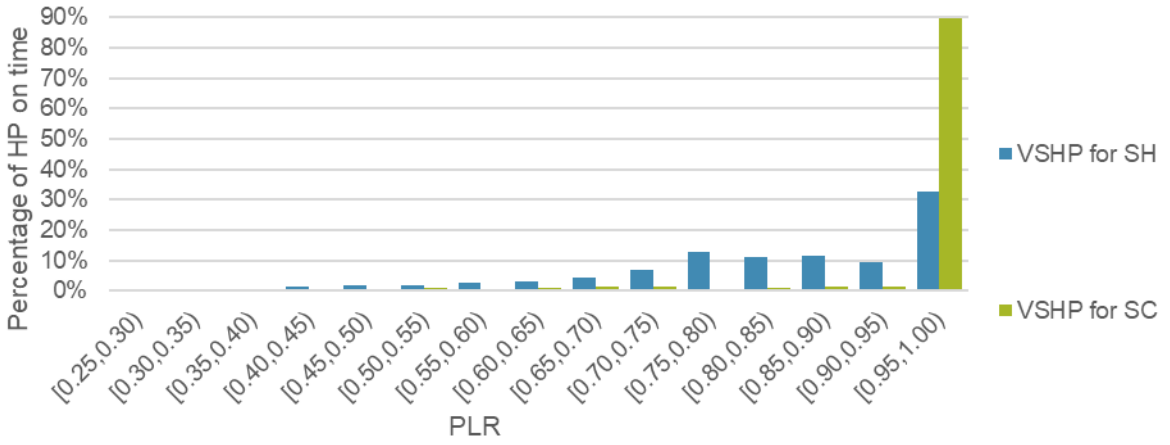

Figure 45: Part load usage of the HP for VSHP for space heating and cooling

Regarding load shifting, the energy flexibility strategies perform better in winter. For example, the variation of price flexibility factor is +1.160 in winter and +0.964 in summer for **MPC cost**, whereas the CO_2 flexibility factor increases by +0.250 in winter and by +0.114 in summer for **MPC CO_2-free**, and by +0.351 in winter and by +0.159 in summer for **MPC CO_2 factor**. On the other hand, considering the reduction of electricity, cost, and of CO_2 emissions, the **MPC** strategies perform better in summer. For example, when compared to **VSHP**, **MPC electricity** in summer reduces the electricity consumption by 3.27% more than in winter, and similarly **MPC cost** decreases the cost by 18.60% more, while **MPC CO_2-free** and **MPC CO_2 factor** in summer reach a higher reduction of

CO_2 emission of 6.27% and of 6.70% than in summer, respectively. This difference may be because the MPC algorithm is able to unlock the use of low part load ratio in summer, as it was not done with the PID control system, as explained previously, so there was a higher margin of improvement.

In addition, it can be observed how the different thermal demands are affected by the **MPC** strategies in terms of quantity variation and load shifting. SH decreases less than 3.50% in all the **MPC** winter scenarios except for **MPC cost** where it grows by 16.76% (because of the higher HP use at night), while SC demand decreases between 7.92% and 20.07% (this may be explained by the ability to use the HP at a lower part load ratio of the **MPC** scenarios), and DHW demand varies less than 8.00% in the **MPC** strategies in comparison with scenario **VSHP**. Figure 46 and Figure 47 show the energy and CO_2 flexibility factor of the HP electricity consumption connected to DHW and SH in January and to DHW and SC in July, respectively. For scenario **MPC cost**, the main load shifting is achieved in DHW, since in winter the price flexibility factor increases by 1.418 for DHW and by 1.142 for SH, and in summer the situation is similar with a growth of 1.218 for DHW and a rise of 0.853 for SC. For scenario **MPC CO_2-free**, in winter the electricity consumption is shifted for DHW and SH with an increase of 0.263 and 0.332 of the respective CO_2 flexibility factors, whereas in summer the CO_2 flexibility factor grows for DHW (+0.687) and diminishes for SC (-0.065). For scenario **MPC CO_2 factor**, in both seasons HP electricity consumption supplying DHW demand is shifted more than space heating/cooling; in fact, the increase of the DHW flexibility indicator is of 0.762 in winter and of 0.647 in summer, whilst SH flexibility factor rises by 0.329 and SC flexibility factor by 0.040. Therefore, it can be concluded that heat pump electricity consumption due to DHW demand can be more easily moved compared to the one related to either space cooling or heating. Moreover, in the CO_2 minimization strategies, it can be noticed that the price flexibility factor for DHW decreases compared to scenario **VSHP**, thus producing an adverse effect, the increase of cost, but this is not reflected in the total electricity cost because this effect is counterbalanced by the importance of the SC demand.

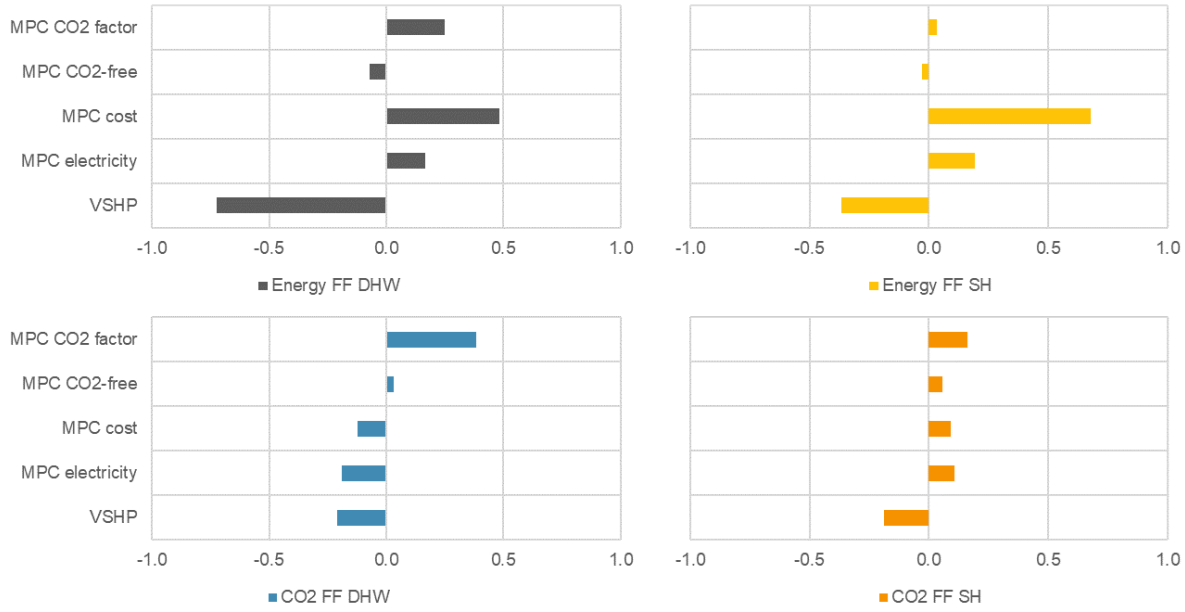

Figure 46: Flexibility factors for SH and DHW in winter

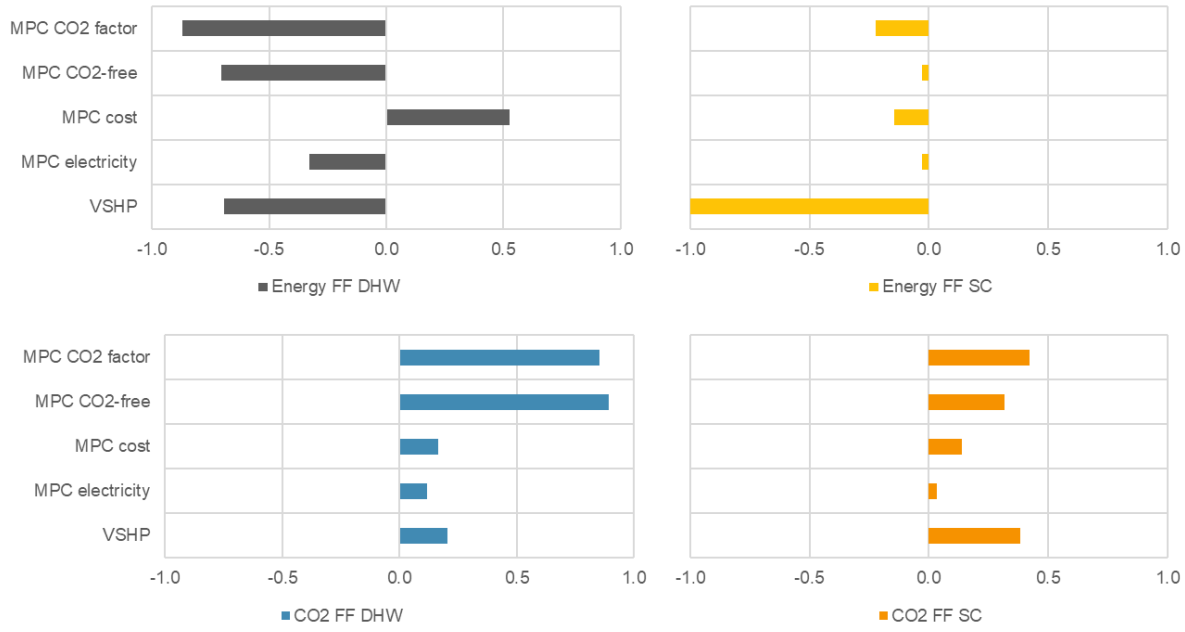

Figure 47: Flexibility factors for SC and DHW in summer

8. Conclusion

In this master's thesis project, the aim was to assess the energy flexibility potential of a residential building located in the Mediterranean climate through dynamic building simulations in TRNSYS, coupled with MPC strategies implemented in MATLAB which control the operation of the domestic variable speed heat pump. Due to the lack of VSHP models in TRNSYS, a model of this type of HP was developed and its performance compared to a FCHP.

This study has shown that the developed VSHP model is able to exploit the advantage of a variable speed heat pump, namely the ability of working at part load where the efficiency is higher, and, thus, achieve better results than a FCHP, and this is especially true when the developed model is applied in energy flexibility strategies.

Regarding the assessment of the energy flexibility potential, the four applied **MPC** strategies were successful in achieving their proposed goal. The **MPC electricity** scenario managed to reduce the electricity consumption by 38.06% in January and by 41.33% in July and the **MPC cost** scenario effectively shifts the HP electrical consumption to low-price hours with an increase of the price flexibility factor of +1.160 in winter and of +0.733 in summer. With respect to the last two scenarios, **MPC CO_2 factor** performed better than **MPC CO_2-free** in terms of load shifting towards periods of low CO_2 pollution, yet the latter achieved a higher CO_2 emission reduction in comparison with the former. Comparing the control signals, the electricity price performed better than the two signals related to CO_2 emission, because it has a clearer and more repetitive trend.

Furthermore, the thermal comfort of the occupants is maintained when flexibility is activated because the long-term percentage of dissatisfied occupants is well below the discomfort value of 20% in every **MPC** scenario, even if this indicator slightly increases compared to the **VSHP** scenario, with a maximum increase of 0.66% in **MPC CO_2 factor** simulated in January. However, in the analysis of the percentage outside the range and of the temperature profile, it was noticed that the winter **MPC electricity**, **MPC CO_2-free**, **MPC CO_2 factor** scenarios tend to maintain the temperature close to the lower comfort boundary, usually 1.0 °C colder than the **VSHP** scenario, and that the winter **MPC cost** scenario heats the building at night, reaching temperatures more than 3.0 °C higher than the **VSHP** scenario. These differences from the thermostat control system needs to be carefully considered when implemented into real buildings, because, if the occupants are accustomed to lower temperatures at night and higher temperatures during the day, comfort issues might appear. On the other hand, in the summer **MPC** simulations, the indoor temperature profile has a high similarity with thermally-driven control scenario.

In addition, regarding the difference in performance among seasons, the **MPC** strategies achieved better results in winter in terms of load shifting of the HP power consumption, whereas the **MPC**

scenarios performed better in summer, when the decrease of electricity consumption and cost, and the emission of carbon dioxide are considered.

Furthermore, this master's thesis project has found that generally DHW demand is more easily shifted compared to the one related to either space cooling or heating.

Another interesting aspect identified by this study is that **MPC** strategies tend to use the VSHP at low part load ratio, close to the minimum operation limit, and this finding should be taken into consideration in future work since the part load performance curve is different from model to model and working at extremely low PLR might not correspond to a high PLF as it is in this study. Therefore, the declared savings might not be as important in reality, since the estimated part load curve is based on manufacturer data and not on experimental data, and other efficiency losses that were not considered in this study might occur in the real operation of a heat pump.

Concerning the drawbacks of model predictive control encountered in this study, they mainly consist in the efforts that are necessary to implement and run the strategies, for example: the time required to identify an accurate reduced building model, the difficulty in coupling the programs – TRNSYS and MATLAB – in a co-simulation platform, and the high computational time required to run the simulations, between 2 and 5 hours depending on the case, compared to the few minutes of the base case. Moreover, other general disadvantages of MPC were experienced, like the high CPU usage demanded to solve the OCP problem, and the lack of precision of the MPC in the forecast of the system, that sometimes provokes the controlled variables to fall outside the boundaries. In order to solve this last issue, a manual control of the heat pump, that indicates the thermal power needed to re-establish the controlled variable inside the boundaries, was introduced. This HP manual control was activated up to 10% of total simulation time (start-up period + analysed week), especially during the simulation start-up that is not considered in the analysed results.

In conclusion, the main goals of the master's thesis were achieved and MPC strategies showed to be a promising technique that is able to provide energy flexibility in buildings equipped with heat pumps, without jeopardizing the comfort of the occupants. Further work should focus on the implementation of model predictive control strategies into real buildings in order to prove whether the MPC algorithm can be successfully implemented in reality, and to obtain detailed feedback from building occupants regarding the thermal comfort. Moreover, further research might explore a comparison between the applied MPC strategies and RBC strategies in order to determine if the advantage of using MPC is worth the higher computation effort and the additional complexity.

Bibliography

1. EUROPEAN COMMISSION. Proposal for a Directive of the European Parliament and of the Council amending Directive 2010/31/EU on the energy performance of buildings 2016/0381 (COD). [online]. 2016. Vol. 0381. Available from: http://eur-lex.europa.eu/legal-content/EN/TXT/PDF/?uri=CELEX:52016PC0765&from=EN
2. EUROPEAN HEAT PUMP ASSOCIATION (EHPA). EHPA Stats. [online]. 2018. [Accessed 3 July 2018]. Available from: http://stats.ehpa.org/hp_sales/story_sales/
3. JENSEN, Søren Østergaard, MARSZAL-POMIANOWSKA, Anna, LOLLINI, Roberto, PASUT, Wilmer, KNOTZER, Armin, ENGELMANN, Peter, STAFFORD, Anne and REYNDERS, Glenn. IEA EBC Annex 67 Energy Flexible Buildings. *Energy and Buildings* [online]. 2017. Vol. 155, p. 25–34. DOI 10.1016/j.enbuild.2017.08.044. Available from: http://dx.doi.org/10.1016/j.enbuild.2017.08.044
4. UNION OF CONCERNED SCIENTISTS. Benefits of Renewable Energy Use. *Union of Concerned Scientists: science for a healthy planet and safer world* [online]. 2017. [Accessed 8 May 2018]. Available from: https://www.ucsusa.org/clean-energy/renewable-energy/public-benefits-of-renewable-power#bf-toc-2
5. DARMANI, Anna, ARVIDSSON, Niklas, HIDALGO, Antonio and ALBORS, Jose. What drives the development of renewable energy technologies? Toward a typology for the systemic drivers. *Renewable and Sustainable Energy Reviews* [online]. 2014. Vol. 38, p. 834–847. DOI 10.1016/j.rser.2014.07.023. Available from: http://dx.doi.org/10.1016/j.rser.2014.07.023
6. GAN, Jianbang and SMITH, C. T. Drivers for renewable energy: A comparison among OECD countries. *Biomass and Bioenergy* [online]. 2011. Vol. 35, no. 11, p. 4497–4503. DOI 10.1016/j.biombioe.2011.03.022. Available from: http://dx.doi.org/10.1016/j.biombioe.2011.03.022
7. EUROPEAN PARLIAMENT. Directive 2009/28/EC of the European Parliament and of the Council of 23 April 2009. *Official Journal of the European Union*. 2009. Vol. 140, no. 16, p. 16–62. DOI 10.3000/17252555.L_2009.140.eng.
8. TABULA PROJECT TEAM. Typology Approach for Building Stock Energy Assessment - Main Results of the TABULA project. [online]. 2012. No. June 2009, p. 43. Available from: https://ec.europa.eu/energy/intelligent/projects/sites/iee-projects/files/projects/documents/tabula_final_report_en.pdf
9. EUROPEAN COMMISSION. EU Buildings Database. *European Commission - Energy* [online]. 2018. [Accessed 8 May 2018]. Available from: https://ec.europa.eu/energy/en/eu-buildings-database
10. LE DRÉAU, J. and HEISELBERG, P. Energy flexibility of residential buildings using short term heat storage in the thermal mass. *Energy*. 2016. Vol. 111, p. 991–1002. DOI 10.1016/j.energy.2016.05.076.
11. REYNDERS, G., NUYTTEN, T. and SAELENS, D. Potential of structural thermal mass for demand-side management in dwellings. *Building and Environment* [online]. 2013. Vol. 64, p. 187–199. DOI 10.1016/j.buildenv.2013.03.010. Available from: http://dx.doi.org/10.1016/j.buildenv.2013.03.010
12. PATTEEUW, Dieter, REYNDERS, Glenn, BRUNINX, Kenneth, PROTOPAPADAKI, Christina, DELARUE, Erik, D'HAESELEER, William, SAELENS, Dirk and HELSEN, Lieve. CO2-abatement cost of residential heat pumps with active demand response: Demand- and supply-side effects. *Applied Energy* [online]. 2015. Vol. 156, p. 490–501. DOI 10.1016/j.apenergy.2015.07.038. Available from: http://dx.doi.org/10.1016/j.apenergy.2015.07.038
13. PÉAN, Thibault Q., SALOM, Jaume and COSTA-CASTELLÓ, Ramon. Review of control strategies for improving the energy flexibility provided by heat pump systems in buildings. *Journal of Process Control* [online]. 2018. DOI 10.1016/j.jprocont.2018.03.006. Available from: https://doi.org/10.1016/j.jprocont.2018.03.006
14. CLAUSS, John, FINCK, Christian, VOGLER-FINCK, Pierre and BEAGON, Paul. Control strategies for building energy systems to unlock demand side flexibility – A review. In : *15th International Conference of the International Building Performance Simulation Association (IBPSA)*. San Francisco, CA, USA, 2017. p. 611–620.

15. DE CONINCK, Roel and HELSEN, Lieve. Practical implementation and evaluation of model predictive control for an office building in Brussels. *Energy and Buildings* [online]. 2016. Vol. 111, p. 290–298. DOI 10.1016/j.enbuild.2015.11.014. Available from: http://dx.doi.org/10.1016/j.enbuild.2015.11.014

16. REYNDERS, Glenn, LOPES, Rui Amaral, MARSZAL-POMIANOWSKA, Anna, AELENEI, Daniel, MARTINS, João and SAELENS, Dirk. Energy Flexible Buildings: An evaluation of definitions and quantification methodologies applied to thermal storage. *Energy and Buildings* [online]. 2018. Vol. 166, p. 372–390. DOI 10.1016/j.enbuild.2018.02.040. Available from: http://linkinghub.elsevier.com/retrieve/pii/S037877881732947X

17. NØRGÅRD, Per; *Characterisation and quantification of flexibilities in the energy exchanges between buildings and the energy system(s)*. 2015.

18. REYNDERS, Glenn, AMARAL LOPES, Rui, MARSZAL-POMIANOWSKA, Anna, AELENEI, Daniel and MARTINS, João. Energy Flexible Buildings: A review of definitions and quantification methodologies. *Energy and Buildings*. 2018. Vol. Submitted. DOI 10.1016/j.enbuild.2018.02.040.

19. STINNER, Sebastian, HUCHTEMANN, Kristian and MÜLLER, Dirk. Quantifying the operational flexibility of building energy systems with thermal energy storages. *Applied Energy* [online]. 2016. Vol. 181, p. 140–154. DOI 10.1016/j.apenergy.2016.08.055. Available from: http://dx.doi.org/10.1016/j.apenergy.2016.08.055

20. DE CONINCK, Roel and HELSEN, Lieve. Quantification of flexibility in buildings by cost curves - Methodology and application. *Applied Energy* [online]. 2016. Vol. 162, p. 653–665. DOI 10.1016/j.apenergy.2015.10.114. Available from: http://dx.doi.org/10.1016/j.apenergy.2015.10.114

21. KONDZIELLA, Hendrik and BRUCKNER, Thomas. Flexibility requirements of renewable energy based electricity systems - A review of research results and methodologies. *Renewable and Sustainable Energy Reviews* [online]. 2016. Vol. 53, p. 10–22. DOI 10.1016/j.rser.2015.07.199. Available from: http://dx.doi.org/10.1016/j.rser.2015.07.199

22. YIN, Rongxin, KARA, Emre C., LI, Yaping, DEFOREST, Nicholas, WANG, Ke, YONG, Taiyou and STADLER, Michael. Quantifying flexibility of commercial and residential loads for demand response using set-point changes. *Applied Energy* [online]. 2016. Vol. 177, p. 149–164. DOI 10.1016/j.apenergy.2016.05.090. Available from: http://dx.doi.org/10.1016/j.apenergy.2016.05.090

23. ULBIG, Andreas and ANDERSSON, Göran. Analyzing operational flexibility of electric power systems. *International Journal of Electrical Power and Energy Systems* [online]. 2015. Vol. 72, p. 155–164. DOI 10.1016/j.ijepes.2015.02.028. Available from: http://dx.doi.org/10.1016/j.ijepes.2015.02.028

24. LOPES, Rui Amaral, CHAMBEL, Adriana, NEVES, João, AELENEI, Daniel and MARTINS, João. A Literature Review of Methodologies Used to Assess the Energy Flexibility of Buildings. *Energy Procedia* [online]. 2016. Vol. 91, p. 1053–1058. DOI 10.1016/j.egypro.2016.06.274. Available from: http://dx.doi.org/10.1016/j.egypro.2016.06.274

25. SIX, Daan, DESMEDT, Johan, BAEL, Johan V A N and VANHOUDT, Dirk. Exploring the Flexibility Potential of Residential Heat Pumps. In : *21st International Conference on Electricity Distribution*. Frankfurt, 2011. p. 1–4.

26. NUYTTEN, Thomas, CLAESSENS, Bert, PAREDIS, Kristof, VAN BAEL, Johan and SIX, Daan. Flexibility of a combined heat and power system with thermal energy storage for district heating. *Applied Energy* [online]. 2013. Vol. 104, p. 583–591. DOI 10.1016/j.apenergy.2012.11.029. Available from: http://dx.doi.org/10.1016/j.apenergy.2012.11.029

27. D'HULST, R., LABEEUW, W., BEUSEN, B., CLAESSENS, S., DECONINCK, G. and VANTHOURNOUT, K. Demand response flexibility and flexibility potential of residential smart appliances: Experiences from large pilot test in Belgium. *Applied Energy* [online]. 2015. Vol. 155, p. 79–90. DOI 10.1016/j.apenergy.2015.05.101. Available from: http://dx.doi.org/10.1016/j.apenergy.2015.05.101

28. DE CONINCK, R. and HELSEN, L. Bottom-Up Quantification of the Flexibility Potential of Buildings. In : *13th Conference of International Building Performance Simulation Association, Chambéry, France,*

August 26-28 [online]. 2013. p. 3250–3258. Available from: http://www.ibpsa.org/proceedings/BS2013/p_1119.pdf

29. OLDEWURTEL, Frauke, STURZENEGGER, David, ANDERSSON, Goran, MORARI, Manfred and SMITH, Roy S. Towards a standardized building assessment for demand response. In : *Proceedings of the IEEE Conference on Decision and Control*. Florence, Italy, 2013. p. 7083–7088. ISBN 9781467357173.
30. REYNDERS, Glenn. *Quantifying the impact of building design on the potential of structural storage for active demand response in residential buildings*. KU Leuven, 2015.
31. REYNDERS, Glenn, DIRIKEN, Jan and SAELENS, Dirk. A generic quantification method for the active demand response potential of structural storage in buildings. *14th International Conference of the International Building Performance Simulation Association (IBPSA)*. 2015. No. March 2016.
32. DERU, M and TORCELLINI, P. *Performance Metrics Research Project - Final Report*. Golden, Colorado, USA, 2005.
33. MARSZAL-POMIANOWSKA, Anna, STOUSTRUP, Jakob, WIDÉN, Joakim and LE DRÉAU, Jérôme. Simple flexibility factor to facilitate the design of energy-flex-buildings. In : *15th International Conference of the International Building Performance Simulation Association (IBPSA)*. 2017. p. 1205–1212.
34. DAR, Usman Ijaz, SARTORI, Igor, GEORGES, Laurent and NOVAKOVIC, Vojislav. Advanced control of heat pumps for improved flexibility of Net-ZEB towards the grid. *Energy and Buildings* [online]. 2014. Vol. 69, p. 74–84. DOI 10.1016/j.enbuild.2013.10.019. Available from: http://dx.doi.org/10.1016/j.enbuild.2013.10.019
35. MASY, Gabrielle, GEORGES, Emeline, VERHELST, Clara, LEMORT, Vincent and ANDRÉ, Philippe. Smart Grid Energy Flexible Buildings Through The Use Of Heat Pumps In The Belgian Context. *Science and Technology for the Built Environment* [online]. 2015. Vol. 21, p. 800–811. DOI 10.1080/23744731.2015.1035590. Available from: https://orbi.ulg.ac.be/handle/2268/185768
36. REYNDERS, Glenn, DIRIKEN, Jan and SAELENS, Dirk. Generic characterization method for energy flexibility: Applied to structural thermal storage in residential buildings. *Applied Energy* [online]. 2017. Vol. 198, p. 192–202. DOI 10.1016/j.apenergy.2017.04.061. Available from: http://dx.doi.org/10.1016/j.apenergy.2017.04.061
37. PÉAN, Thibault Q, TORRES, Bismark, SALOM, Jaume and ORTIZ, Joana. Representation of daily profiles of building energy flexibility. . 2017.
38. TORRES RUILOVA, Bismark. *Evaluation of energy flexibility of buildings using structural thermal mass*. 2017.
39. ARENTSEN, Michael Guldbæk, JUHLER-VERDONER, Helle, MØLLER JØRGENSEN, Jeannette, STOUGAARD KIIL, Ulrik and HOLST, Marie. *Market models for aggregators - activation of flexibility*. 2017.
40. REYNDERS, Glenn, LOPES, Rui Amaral, JUNKER, Rune Grønborg and MADSEN, Henrik. *IEA EBC Annex 67 Common exercise 4: Evaluation of characterization methodology for energy flexibility based on Flexibility Function and Flexibility Characteristics*. 2018.
41. ARTECONI, Alessia, PATTEEUW, Dieter, BRUNINX, Kenneth, DELARUE, Erik, D'HAESELEER, William and HELSEN, Lieve. Active demand response with electric heating systems: Impact of market penetration. *Applied Energy* [online]. 2016. Vol. 177, p. 636–648. DOI 10.1016/j.apenergy.2016.05.146. Available from: http://dx.doi.org/10.1016/j.apenergy.2016.05.146
42. HONG, Jun, JOHNSTONE, Cameron, TORRITI, Jacopo and LEACH, Matthew. Discrete demand side control performance under dynamic building simulation: A heat pump application. *Renewable Energy* [online]. 2012. Vol. 39, no. 1, p. 85–95. DOI 10.1016/j.renene.2011.07.042. Available from: http://dx.doi.org/10.1016/j.renene.2011.07.042
43. LEE, Kyoung Ho, JOO, Moon Chang and BAEK, Nam Choon. Experimental evaluation of simple thermal storage control strategies in low-energy solar houses to reduce electricity consumption during grid on-peak periods. *Energies*. 2015. Vol. 8, no. 9, p. 9344–9364. DOI 10.3390/en8099344.
44. MIARA, Marek, GUNTHER, Danny, LEITNER, Zaphod L. and WAPLER, Jeannette. Simulation of an Air-to-Water Heat Pump System to Evaluate the Impact of Demand-Side-Management Measures on Efficiency and Load-Shifting Potential. *Energy Technology*. 2014. Vol. 2, no. 1, p. 90–99.

DOI 10.1002/ente.201300087.

45. MADANI, Hatef, CLAESSON, Joachim and LUNDQVIST, Per. A descriptive and comparative analysis of three common control techniques for an on/off controlled Ground Source Heat Pump (GSHP) system. *Energy and Buildings* [online]. 2013. Vol. 65, p. 1–9. DOI 10.1016/j.enbuild.2013.05.006. Available from: http://dx.doi.org/10.1016/j.enbuild.2013.05.006
46. KANDLER, Christian, WIMMER, Patrick and HONOLD, Johannes. Predictive control and regulation strategies of air-to-water heat pumps. *Energy Procedia* [online]. 2015. Vol. 78, p. 2088–2093. DOI 10.1016/j.egypro.2015.11.239. Available from: http://dx.doi.org/10.1016/j.egypro.2015.11.239
47. VERHELST, Clara. *Model Predictive Control of Ground Coupled Heat Pump Systems for Office Buildings*. Katholieke Universiteit Leuven, 2012.
48. DE CONINCK, R., BAETENS, R., SAELENS, D., WOYTE, A. and HELSEN, L. Rule-based demand-side management of domestic hot water production with heat pumps in zero energy neighbourhoods. *Journal of Building Performance Simulation*. 2014. Vol. 7, no. 4, p. 271–288. DOI 10.1080/19401493.2013.801518.
49. DE CONINCK, R, BAETENS, R, VERBRUGGEN, B, DRIESEN, J, SAELENS, D and HELSEN, L. Modelling and simulation of a grid connected photovoltaic heat pump system with thermal energy storage using Modelica. *8th International Conference on System Simulation in Buildings*. 2010. Vol. 2010, no. June, p. 1–21.
50. CARVALHO, Anabela D., MOURA, Pedro, VAZ, Gilberto C. and DE ALMEIDA, Anibal T. Ground source heat pumps as high efficient solutions for building space conditioning and for integration in smart grids. *Energy Conversion and Management* [online]. 2015. Vol. 103, p. 991–1007. DOI 10.1016/j.enconman.2015.07.032. Available from: http://dx.doi.org/10.1016/j.enconman.2015.07.032
51. NEWSHAM, Guy R. and BOWKER, Brent G. The effect of utility time-varying pricing and load control strategies on residential summer peak electricity use: A review. *Energy Policy* [online]. 2010. Vol. 38, no. 7, p. 3289–3296. DOI 10.1016/j.enpol.2010.01.027. Available from: http://dx.doi.org/10.1016/j.enpol.2010.01.027
52. OCHSENDELF, Henning and CORRADI, Olivier. Integration of fluctuating energy by electricity price control. . 2011. P. 119.
53. SCHIBUOLA, Luigi, SCARPA, Massimiliano and TAMBANI, Chiara. Demand response management by means of heat pumps controlled via real time pricing. *Energy and Buildings* [online]. 2015. Vol. 90, p. 15–28. DOI 10.1016/j.enbuild.2014.12.047. Available from: http://dx.doi.org/10.1016/j.enbuild.2014.12.047
54. PÉAN, Thibault Q., SALOM, Jaume and ORTIZ, Joana. Potential and optimization of a price-based control strategy for improving energy flexibility in Mediterranean buildings. *Energy Procedia* [online]. 2017. Vol. 122, p. 463–468. DOI 10.1016/j.egypro.2017.07.292. Available from: https://doi.org/10.1016/j.egypro.2017.07.292
55. PÉAN, Thibault, ORTIZ, Joana and SALOM, Jaume. Impact of Demand-Side Management on Thermal Comfort and Energy Costs in a Residential nZEB. *Buildings* [online]. 2017. Vol. 7, no. 2, p. 37. DOI 10.3390/buildings7020037. Available from: http://www.mdpi.com/2075-5309/7/2/37
56. EUROPEAN UNION. Directive of 2009/72/EC of the European Parliament and of the Council of 13 July 2009 Concerning Common Rules for the Internal Market in Electricity and Repealing Directive 2003/54/EC. *Official Journal of the European Union*. 2009. Vol. L211, no. August, p. L 211/55-L 211/93. DOI 10.1126/science.202.4366.409.
57. KLEIN, Konstantin, KILLINGER, Sven, FISCHER, David, STREULING, Christoph, SALOM, Jaume and CUBI, Eduard. Comparison of the future residual load in fifteen countries and requirements to grid-supportive building operation. *Eurosun 2016*. 2016. No. October, p. 11–14.
58. PAWLOWSKI, Andrzej, GUZMAN, José Luis, RODRÍGUEZ, Francisco, BERENGUEL, Manuel and SANCHEZ, Jorge. Application of time-series methods to disturbance estimation in predictive control problems. *IEEE International Symposium on Industrial Electronics*. 2010. P. 409–414. DOI 10.1109/ISIE.2010.5637867.

59. SALPAKARI, Jyri and LUND, Peter. Optimal and rule-based control strategies for energy flexibility in buildings with PV. *Applied Energy* [online]. 2016. Vol. 161, p. 425–436. DOI 10.1016/j.apenergy.2015.10.036. Available from: http://dx.doi.org/10.1016/j.apenergy.2015.10.036

60. TAHERSIMA, Fatemeh, STOUSTRUP, Jakob, RASMUSSEN, Henrik and MEYBODI, Soroush a. Economic COP optimization of a heat pump with hierarchical model predictive control. *2012 IEEE 51st IEEE Conference on Decision and Control (CDC)* [online]. 2012. P. 7583–7588. DOI 10.1109/CDC.2012.6425810. Available from: http://ieeexplore.ieee.org/lpdocs/epic03/wrapper.htm?arnumber=6425810

61. LI, Xiwang and MALKAWI, Ali. Multi-objective optimization for thermal mass model predictive control in small and medium size commercial buildings under summer weather conditions. *Energy* [online]. 2016. Vol. 112, p. 1194–1206. DOI 10.1016/j.energy.2016.07.021. Available from: http://dx.doi.org/10.1016/j.energy.2016.07.021

62. VERHELST, Clara, DEGRAUWE, David, LOGIST, Filip, IMPE, Jan Van and HELSEN, Lieve. Multi-objective optimal control of an air-to-water heat pump for residential heating. *Building Simulation*. 2012. Vol. 5, no. 3, p. 281–291. DOI 10.1007/s12273-012-0061-z.

63. PEDERSEN, T. S., ANDERSEN, P. and NIELSEN, K. M. Central control of heat pumps for smart grid purposes tested on single family houses. *2013 10th IEEE International Conference on Networking, Sensing and Control, ICNSC 2013*. 2013. P. 118–123. DOI 10.1109/ICNSC.2013.6548722.

64. KAJGAARD, Mikkel Urban, MOGENSEN, Jesper, WITTENDORFF, Anders, VERESS, Attila Todor and BIEGEL, Benjamin. Model predictive control of domestic heat pump. *2013 American Control Conference* [online]. 2013. P. 2013–2018. DOI 10.1109/ACC.2013.6580131. Available from: http://ieeexplore.ieee.org/document/6580131/

65. HALVGAARD, Rasmus, POULSEN, Niels Kjolstad, MADSEN, Henrik and JORGENSEN, John Bagterp. Economic Model Predictive Control for building climate control in a Smart Grid. *2012 IEEE PES Innovative Smart Grid Technologies (ISGT)* [online]. 2012. P. 1–6. DOI 10.1109/ISGT.2012.6175631. Available from: http://ieeexplore.ieee.org/document/6175631/

66. SANTOS, Rui Mirra, ZONG, Yi, SOUSA, Joao M. C., MENDONCA, Luis and THAVLOV, Anders. Nonlinear economic model predictive control strategy for active smart buildings. *2016 IEEE PES Innovative Smart Grid Technologies Conference Europe (ISGT-Europe)* [online]. 2016. P. 1–6. DOI 10.1109/ISGTEurope.2016.7856245. Available from: http://ieeexplore.ieee.org/document/7856245/

67. BIANCHINI, Gianni, CASINI, Marco, VICINO, Antonio and ZARRILLI, Donato. Demand-response in building heating systems: A Model Predictive Control approach. *Applied Energy* [online]. 2016. Vol. 168, p. 159–170. DOI 10.1016/j.apenergy.2016.01.088. Available from: http://dx.doi.org/10.1016/j.apenergy.2016.01.088

68. DAHL KNUDSEN, Michael and PETERSEN, Steffen. Demand response potential of model predictive control of space heating based on price and carbon dioxide intensity signals. *Energy and Buildings* [online]. 2016. Vol. 125, p. 196–204. DOI 10.1016/j.enbuild.2016.04.053. Available from: http://dx.doi.org/10.1016/j.enbuild.2016.04.053

69. SICHILALU, Sam M. and XIA, Xiaohua. Optimal power dispatch of a grid tied-battery-photovoltaic system supplying heat pump water heaters. *Energy Conversion and Management* [online]. 2015. Vol. 102, p. 81–91. DOI 10.1016/j.enconman.2015.03.087. Available from: http://dx.doi.org/10.1016/j.enconman.2015.03.087

70. MENDOZA-SERRANO, David I. and CHMIELEWSKI, Donald J. Smart grid coordination in building HVAC systems: EMPC and the impact of forecasting. *Journal of Process Control* [online]. 2014. Vol. 24, no. 8, p. 1301–1310. DOI 10.1016/j.jprocont.2014.06.005. Available from: http://dx.doi.org/10.1016/j.jprocont.2014.06.005

71. MA, Jingran, QIN, S. Joe and SALSBURY, Timothy. Application of economic MPC to the energy and demand minimization of a commercial building. *Journal of Process Control* [online]. 2014. Vol. 24, no. 8, p. 1282–1291. DOI 10.1016/j.jprocont.2014.06.011. Available from: http://dx.doi.org/10.1016/j.jprocont.2014.06.011

72. VÁŇA, Zdeněk, CIGLER, Jiří, ŠIROKÝ, Jan, ŽÁČEKOVÁ, Eva and FERKL, Lukáš. Model-based energy efficient control applied to an office building. *Journal of Process Control*. 2014. Vol. 24, no. 6, p. 790–797. DOI 10.1016/j.jprocont.2014.01.016.

73. STURZENEGGER, David, GYALISTRAS, Dimitrios, MORARI, Manfred and SMITH, Roy S. Model Predictive Climate Control of a Swiss Office Building: Implementation, Results, and Cost-Benefit Analysis. *IEEE Transactions on Control Systems Technology*. 2016. Vol. 24, no. 1, p. 1–12. DOI 10.1109/TCST.2015.2415411 Y3 - 07.01.2016 U6 - http://ieeexplore.ieee.org/ielx7/87/7361777/07087366.pdf?tp=&arnumber=7087366&isnumber=7361777 M4 - Citavi.

74. TOERSCHE, H. A., BAKKER, V., MOLDERINK, A., NYKAMP, S., HURINK, J. L. and SMIT, G. J.M. Controlling the heating mode of heat pumps with the TRIANA three step methodology. *2012 IEEE PES Innovative Smart Grid Technologies, ISGT 2012*. 2012. P. 1–7. DOI 10.1109/ISGT.2012.6175662.

75. HEDEGAARD, Rasmus Elbæk, PEDERSEN, Theis Heidmann and PETERSEN, Steffen. Multi-market demand response using economic model predictive control of space heating in residential buildings. *Energy and Buildings* [online]. 2017. Vol. 150, p. 253–261. DOI 10.1016/j.enbuild.2017.05.059. Available from: http://dx.doi.org/10.1016/j.enbuild.2017.05.059

76. KLEIN, Konstantin, HERKEL, Sebastian, HENNING, Hans Martin and FELSMANN, Clemens. Load shifting using the heating and cooling system of an office building: Quantitative potential evaluation for different flexibility and storage options. *Applied Energy* [online]. 2017. Vol. 203, p. 917–937. DOI 10.1016/j.apenergy.2017.06.073. Available from: http://dx.doi.org/10.1016/j.apenergy.2017.06.073

77. ALIBABAEI, Nima, FUNG, Alan S. and RAAHEMIFAR, Kaamran. Development of Matlab-TRNSYS co-simulator for applying predictive strategy planning models on residential house HVAC system. *Energy and Buildings* [online]. 2016. Vol. 128, p. 81–98. DOI 10.1016/j.enbuild.2016.05.084. Available from: http://dx.doi.org/10.1016/j.enbuild.2016.05.084

78. UNIVERSAL SMART ENERGY FRAMEWORK (USEF). *USEF: Workstream on Aggregator Implementation Models - Recommended practices and key considerations for a regulatory framework and market design on explicit Demand Response*. 2017.

79. MA, Zheng, DALMACIO BILLANES, Joy, KJARGAARD, Mikkel Baun and JORGENSEN, Bo Norregaard. Energy flexibility in retail buildings: From a business ecosystem perspective. In : *International Conference on the European Energy Market, EEM*. 2017. ISBN 9781509054992.

80. MA, Zheng, BILLANES, Joy Dalmacio and JORGENSEN, Bo Norregaard. A business ecosystem driven market analysis: The bright green building market potential. In : *2017 IEEE Technology and Engineering Management Society Conference, TEMSCON 2017*. 2017. p. 79–85. ISBN 9781509011148.

81. LEHEC, Guillaume. *The Flexibility Aggregator – the example of the GreenLys Project*. 2014.

82. VAN DE KAA, G. *Standards Battles for Complex Systems*. 2009. Rotterdam, Netherlands : Erasmus Research Institute of Management.

83. MA, Zheng, BADI, Adrian and JORGENSEN, Bo Norregaard. Market opportunities and barriers for smart buildings. In : *2016 IEEE Green Energy and Systems Conference (IGSEC)* [online]. 2016. p. 1–6. ISBN 978-1-5090-2294-6. Available from: http://ieeexplore.ieee.org/document/7790078/

84. MLECNIK, Erwin. Goodbye Passive House, Hello Energy Flexible Building? In : *Proceedings of PLEA 2016 36th International Conference on Passive and Low Energy Architecture*. 2016.

85. VAN DER LAAN, Marten. *Universal Smart Energy Framework: a solid foundation for smart energy futures*. 2017. Amsterdam, Netherlands.

86. LI, Rongling, DANE, Gamze, FINCK, Christian and ZEILER, Wim. Are building users prepared for energy flexible buildings?—A large-scale survey in the Netherlands. *Applied Energy* [online]. 2017. Vol. 203, p. 623–634. DOI 10.1016/j.apenergy.2017.06.067. Available from: http://dx.doi.org/10.1016/j.apenergy.2017.06.067

87. SMART ENERGY DEMAND COALITION (SEDC). *Explicit Demand Response in Europe - Mapping the Markets 2017* [online]. Brussels, Belgium, 2017. Available from: http://www.smarten.eu/wp-

content/uploads/2017/04/SEDC-Explicit-Demand-Response-in-Europe-Mapping-the-Markets-2017.pdf

88. MICROSOFT. Bing Maps. [online]. 2018. Available from: https://www.bing.com/maps

89. METEOBLUE. Clima Terrassa - meteoblue. *meteoblue.com* [online]. 2018. [Accessed 24 May 2018]. Available from: https://www.meteoblue.com/es/tiempo/pronostico/modelclimate/terrassa_españa_3108286

90. INSTITUT CATALÀ D'ENERGIA. *Rehabilitació energètica d'edificis, Col•lecció Quadern Pràctic Nº 10* [online]. Barcelona, Spain, 2016. Available from: http://icaen.gencat.cat/web/.content/10_ICAEN/17_publicacions_informes/04_coleccio_QuadernPractic/quadern_practic/arxius/10_rehabilitacio_edificis.pdf

91. INSTITUT CATALÀ D'ENERGIA. *Normativa d'Aïllament Tèrmic d'Edificis: NRE-AT-87*. Barcelona, Spain, 1987.

92. ORTIZ, Joana, FONSECA I CASAS, Antoni, SALOM, Jaume, GARRIDO SORIANO, Nuria and FONSECA I CASAS, Pau. Cost-effective analysis for selecting energy efficiency measures for refurbishment of residential buildings in Catalonia. *Energy and Buildings* [online]. 2016. Vol. 128, p. 442–457. DOI 10.1016/j.enbuild.2016.06.059. Available from: http://dx.doi.org/10.1016/j.enbuild.2016.06.059

93. ORTIZ, Joana, FONSECA, Antoni, SALOM, Jaume, GARRIDO, Nuria, FONSECA, Pau and RUSSO, Verdiana. Comfort and economic criteria for selecting passive measures for the energy refurbishment of residential buildings in Catalonia. *Energy and Buildings* [online]. 2016. Vol. 110, p. 195–210. DOI 10.1016/j.enbuild.2015.10.022. Available from: http://dx.doi.org/10.1016/j.enbuild.2015.10.022

94. ORTIZ, Joana, GUARINO, Francesco, SALOM, Jaume, CORCHERO, Cristina and CELLURA, Maurizio. Stochastic model for electrical loads in Mediterranean residential buildings: Validation and applications. *Energy and Buildings* [online]. 2014. Vol. 80, p. 23–36. DOI 10.1016/j.enbuild.2014.04.053. Available from: http://dx.doi.org/10.1016/j.enbuild.2014.04.053

95. CEN. *EN 15316-1: Heating systems in buildings - Method for calculation of system energy requirements and system efficiencies - Part 3-1 Domestic hot water systems, characterisation of needs (tapping requirements)*. 2007.

96. INSTITUTO PARA LA DIVERSIFICACIÓN Y AHORRO DE LA ENERGÍA (IDAE). *Guía Técnica Agua Caliente Sanitaria Central*. 2010. Madrid, Spain. ISBN 9788496680524.

97. FUENTES, Elena, WADDICOR, David, FANNAN, Mohammed Omar and SALOM, Jaume. Improved methodology for testing the part load performance of water-to-water heat pumps. In : *12th IEA Heat Pump Conference 2017*. 2017.

98. FUENTES, E., WADDICOR, D. A. and SALOM, J. Improvements in the characterization of the efficiency degradation of water-to-water heat pumps under cyclic conditions. *Applied Energy* [online]. 2016. Vol. 179, p. 778–789. DOI 10.1016/j.apenergy.2016.07.047. Available from: http://dx.doi.org/10.1016/j.apenergy.2016.07.047

99. DONGELLINI, Matteo, NALDI, Claudia and MORINI, Gian Luca. Seasonal performance evaluation of electric air-to-water heat pump systems. *Applied Thermal Engineering* [online]. 2015. Vol. 90, p. 1072–1081. DOI 10.1016/j.applthermaleng.2015.03.026. Available from: http://dx.doi.org/10.1016/j.applthermaleng.2015.03.026

100. SCHIBUOLA, L., SCARPA, M. and TAMBANI, C. Modelling of HVAC system components for building dynamic simulation. *Proceedings of BS 2013: 13th Conference of the International Building Performance Simulation Association*. 2013. P. 1103–1109.

101. PIECHURSKI, Krzysztof, SZULGOWSKA-ZGRZYWA, Małgorzata and DANIELEWICZ, Jan. The impact of the work under partial load on the energy efficiency of an air-to-water heat pump. . 2017. Vol. 00072. DOI 10.1051/e3sconf/20171700072.

102. BETTANINI, Ernesto, GASTALDELLO, Alessio and SCHIBUOLA, Luigi. Simplified models to simulate part load performances of air conditioning equipments. *Eighth International IBPSA Conference Eindhoven, Netherlands August 11-14, 2003* [online]. 2003. P. 107–114. Available from: http://www.ibpsa.org/proceedings/BS2003/BS03_0107_114.pdf

103. EUROPEAN COMMITTEE FOR STANDARDIZATION (CEN). *EN 14825-2013: Air conditioners, liquid chilling packages and heat pumps, with electrically driven compressors, for space heating and cooling -Testing and rating at part load conditions and calculation of seasonal performance*. 2013. Brussels, Belgium.

104. HITACHI AIR CONDITIONING PRODUCTS EUROPE. *Technical Catalogue - Yutaki Series*. 2016. Vacarisses, Barcelona, Spain : Hitachi Air Conditioning Products Europe.

105. FILLIARD, Bruno;, GUIAVARCH, Alain; and PEUPORTIER, Bruno; Performance evaluation of an air-to-air heat pump coupled with temperate air-sources integrated into a dwelling. In : *11th Conference of International Building Performance Simulation Association* [online]. Glasgow, Scotland, 2009. p. 2266–2273. Available from: http://hal.archives-ouvertes.fr/hal-00574663/

106. SWEDISH ENERGY AGENCY. Luftvattenvärmepumpar. [online]. 2018. [Accessed 19 July 2018]. Available from: http://www.energimyndigheten.se/tester/tester-a-o/luftvattenvarmepumpar/

107. BURBA, Maurizio. Improved energy efficiency of air cooled chillers. . 2013. No. January, p. 50–53.

108. HIGH PERFORMING BUILDINGS MAGAZINE. Daikin Technology and Innovation Center, Osaka, Japan. [online]. 2018. [Accessed 15 September 2018]. Available from: http://www.hpbmagazine.org/Daikin-Technology-and-Innovation-Center-Osaka-Japan/

109. DONGELLINI, Matteo, ABBENANTE, Massimiliano and MORINI, Gian Luca. A strategy for the optimal control logic of heat pump systems: impact on the energy consumptions of a residential building. In : *12th IEA Heat Pump Conference 2017*. Rotterdam, Netherlands, 2017. ISBN 0512090467.

110. UNIVERSITY OF WISCONSIN-MADISON. *TRNSYS, a Transient Simulation Program*. 2012. Madison, Wisconsin, USA. 17.1.

111. RED ELÉCTRICA DE ESPAÑA. Término de facturación de energía activa del PVPC. *Red Eléctrica de España* [online]. 2017. [Accessed 8 May 2018]. Available from: https://www.esios.ree.es/es/pvpc

112. DAR, Usman Ijaz, SARTORI, Igor, GEORGES, Laurent and NOVAKOVIC, Vojislav. Improving the interaction between netZEB and the grid using advanced control of HP. *13th Conference of International Building Performance Simulation Association, Chambéry, France*. 2013. P. 1365–1372.

113. CARLUCCI, S. *Thermal Comfort Assessment of Buildings*. Mlano, Italy : Springer - Briefs in Applied Sciences and Technology, 2013.

114. ORTIZ, Joana. *Detailed energy and comfort simulation of integral refurbishment of existing buildings in Catalonia* [online]. Universitat Politècnica de Catalunya, 2016. Available from: http://hdl.handle.net/2117/106274

115. REYNDERS, G., DIRIKEN, J. and SAELENS, D. Quality of grey-box models and identified parameters as function of the accuracy of input and observation signals. *Energy and Buildings* [online]. 2014. Vol. 82, p. 263–274. DOI 10.1016/j.enbuild.2014.07.025. Available from: http://dx.doi.org/10.1016/j.enbuild.2014.07.025

116. BACHER, Peder and MADSEN, Henrik. Identifying suitable models for the heat dynamics of buildings. *Energy and Buildings* [online]. 2011. Vol. 43, no. 7, p. 1511–1522. DOI 10.1016/j.enbuild.2011.02.005. Available from: http://dx.doi.org/10.1016/j.enbuild.2011.02.005

117. THE MATHWORKS INC. *MATLAB* [online]. 2018. Natick, Massachusetts, United States. Release 2018a. Available from: https://es.mathworks.com/products/matlab.html

118. LOFBERG, J. YALMIP : a toolbox for modeling and optimization in MATLAB. *2004 IEEE International Conference on Robotics and Automation (IEEE Cat. No.04CH37508)* [online]. 2004. P. 284–289. DOI 10.1109/CACSD.2004.1393890. Available from: http://ieeexplore.ieee.org/document/1393890/

119. GUROBI OPTIMIZATION LLC. Gurobi Software. [online]. 2018. Available from: http://www.gurobi.com

120. PÉAN, Thibault, SALOM, Jaume and COSTA-CASTELLÓ, Ramon. Configurations of model predictive control to exploit energy flexibility in building thermal loads. In : .

121. RED ELÉCTRICA DE ESPAÑA. Porcentaje de Generación Libre de CO2. [online]. 2018. [Accessed 7 September 2018]. Available from: https://www.esios.ree.es/es/analisis/10033

122. SALOM, Jaume, MARSZAL, Anna Joanna, WIDÉN, Joakim, CANDANEDO, José and

LINDBERG, Karen Byskov. Analysis of load match and grid interaction indicators in net zero energy buildings with simulated and monitored data. *Applied Energy* [online]. 2014. Vol. 136, p. 119–131. DOI 10.1016/j.apenergy.2014.09.018. Available from: http://dx.doi.org/10.1016/j.apenergy.2014.09.018

123. SALOM, Jaume, MARSZAL, Anna Joanna, CANDANEDO, José, WIDÉN, Joakim, LINDBERG, Karen Byskov and SARTORI, Igor. Analysis Of Load Match and Grid Interaction Indicators in NZEB with High-Resolution Data. *A report of Subtask A, IEA Task 40/Annex 52 Towards Net Zero Energy Solar Buildings* [online]. 2014. P. 102. Available from: https://nachhaltigwirtschaften.at/resources/iea_pdf/endbericht_201417_iea_shc_task40_ebc_annex_52_anhang05.pdf

124. BAETENS, R, DE CONINCK, R, HELSEN, L and SAELENS, D. The Impact of Load Profile on the Grid-Interaction of Building Integrated Photovoltaic (BIPV) Systems in Low-Energy Dwellings. *Journal of Green Building*. 2010. Vol. 5, no. 4, p. 137–147. DOI 10.3992/jgb.5.4.137.

125. VANHOUDT, D., GEYSEN, D., CLAESSENS, B., LEEMANS, F., JESPERS, L. and VAN BAEL, J. An actively controlled residential heat pump: Potential on peak shaving and maximization of self-consumption of renewable energy. *Renewable Energy* [online]. 2014. Vol. 63, p. 531–543. DOI 10.1016/j.renene.2013.10.021. Available from: http://dx.doi.org/10.1016/j.renene.2013.10.021

126. KLEIN, K, KALZ, D and HERKEL, S. Grid Impact of a Net-Zero Energy Building With BIPV Using Different Energy Management Strategies. *Cisbat 2015*. 2015. P. 579–584.

Appendix 1: General Key Performance Indicators

Self-generation/consumption (or load/supply cover factor) (48, 122–126)

Self-generation γ_l and self-consumption γ_s are defined respectively as the proportion of electrical demand met by on-site generation and the proportion of on-site generation consumed by building. The mathematical definitions are presented below:

$$\gamma_l = \frac{\int_0^T \min[g(t)-S(t)-\xi(t);l(t)]dt}{\int_0^T l(t)dt} \quad \text{(A1.74)}$$

$$\gamma_s = \frac{\int_0^T \min[g(t)-S(t)-\xi(t);l(t)]dt}{\int_0^T g(t)dt} \quad \text{(A1.75)}$$

Where $g(t)$ is the on-site electricity generation, $S(t)$ is the energy storage balance, $\xi(t)$ are the energy losses, and $l(t)$ is the energy load.

These two KPIs are accepted by international research groups, e.g. IEA EBC Annex 52: "Heat Pumping Technologies" and are able to show the seasonal or daily performance of various generator types, such as PV or combined heat and power, independently from any emission or energy saving of the entire energy system, as well as to enable the comparison of different control strategies.

Peak power generation/load (122)

Peak power generation $\bar{G}$ and peak power load are defined as the peak value of the on-site generation and the peak value of the demand normalized by the nominal capacity of the grid connection E_{des} (122). In mathematical terms:

$$\bar{G} = \frac{\max[g(t)]}{E_{des}} \quad \text{(A1.76)}$$

$$\bar{L} = \frac{\max[l(t)]}{E_{des}} \quad \text{(A1.77)}$$

These metrics are useful to determine the peak period of generation or load demand, to allow the comparison to net energy export and net energy import, and, moreover, to set boundaries to load duration curves and carpet plots of the demand.

Loss of load probability (122)

It is the percentage of time when on-site generation is less than local demand, in other words, the percentage of time when the system imports electricity from the grid. The following equations give the mathematical definition:

$$LOLP_b = \frac{\int_0^T (f(t)dt}{T} \quad \text{(A1.78)}$$

Where $f(t)$ is equal to 1 when the net energy exported to the grid is lower than 0 while it is equal to 0 when the net energy exported to the grid is higher than 0. This indicator is used to design PV/energy system, but it does not give an indication on the amount of imported electricity.

Grid feed-in (59)

It is defined as the amount of energy exported to the grid:

$$GFI = \int_0^T E_{net\ export}(t)dt \quad \text{(A1.79)}$$

The minimisation of this indicator achieves a higher self-consumption factor, and it is a more efficient method to satisfy grid integration regulation than simple curtailment.

Appendix 2: Heat Pump Performance Data

Table A2.20: full load heating capacity

Manufacturer full load data											
Full load heating capacity [kW]		Ambient temperature [°C]									
		-20	-15	-10	-7	-2	2	7	12	15	20
Water outlet temperature [°C]	60	NA	NA	6.5	6.8	6.9	7.0	8.5	10.2	11.2	13.0
	55	NA	NA	7.2	9.7	9.9	10.5	13.5	14.4	14.8	15.5
	50	NA	NA	7.8	9.9	10.0	10.9	13.8	14.8	15.4	16.3
	45	7.2	8.3	9.4	10.0	10.6	11.5	14.1	15.3	16.0	17.0
	40	8.1	9.0	9.8	10.3	11.0	11.8	14.7	15.7	16.3	17.3
	35	9.0	9.6	10.3	10.6	11.8	12.8	15.2	16.0	16.5	17.5
	30	10.0	10.8	11.5	12.0	12.7	13.3	15.9	16.6	17.0	17.7
	25	11.6	12.2	12.7	13.0	13.7	13.6	16.1	17.0	17.5	18.4
	20	13.3	13.6	13.8	14.0	14.7	13.8	16.3	17.4	18.1	19.2

Table A2.21: coefficient of performance at full load

Manufacturer full load data											
COP at full load [-]		Ambient temperature [°C]									
		-20	-15	-10	-7	-2	2	7	12	15	20
Water outlet temperature [°C]	60	NA	NA	1.50	1.65	1.92	2.20	2.50	2.80	2.96	3.20
	55	NA	NA	1.67	1.74	2.04	2.35	2.84	2.78	2.75	4.42
	50	NA	NA	1.97	2.19	2.40	2.60	3.19	3.33	3.41	3.53
	45	1.79	2.04	2.30	2.45	2.68	2.90	3.66	4.10	4.38	4.87
	40	1.95	2.17	2.41	2.55	2.80	3.01	4.12	4.60	4.91	5.48
	35	2.10	2.30	2.51	2.65	2.90	3.10	4.65	5.19	5.57	6.23
	30	2.30	2.55	2.81	2.98	3.26	3.50	4.80	5.91	6.78	6.82
	25	2.62	2.82	3.03	3.17	3.45	3.76	5.71	6.20	6.52	7.23
	20	2.92	3.08	3.26	3.35	3.63	3.98	6.97	6.52	6.29	7.66

Table A2.22: part load heating capacity

Manufacturer and estimated part load data											
Part load heating capacity [kW]		Ambient temperature [°C]									
		-20	-15	-10	-7	-2	2	7	12	15	20
Water outlet temperature [°C]	60	NA	NA	6.63	8.35	6.53	5.08	3.46	3.58	NA	NA
	55	NA	NA	7.40	8.60	6.73	5.23	3.52	3.60	NA	NA
	50	NA	NA	8.18	8.85	6.92	5.38	3.58	3.63	NA	NA
	45	NA	NA	8.95	9.10	7.12	5.54	3.64	3.65	NA	NA
	40	NA	NA	9.73	9.35	7.32	5.69	3.70	3.68	NA	NA
	35	NA	NA	10.50	9.60	7.51	5.84	3.76	3.70	NA	NA
	30	NA	NA	11.28	9.85	7.71	5.99	3.82	3.73	NA	NA
	25	NA	NA	12.05	10.10	7.90	6.15	3.88	3.75	NA	NA
	20	NA	NA	12.83	10.35	8.10	6.30	3.94	3.78	NA	NA

Table A2.23: coefficient of performance at part load

Manufacturer and estimated part load data											
COP at part load [-]		Ambient temperature [°C]									
		-20	-15	-10	-7	-2	2	7	12	15	20
Water outlet temperature [°C]	60	NA	NA	1.46	1.57	2.47	3.20	4.55	5.65	NA	NA
	55	NA	NA	1.70	1.80	2.80	3.60	4.80	5.80	NA	NA
	50	NA	NA	1.94	2.04	3.13	4.00	5.05	5.95	NA	NA
	45	NA	NA	2.18	2.27	3.45	4.40	5.30	6.10	NA	NA
	40	NA	NA	2.41	2.51	3.78	4.80	5.55	6.25	NA	NA
	35	NA	NA	2.65	2.74	4.11	5.20	5.80	6.40	NA	NA
	30	NA	NA	2.89	2.98	4.43	5.60	6.05	6.55	NA	NA
	25	NA	NA	3.13	3.21	4.76	6.00	6.30	6.70	NA	NA
	20	NA	NA	3.36	3.45	5.09	6.40	6.55	6.85	NA	NA